41 0623142 X

ProQuest Number: 10183022

All rights reserved

INFORMATION TO ALL USERS
The quality of this reproduction is dependent upon the quality of the copy submitted.

In the unlikely event that the author did not send a complete manuscript
and there are missing pages, these will be noted. Also, if material had to be removed,
a note will indicate the deletion.

ProQuest 10183022

Published by ProQuest LLC (2017). Copyright of the Dissertation is held by the Author.

All rights reserved.
This work is protected against unauthorized copying under Title 17, United States Code
Microform Edition © ProQuest LLC.

ProQuest LLC.
789 East Eisenhower Parkway
P.O. Box 1346
Ann Arbor, MI 48106 – 1346

Gas Sensing Applications of Phthalocyanine Thin Films

THOMAS STARKE

A thesis submitted in partial fulfilment of the requirements of The
Nottingham Trent University for the Degree of Doctor of Philosophy

March 2000

Abstract

This thesis reports an investigation into the NO_2 sensing properties of copper phthalocyanine (CuPc) thin films at room temperature in air. The gas sensing properties of the CuPc films were investigated using electrical conductivity and surface acoustic wave (SAW) sensing devices. Conductivity and SAW sensors were employed to detect changes of the film properties upon NO_2 exposure in electrical conductivity and mass loading respectively.

Initially, the response of electrical conductivity and SAW sensors incorporating an untreated layer of CuPc was investigated. Laser illumination of the films during the sensing experiments was found to have a significant effect on the mass loading response but little effect on the change in electrical conductivity. From these experiments it was suggested that NO_2 adsorption on CuPc may be dominated by two different mechanisms, surface adsorption and bulk diffusion. It was also suggested that a reduction of one of these components would lead to a more controllable response.

In order to minimise the effect of bulk diffusion, some of the CuPc films were doped with NO_2 after deposition so filling the strongly bound bulk adsorption sites. In other devices, cooling of the CuPc layer in liquid nitrogen was used after deposition to change the surface structure in order to facilitate bulk diffusion. It was shown that these post-deposition treatment significantly changed the response characteristics of the CuPc film.

Response kinetics of the experiments were analysed using the Langmuir and Elovich adsorption models, a method was suggested to determine the concentration of NO_2 within the first few minutes of exposure using the value for the maximum rate of current change. A good correlation between this value and the concentration was found.

Acknowledgements

I would like to thank my supervisors Mike Newton and Glen McHale for their support and encouragement throughout the project. With their help I obtained many skills and learned to overcome difficulties and solve problems.

Thanks to Martin Willis, my third supervisor, for fruitful discussions, useful suggestions and his competent advise.

I am very grateful to my girlfriend, my parents and my grand parents for their strong emotional and financial support.

Special thanks to the technicians Pete, Nick, Steve, Larry and Toni for their practical advice, which often helped to make the impossible work.

Particularly, I would like to thank all my friends and colleges for the good times we spent together, which made my stay in Nottingham to one of the best times in my life.

Finally, I wish to thank the Royal Society for their financial support of the project.

Table of Contents

Chapter 2: LITERATURE REVIEW

Chapter 3: THEORETICAL BACKGROUND

Chapter 4: EXPERIMENTAL METHODS AND DEVELOPEMENT

Chapter 5: RESULTS AND DISCUSSION

Chapter 6: CONCLUSION AND FURTHER WORK

Chapter 1: Introduction

Gas sensors possess a wide range of applications in today's society. Many processes employ gases with properties that require a constant monitoring. Hence, there is an ongoing increase in the demand for cost-effective, rapid response and reliable sensing devices.

Amongst more traditional analysis methods, such as mass spectrometry, IR and UV-absorption and optical techniques, solid state gas sensors have received much attention in recent years. Research groups, industry and public (e.g. environmental groups) are equally interested in the advantages solid state gas sensors offer such as portability and relatively low costs.

There are numerous examples where the control of the concentration and composition of analytes is essential:

-NO_x and CO are the main toxic contents of car exhaust fumes. With a very high number of motorised vehicles these gases are a large contributor to air pollution, particularly in metropolitan areas.

-Industrial plants emitting a large amount of SO_2 are mainly responsible for acid rain and the related environmental damage.

-Coal mines have the problem of accumulating CH_4 in their tunnels. This highly explosive gas has led to a large number of disastrous accidents in the past.

-Ozone (O_3) generated due to pollution at the outskirts of large cities has become a health problem for many people. In the atmosphere it attenuates cosmic UV-radiation to a large extent. A lack of ozone, at the earth's poles may cause serious damage to the human skin, as well as other environmental problems [1].

The requirements on solid state gas sensor are high and only devices that meet these requirements have the chance of being commercialised. This is the reason why solid state gas sensing technology is an intensively investigated field with growing success in commercial applications. The properties of an ideal gas sensing device should be the guide line for the developement of a viable sensor system. They are discussed in the next section.

1.1. Ideal Sensor Properties

It would be impossible to build a sensor for universal application. However, an ideal sensor should be small, economic to produce and run, and solid state for an easier integration with modern electronics. The following list outlines the characteristics expected from an 'ideal' sensor.

- Long term stability: The sensor should be capable of performing over a reasonable long period of time at least in the range of weeks.
- Reproducibility: The response of the sensor should be consistent after each exposure. A commercially viable sensor should retain this characteristics for a high number of exposure cycles.
- Selectivity: The sensor should ideally react to only one gas. It would then be possible to construct an array with a variety of sensors with each one sensitive to only one pollutant.
- Sensitivity: Depending on the gas to be detected the sensor should be sensitive to concentrations from parts per billion (ppb) to parts per million

- Zero drift: The sensitivity should have no drift over its period of operation.
- Rapid response time: Response and recovery of the sensor should be in the range of seconds or minutes at most, especially if used in hazardous environment.
- Portability: Sensors usually operate in hostile or dangerous environments. They should be robust, easy to handle in the field, and easy to install. Ideally the whole sensor should be containable in a box without bulky external devices or cables.

1.2. Project Overview

The aim of this project was to investigate NO_2 detection using copper phthalocyanine thin films which can be operated at room temperature. If NO_2 gas adsorbs on the thin film its properties will change. These changes in properties should represent the presence and the concentration of NO_2.

In this work the copper phthalocyanine film is applied to two types of devices: electrical conductivity and acoustic wave sensors. Both of these sensors belong to the group of solid state sensors and they can detect changes of the conductivity and mass loading in the Pc film. Solid state sensors have the advantage of being small and easily integrated into micro-electronic measurement systems.

Copper Phthalocyanine is a non-toxic organic dye material which has a semiconductive nature and is known to adsorb NO_2 molecules. However, in order to make CuPc gas sensitive devices more viable some problems remain to be solved such as response speed and repeatable sensitivity.

A detailed literature review of the work by other researchers related to the project is given in Chapter 2. It covers acoustic wave gas sensing technology, phthalocyanine gas sensing, and relevant work on gas adsorption kinetics.

A detailed literature review of the work by other researchers related to the project is given in Chapter 2. It covers acoustic wave gas sensing technology, phthalocyanine gas sensing, and relevant work on gas adsorption kinetics. Chapter 3 discusses the relevant theoretical background of the project including phthalocyanines, acoustic wave devices and adsorption kinetics. Chapter 4 outlines the experimental procedures and presents some preliminary experiments in order to understand the properties of the sensors and repeat gas sensing experiments by other research groups.

Chapter 5 investigates the development of a phthlocyanine thin film NO_2 sensing system which shows a fast and reproducible response and which can be operated under room temperature conditions. All experiments were carried out using vacuum sublimed copper phthalocyanine films on conductivity and surface acoustic wave (SAW) sensors.

Since copper phthalocyanines are photo active materials a diode laser was employed to investigate the interaction of the test gas with the phthlocyanine layer by photoexcitation of the CuPc molecules. From this experiments it is suggested that two mechanisms are involved into gas adsorption on copper phthalocyanine: surface adsorption and bulk diffusion. Both these processes showed very different characteristics. It was concluded that surface treatment should be investigated in order to allow one mechanism to dominate the response.

To eliminate bulk diffusion the sensors with the phthalocyanine films were doped with NO_2 which is believed to fill the bulk adsorption sites. In this work these sensors are referred to as doped sensors. These doped sensors showed improved properties towards NO_2 detection compared to untreated films.

Cooling the sensor at liquid nitrogen temperature is believed to increase the contribution of bulk diffusion to the sensor response. In this work these devices are often referred to as cooled sensors. Cooled conductivity and SAW sensors also showed improved gas sensing properties compared to untreated films.

In order to improve the response speed, the adsorption kinetics of doped and cooled sensors were investigated. It was found that the doped sensors follow the Langmuir adsorption model which assumes a constant activation energy of adsorption whereas the cooled sensors fitted better to an Elovich model which allows for a variation in activation energy. From the kinetic responses of the doped and cooled sensors parameters has been extracted and this allows a rapid determination of the NO_2 concentration.

Finally, an initial adsorption rate method is proposed to quantify the test gas concentration which determines the gas concentration at the start of an exposure and can be easily processed by an electronic circuit.

Chapter 2: Literature Review

This chapter provides a detailed literature review of the work related to this project. It indicates the wide variety of work in the interdisciplinary field of solid state sensor technology which provided the basis for this thesis. Initially, an introduction into acoustic wave devices and their gas sensing applications will be presented, then briefly discusses sensor selectivity approaches, followed by an overview of the phthalocyanines and their application in gas detection. The final section outlines problems related to the adsorption kinetics of phthalocyanine materials.

2.1. Acoustic Wave Devices

With the miniaturisation and automation of analysis technology, fast and portable sensing systems have become possible replacing heavy expensive apparatus, such as spectrometers. Because of their high sensitivity and relatively small dimensions, gas sensors based on the propagation of acoustic waves in a piezoelectric solid have drawn the attention of many research groups over the last decade [1,2,3].

An acoustic wave device consists of a piezoelectric substrate with electrodes applied to it. An electrical circuit attached to the electrodes excites an acoustic wave in the piezoelectric material. The system may resonate at a frequency depending on the type and design of the acoustic wave device. The operating frequencies of this group of devices extends through the whole MHz range up to several GHz. Their resonance frequency is usually extremely sensitive to mass deposited on the surface of the piezoelectric substrate.

Sauerbrey [4] derived a relationship between the mass deposited on a quartz crystal resonator and its bulk resonance frequency.

$$\Delta f = -\frac{2f^2 \rho_s}{\left(\mu_q \rho_q\right)^{1/2}} \qquad (2.1)$$

Where ρ_s is the surface mass loading, ρ_q is the mass density of the crystal, μ_q is the shear stiffness of the crystal and f is the centre frequency of oscillation.

Assuming the ability to detect changes of 1Hz Equation (2.1) demonstrates that at operating frequencies of tens of MHz it is possible with an acoustic wave device to detect changes in surface mass loading as low as 10^{-10} gcm^{-2} [5]. This means that a change in surface coverage of less than a monolayer of molecules is measurable. Such a high sensitivity makes these devices especially interesting for gas sensing applications since it is possible to detect small numbers of molecues adsorbed on the surface of the device.

The first devices that were used as mass detectors by Sauerbrey were called quartz crystal microbalances (QCM). QCM's consist of a thin piezoelectric plate with an electrode attached on each side. Between the electrodes a wave is generated which propagates through the solid. This wave can have longitudinal or shear components. The latter is commonly used for QCM's in so-called thickness shear mode (TSM Figure 2.1) devices. However, QCM's are limited in their highest fundamental frequency of oscillation by the thickness of the piezoelectric plate. These devices therefore have a limited mass detection capability.

A second group of acoustic wave devices uses a wave that travels along the surface of the piezoelectric material rather than a bulk wave. In these so-called surface acoustic wave (SAW) devices most of the energy of the acoustic wave is confined to within one wavelength on the surface. The acoustic waves generated on the surface have a lower velocity than bulk waves [6]. SAW devices therefore have no restrictions on substrate thickness. Thus, operating frequencies of many GHz can be achieved, which, in turn results in higher sensitivity to changes in surface mass loading.

SAW devices were first reported after the invention of interdigital transducers (IDT's) by White *et al* [7]. Recently, other acoustic wave device types have been studied such as flexural plate wave (FPW), acoustic plate mode (APM) (Figure 2.1), and Love wave devices [8]. Although there are many other ways of SAW generation such as optical, magnetical or thermal transducers, the IDT is the most commonly used transducer type since it utilises only the electromechanical coupling [9].

A number of piezoelectric materials are suitable for acoustic wave sensor applications. Quartz crystals are widely used for TSM as well as SAW applications. Certain cut directions (e.g. AT-cut) offer the advantage of having zero temperature coefficient around room temperature [10]. Lithium niobate ($LiNbO_3$) and lithium tantalate ($LiTaO_3$) are used for SAW applications because of their high piezoelectric coupling coefficient K^2 (4.8%, 1.6% respectively, Quartz: 0.11%) [6]. The K^2 value indicates how strongly electrical energy is transformed into mechanical energy.

An acoustic wave may propagate along the surface in different modes depending on the propagation direction in relation to the crystal cut [11]. A Rayleigh wave consists of a surface-parallel and a surface-normal displacement component (Figure 2.2) with the surface parallel component also being parallel to the wave propagation direction. With both components having different magnitudes of displacement a single particle on the surface will move in an elliptical path. A Rayleigh wave is accompanied by a travelling electrical field as a result of acoustoelectric coupling. This wave type has a number of attractive attributes such as high electromechanical coupling, low losses and ease of fabrication [12].

With the selection of a different propagation direction a *Gulayev-Bleustein* (GB) *wave* may be generated. The particle displacement is transverse to the wave propagation direction and parallel to the surface. The penetration depth of this wave into the bulk is larger by the factor $1/K^2$ with respect to Rayleigh waves. Therefore, plates should be considered thicker than for Rayleigh wave type devices [12]. The GB wave shows very little response to surface mass loading. However, its velocity is altered due to viscoelastic changes of the surface layer [8]. A comprehensive description of other wave types such as flexural plate waves (FPW) and Love waves which are used in liquid and bio sensing can be found in [13] and [14].

SAW gas sensors generally employ Rayleigh wave devices because their out of plain motion produces excellent sensitivity to surface mass loading. An electrical signal is converted into an acoustic wave with an interdigital transducer (IDT) due to the piezoelectric effect. The wave travels along the surface of the crystal with a velocity five orders of magnitude slower than the electromagnetic wave. It is transformed back into an electrical signal by using the inverse piezoelectric effect. The frequency of the Rayleigh wave is determined by the separation of the IDT fingers. An introduction to design considerations of SAW devices is given by Datta [6]. For gas sensing applications the finger width is often equal to the spacing. Assuming two IDT fingers with alternating charge and the spaces of equal size the finger width will be $\lambda/4$. Typical IDT metallisations have thicknesses of around 100nm and use gold, gold on chromium or aluminium.

Apart from the width of the IDT fingers the number of finger pairs (N) and the aperture (length of overlap of the finger pairs) are crucial parameters for the device performance. The bandwidth becomes narrower with increasing N.

However, in practice if N>100 the losses associated with mass loading of the IDT's and scattering overrule the advantages. The input impedance of the transducers should be matched to the impedances of peripheral devices. Transducer layout and design is not a straight forward procedure and is often done by computational design systems. A number of tested designs suitable for sensing applications is given by Ballantine [3].

A more recent review on the various kinds of acoustic wave mass sensors is given by Ali [15]. The report includes SAW and QCM devices for gas and liquid sensing with regards to their implementation into sensor arrays.

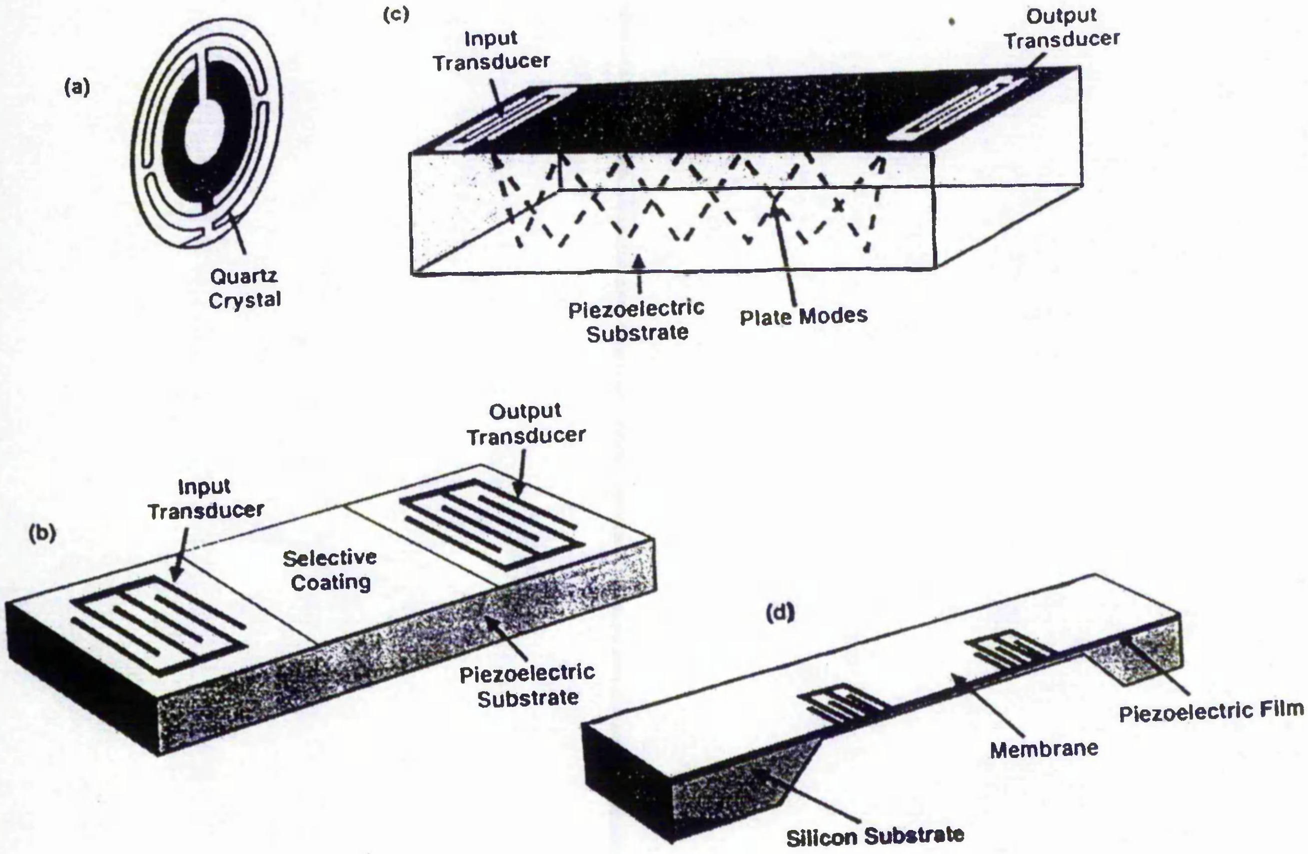

Figure 2.1: Schematic diagrams of the four types of acoustic wave sensors. (a) TSM resonator; (b) SAW sensor; (c) APM sensor; (d) FPW sensor [25]

2.2. SAW Gas Sensors

Surface acoustic wave devices have been studied for their use as high-Q filters and delay lines in signal processing [12]. Other applications of SAW devices include temperature [16] and pressure sensors [17], touch screens [18], monitoring of paper quality and the investigation of properties of viscoelastic films [19, 20].

SAW gas sensors normally operate with a chemically sensitive interface (thin film) applied to the delay path between the two transducers. If an analyte adsorbs on the film the properties of the film such as mass loading and electrical conductivity (chemiresistivity) will change and may alter velocity and amplitude of the surface acoustic wave. In most gas sensing applications a second, uncoated delay line adjacent to the coated SAW path may serve as reference for environmental corrections such as temperature drift. Since SAW delay lines are very sensitive to a number of changes in physical properties such as temperature, pressure, dielectric constant, mass loading, shear stiffness and modulus of the overlayer, subtraction of the reference signal helps to rule out unwanted perturbations, at least to a first approximation [21]. The suppression of unwanted signals due to temperature fluctuations can also be achieved by using temperature stable substrates [22].

Sorption of molecules in the overlayer may change the electrical film conductivity and mass loading. Several groups have investigated sensing techniques based on conductivity changes of a chemiresistive overlayer [23] as well as a mixture of conductivity and mass loading perturbations [24] which can be obtained by measuring the SAW frequency and amplitude. Martin *et al* studied changes in the viscoelastic properties of polymer films upon exposure to solvent vapours

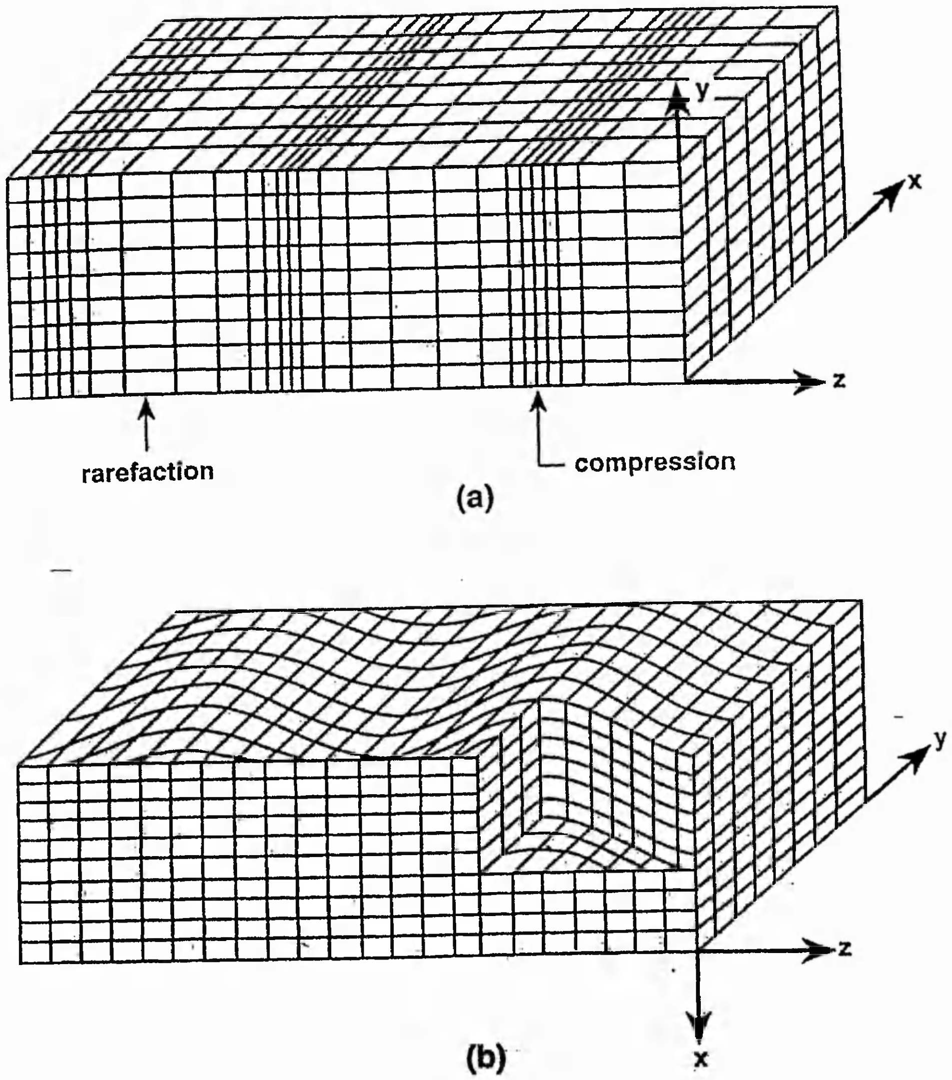

Figure 2.2 : Rayleigh wave propagating in a solid, (a) surface-parallel and (b) surface-normal component [3]

[25]. Using a plot of frequency shift versus attenuation they obtained graphs with a distinctive pattern for each of the solvents.

Although some groups have focused their work on physical sensing mechanisms, the majority of the researchers in this field have concentrated on the investigation of chemical interactions between sensing material and analyte. Their work can be split up into two types: the sensing of volatile compounds/organic vapours and the detection of gases.

2.2.1. Organic Vapours and Volatile Compounds

The detection of odours, organic vapours and volatiles is a challenging task for the sensing technology. A complete selectivity of the films cannot be achieved since many compounds have similar properties which causes cross-sensitivities between different films and analytes. A careful selection and investigation of the sensitising layers applied to the SAW sensors is therefore necessary. Surface acoustic wave devices with their excellent sensitivity to changes in surface mass loading and viscoelastic properties provide the means for the detection of these changes due to gaseous materials.

McGill *et al.* [26] provide a fundamental description of the physical mechanisms of organic vapour sensing for sensitising layers. Models together with the experimental verification for frequency changes of the SAW signal due to adsorption and absorption on polymer interfaces are discussed in their work. Grate *et al.* [27] also investigated sorption mechanisms on fullerene films and correctly predicted relative vapour sensitivities using a linear solvation energy relationship.

Enguang *et al.* [28] studied the performances of a number of different organic films, such as cast and Laingmuir-Blodgett (LB) films, in combination with two-port SAW resonators. It was suggested that the film application and the amount of overlayer material should be controlled prudently in order to avoid spurious signals. LB films were found to have shorter medium term stability than cast organic films.

Ricco *et al.* [29] applied different polymer coatings to a sensor array and employed pattern recognition to distinguish between the responses of the array to different vapours. They stated that the system was able to determine a large number of different analytes and their concentration with a minimum accuracy of 92% within their experimental limits.

Thick films of copper phthalocyanine (CuPc) were used as a sensing interface by Urbanczyk *et al* [30] to study various organic compound vapours. A large area of sensitising layer was shown to maximise the response. They used a metallised reference path to short circuit the electrical field associated with the surface wave regardless of the condensation level of the vapour to avoid degradation of the signal. The best sensitivity was obtained from Trichloroethylene with approximately 0.1Hz/ppm and response times of several minutes.

One of the first industrial applications for vapour detection using SAW technology is reported by Wessa *et al.* [31]. Their system consisted of nine SAW delay lines and a neural network/pattern recognition system. With this configuration it was possible to determine the concentrations of industrial vapours and vapour mixtures in the solvent mixer of a HPLC-system.

SAW technology is, of course, not only suitable for the detection of volatile compounds but also to detect gases. The next section provides an overview of the research that has been carried out in this field.

2.2.2. Gas Detection

A large emphasis has been put on the detection of gases with industrial and environmental importance. Many groups have investigated different overlayer materials such as metal oxides, organic semiconducters, polymers, pure metal films and even a plain surface as gas sensitive interfaces in combination with the SAW technology. The following examples illustrate the great variety of work that has been done in the field of gas sensitive films for surface acoustic wave devices.

In the field of organic semiconductors Ricco *et al.* [21] used a lead phthalocyanine (PbPc) coated SAW device for the detection of NO_2 in N_2. The sensor response was based on changes in the conductivity of the chemiresistive overlayer. It was calculated that the contribution to the sensor response due to the conductivity change of the overlayer exceeds the mass loading contribution by four orders of magnitude for their system.

On the basis of Ricco *et al's* model [21] Rügemer and co-workers [32] developed a surface acoustic wave based detection system for a CuPc sensitising layer using attenuation of the SAW amplitude as the measured quantity, as attenuation measurements provide a higher temperature stability. By measuring the electrical conductivity through attenuation the IDT's have no direct contact with the film. It therefore reduces problems such as drift and nonlinear current/voltage characteristics associated with the interaction of film and electrodes as encountered in common conductivity based gas sensing devices (chemiresistors). Their system was tested in the field as environmental NO_x monitor. The results over a 24 hour period showed good agreement with a commercial chemoluminescence monitoring system.

Rebiere *et al.* [33] studied the influence of humidity for SAW based NO_2 sensors with copper phthalocyanine as sensitising layer. Changing concentrations of water vapour were found to have only a slight effect on the sensitivity of the sensor, but caused a significant decrease in response time.

Anisimkin and co-workers [34] investigated the use of Pd based sensors for the detection of NO_2. Two different sorts of overlayers were investigated: annealed and non-annealed thin films. Changes in mass loading and elastic modulus were tested and allowed an independent analysis of surface and bulk phenomena. For certain conditions the annealed and non-annealed films were founds to give responses with a positive frequency shift. A positive frequency shift upon exposure to gases such as carbon dioxide, methane and ethane using ultra thin PDMS films was also reported by Ahuja *et al.* [35]. They believe that at high frequencies the change in modulus of the polymer film becomes significant and may overrule the changes due to mass loading. This was especially found for penetrant gases with a low solubility.

Lee *et al.* [36] proposed a SO_2 sensor with a very short recovery time. Cadmium sulphide (CdS) served as overlayer material. CdS was found to give more satisfactory results upon SO_2 exposure than previously investigated materials such as triethanolamine (TEA), diethanolamine (DEA) and tungsten trioxide (WO_3). Their system was capable of measuring concentrations of less than 200ppm of SO_2 in air. WO_3 was employed by Galipeau *et al.* [37] for the detection of H_2S. Their sensor response was mainly dependent on changes in sheet conductivity. The use of 27° rotated Y-cut temperature compensated quartz substrates seems to provide enhanced signal stability. At 40% relative humidity the detection limit was at around 1ppm of H_2S in air in their experiments.

Molecular sieves such as Zeolite applied to surface acoustic wave devices have been the subject of study for Shul'ga *et al* [38]. Their films showed a very good sensitivity towards small concentrations of ammonia even at high relative humidities of the ambient air.

Penza *et al.* [39] used LB polypyrrole films as sensitising layer for the monitoring of NH_3 gas and reported good selectivity of these films with a detection limit of approximately 46ppm. Their sensors responded well to NH_3 up to relative humidities of 40%.

A novel approach to the application of SAW based gas sensors was introduced by Hoyt an co-workers [40]. In a dual delay line configuration, both SAW paths were coated with different sensitising layers. Instead of the common differential method, a 'region of influence pattern recognition' method was applied. A robust quantification of CO_2 at low relative humidity was achieved with their system.

An automated SAW sensor testing system as a transition from laboratory to industrial applications was proposed by Nieuwenhuizen *et al.* [41]. It allowed a flexible, but reliable testing of sensor performance for a wide range of gases and vapours. Amongst other overlayer materials and analytes their work presents results for the testing of a CuPc based SAW device as NO_2 sensor.

Temperature stability is one of the main problems in SAW gas sensing. Hechner and Wrobel [42] investigated the influence of the crystalline structure of CuPc on the temperature stability of SAW gas sensors. They concluded that the implementation of a reference delay line for compensation of ambient temperature variations should be used with great caution since it compensates fluctuations only in the first approximation. It was found that a β-CuPc layer provides several times better temperature stability of the delay line than an α-CuPc layer of the same thickness.

A review of the field of sensitising layers for SAW devices together with the different approaches for selectivity is given by Ricco *et al.* [43]. SAW gas sensor research groups however, not only focussed on the interaction of the chemically active interface with the test gas but also on physical mechanisms underlying these processes in order to improve the sensor performance as described in the following section.

2.2.3. SAW Device Designs for Gas Sensing

In addition to the improvement of SAW delay lines and filters which has been intensively investigated [6,12] some work has also been reported on improving the performance of SAW gas sensors by introducing novel device designs that may exploit less obvious mechanisms of the SAW technology.

A two-port SAW resonator as gas sensor was reported by Bowers *et al.* [44]. Reflectors on both sides of the delay line were employed to generate a standing wave between the transducers with very narrow bandwidth. They suggested that the advantage of this configuration lies in its higher stability compared to conventional delay lines.

Becker and co-workers [45] proposed the use of a multistrip coupler [6] in the delay path. They pointed out that this configuration might be useful for SAW sensors with chemiresistive overlayers. For a CoPc overlayer exposed to NO_2 a sub-ppm sensitivity as well as high temperature stability was reported by measuring the attenuation of the SAW amplitude.

An improvement in device sensitivity employing a SAW device with a fundamental frequency as high as 1GHz was reported by Dickert *et al.* [46]. A higher device sensitivity proportional to f^2 was observed whereas the noise level only increased linearly. In their work they used the common differential delay line design.

Anisimkin *et al.* [47,48] showed that the response upon gas exposure of SAW devices can be increased, speeded up, cancelled and selected for a given selective layer by changing the substrate material and orientation. It was stated that SAW devices unlike other chemical sensors respond to a test gas in accordance not only with the properties of the sorbent film but with those of the substrate material as well.

Kryshtal *et al.* [49] proposed an electronically tuneable surface acoustic wave chemosensor. A metallic waveguide is placed on the substrate surface. Two electrodes are applied on either side of the waveguide with a voltage applied between them. This configuration gives rise to local perturbations of the substrate properties around the waveguide and leads to a selective response of the sensor. Experiments without using a sorbent layer showed a selective response for different alcohol vapours.

Another no-sorbent-layer approach was proposed by Penza *et al.* [50] to provide an efficient solution for the open questions of ageing and stability of SAW sensors. A selective response was achieved by exploiting the physical effects of gas flow rate and thermal conductivity. Gases could be detected over a wide concentration range and a detection of inert gases such as CH_4 was possible. A theoretical analysis of these kind of sensors would be of interest since it could expand the range of applications.

In an enclosed monitoring environment it can be a difficult task to provide stable and non-interfering electrical connections to peripheral devices due to the often hostile conditions. Therefore, some groups have worked on the use of wireless

SAW applications as sensors which work as passive radio requestable devices. Consisting only of substrate with metallisation these devices can withstand temperatures of more than 1000°C, a high rate of radiation, and powerful electromagnetic interference. However, because of the wireless configuration the implementation of these devices meets additional challenges. Pohl *et al.* [51] describe a radio requestable sensor for ultrafast measurements of light, pressure and temperature with the potential for the use as gas detector. If the reflecting transducer is connected to a conductivity sensor, the system can be used as a passive remote controlled chemiresistor.

Modern computer technology enables researchers to advance their work towards more complex systems which can be implemented by the use of sophisticated algorithms. These methods play an important role for the progress of sensing systems. Some of its examples will be described next.

2.3. Chemical Selectivity using Pattern Recognition

Chemical selectivity is a requirement for most sensor applications since

a) chemiresistive overlayers are normally cross-sensitive to a number of different analytes and
b) interfering gases may be present in the tested environment.

In order to specify the tested analyte a sensor array with a number of different sensitising layers may be used. Each layer should respond in a different way to a certain substance whilst responding to a range of analytes. The resulting signals produce a unique pattern “finger print” that can be recognised by the computer after a learning process.

Early work by Ballantine *et al.* [52] applied pattern recognition to investigate the physical and chemical mechanisms of vapour/coating interaction. Chuang *et al.* [53] used a neural network with backpropagation algorithm together with an array of three SAW sensors. This array was compared with the equivalent system using TSM AT-cut quartz crystals. It was empirically found that the learning speed of the array was twice as high for the SAW sensors than for the TSM devices.

Pattern recognition techniques have been applied to a whole range of solid state gas sensor types. Hong and co-workers [54] built a sensor array based on four conductivity sensors. A minimum recognition probability of 80% for each of the twelve tested analytes was realised.

An array of TSM sensors was applied by Deng *et al.* [55] to demonstrate the feasibility of determining fish freshness by the odors they produced. Although a higher number of devices was applied it was suggested that an array of four sensors would be sufficient to recognise a large variety of substances.

Ricco *et al.* [29] presented a study of SAW sensor arrays confirming Deng's [55] statement that four sensors with chemically independent interfaces provide satisfactory results for a large number of analytes. Maximum chemical independence is often provided by films from very different material families. It can be important to choose array elements carefully to minimise the identification errors. Visually empirical region of influence pattern recognition (VERI) was employed to determine a large number of analytes as well as their concentrations [39].

An array of two pellistors (microcalorimetic sensors) was used as sensing elements for the recognition of methane and butane by Sommer *et al.* [56]. In their experiments they determined the concentrations of the two combustibles by neural networks with a maximum error of 10% and 4% respectively.

As previously stated, SAW sensors are sensitive to changes in film properties such as conductivity, mass loading, viscoelasticity, dielectric constant etc. Combining the conductivity and mass loading responses of the sensor with a pattern recognition system Kungi *et al.* [57] reported a reasonable distinction between different organic vapours.

A novel approach to the problem of sensor arrays proposed by Anisimkin *et al.* employs a single overlayer with four delay lines placed around it. Due to the different propagation directions of the SAW's on the quartz substrate different modes are generated. Applying pattern recognition techniques a distinct response for each of the tested analytes was obtained. Ageing and instabilities seem to be better controllable since there is only one overlayer material used [11].

The examples presented above show the variety of applications and the range of possibilities for further research in the field of gas detection. However, one group of materials, phthalocyanines, has been studied particularly intesive because it holds the promise of good response towards the detection of oxidising and reducing agents. This group of organic semiconductors is described in the next section.

2.4. Phthalocyanines

In 1933 Linstead reported a substance consisting of pyrrole units linked in a circular manner by methine and azamethine bridges and called them phthalocyanines [58]. However, Pc's were probably first discovered in 1907 by Braun and Tscherniak [59] as by-product of O-cyanobezamide.

Phthalocyanines are versatile substances with a wide range of applications. Conventional dyes, catalysis, coatings for CD-ROM's, cancer agents and possible photoconductive devices are some of many applications for this group of organic materials [60,61,62]. Good overviews of the Pc's available today and the methods of synthesis of many of them are given by Leznoff and Lever [63], Moser and Thomas [64] and McKeown [65].

2.4.1. Structure of Phthalocyanines

Most of the work which was carried out in this field investigates the properties of mono-phthalocyanines such as CuPc. However, other structures exist such as the non-planar di-phthalocyanines and the bis-phthalocyanines where a metal atom is sandwiched between two Pc macrocycles [66].

In planar mono-Pc's ($C_{32}H_{18}N_8$) atoms are arranged as four benzene rings connected via hydrogen and nitrogen. In metal substituted Pc's (MPc's) a di-valent metal atom straddles at the centre of the molecule taking the place of two hydrogens (Figure 2.3). Most of the MPc's are planar. However, if the central atom is too large to be contained inside the ring structure it will extend out of the plane of the ring. A distinction is made between molecules which are symmetrical with respect to the Pc plane and molecules that are not symmetrical. These substances are regarded as type 1 and type 2 respectively [67].

The molecular arrangement is very important since many physical and chemical properties strongly depend on it. Pc's appear in a number of different morphologies although mainly the properties of the α and β phase have been investigated. The constitution of the two phases differs only in their stacking angle e.g. 26.5° and 45.8° for α-CuPc and β-CuPc respectively [66].

2.4.2. Phthalocyanine Films

Different types of Pc films are used for gas sensing applications e.g. vacuum sublimed, Langmuir Blodgett, spin coated and screen printed films. Vacuum sublimation can be used for Pc's because of their high thermal stability. This method is preferable if very clean films are required. In combination with entrainer sublimation a contamination figure of 1 in 10^5 is attainable. This is still high compared with single crystals of Ge or Si with an impurity concentration of 1 in 10^{12} [66] being used in commercial semiconductor devices. Films of α-phase are produced when the substrate material is held below 150°C during the evaporation. If the substrate is heated above this temperature, or if it is subject to post deposition annealing, a β-phase can be formed the latter being independent of the phase of the material before deposition. If the evaporation takes place at high rate (e.g. 5nm/s) on a substrate with room temperature the film can be regarded as amorphous [68].

The Langmuir-Blodgett technique offers the advantage of producing highly uniform films of single-monolayer thickness. Peripherally or axially substituted Pc's are dissolved in a non-polar solvent. This solution is spread onto a water surface in a LB-trough. After the solvent has evaporated two bars are used to slowly compress the molecules on the surface until a monolayer is formed. The substrate is then lifted vertically out of the water with the monolayer sticking to the substrate. Multilayers can be formed by repeating this procedure [69].

Pc films can also be applied by spin coating. Because of its convenience this technique has received increasing attention by many groups. Substituted Pc's are dissolved in an appropriate solution (e.g. $CHCl_3$) and spun onto a pre-prepared substrate. After the solvent has evaporated a thin Pc-film remains [70].

Thick films of PbPc have been applied by screen printing technique and compared to conventional thermally evaporated films by Cranny et al. [71]. The overall properties of these films are comparable to their thermally evaporated counterparts. However, screen printed films are far more conducive to volume manufacturing because of their quicker, easier, and cheaper production.

2.4.3. Electrical Conduction in Phthalocyanines

The conductivity of solid state materials can be divided into three classes: insulators, semiconductors and conductors. Conductors have high conductivities (10^4 to 10^6 mho/cm) whereas insulators have low conductivities (10^{-18} to 10^{-8} mho/cm). The conductivity of conventional semiconductors lies between that of conducting materials and insulators. With a conductivity close to that of insulators Pc's can be regarded as weakly semiconducting materials.

It has been suggested that at relatively low electrical fields conduction in phthalocyanines is dominated by thermally-generated charge carriers and can be approximated by a linear current - voltage relationship following Ohm's law. In this project the bias voltage for the conductivity sensors was always set to 1V in order to operate in that ohmic regime [66].

Other models exist that describe conduction at higher electrical fields i.e. higher bias voltage applied to phthalocyanines. If the concentration of charge carriers injected by the electrodes becomes greater than the concentration of thermally generated carriers space charge limited conduction (SCLC) occurs. High fields

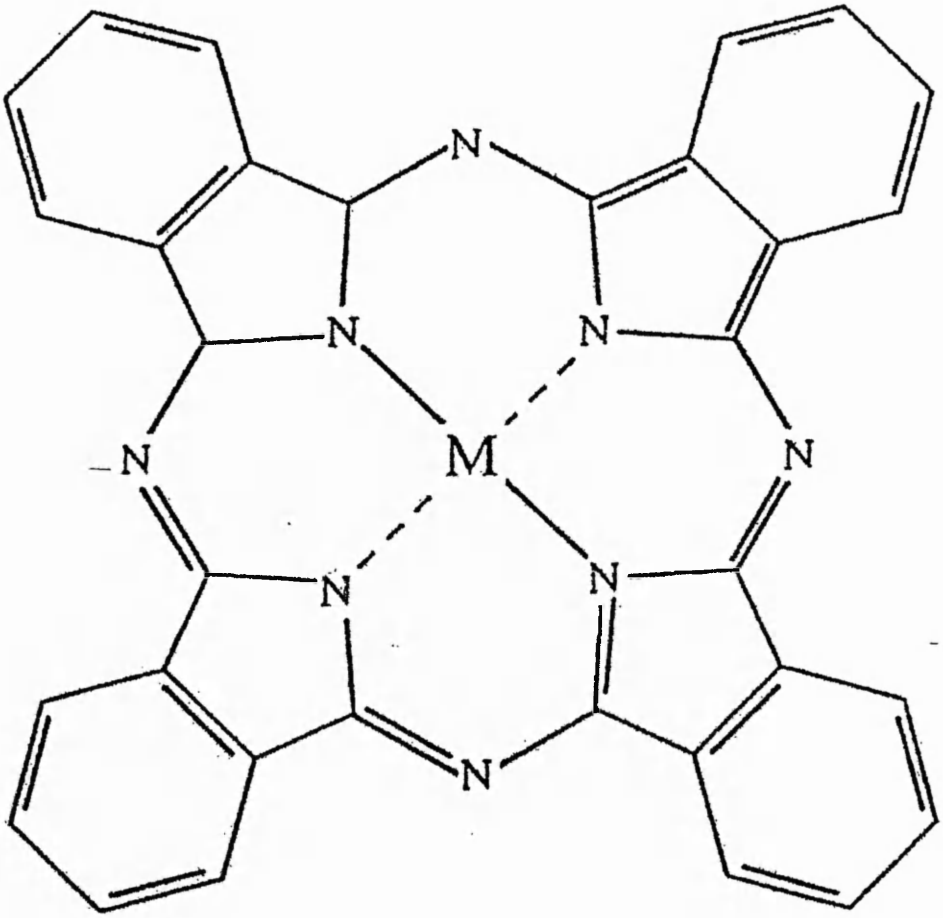

Figure 2.3: Structure of metal substituted phthalocyanine [65]

cause a SCLC current which can be described by the Child-Langmuir law $J \propto V^s$ where the power s has a value of 2. This model suggests the existence of a discrete trapping level in the forbidden band gap of the semiconductor [72]. If there exists an exponential distribution of trap levels in the band gap s was experimentally found to be greater than 2 [73].

2.4.4. Phthalocyanine Gas Sensing

Phthalocyanines are intensively studied materials with regards to gas sensor applications, however, it is still found difficult to exploit their full potential because of the complexity of the mechanisms involved. Pc's show changes in their electrical conductivity when exposed to a large range of gases such as NO_x, O_3, Cl_2, F_2, BF_3, SO_2, H_2S and HCl [74]. Gas sensing for strongly oxidising gases such as O_3 and NO_2 is realised through a charge transfer interaction in which the gas molecule to be sensed acts as a π-electron acceptor forming a redox couple. The positive charge produced is then delocalised over the Pc ring causing an increase in conductivity. Many groups have worked on different aspects of Pc gas sensors. Fields of interest include film morphologies, types of overlayers and thickness, different sensor types (SAW, TSM, FET, capacitance, conductivity), substituted Pc's (symmetrical, asymmetrical), adsorption and desorption mechanisms, transient and stationary response characteristics and many more. A review on Pc gas sensing is given by Zhou *et al.* [75]. Guillaud *et al.* [76] provide a more recent review on the conductivity based phthalocyanine gas sensors. Although many groups have worked on Pc based gas sensors commercial devices are still rare because of slow response and recovery time, drift and insufficient recovery of the signal.

Clifford and Tuma [77] carried out a very detailed investigation into the behaviour of a commercial SnO_2 gas sensor (Taguchi Gas Sensor). By applying an extensive mathematical framework it was possible to determine responses of the sensor to several test gases under widely varying conditions to a high degree of accuracy. Although the problem is somewhat more complex in the case of organic semiconductors their investigation could serve as an example for a detailed study of the viability of Pc gas sensors. The following paragraphs describe investigations into different aspects of gas detection for phthalocyanine based chemiresistors.

A gas diffusion model to describe the conductance changes in Pc Langmuir-Blodgett films was proposed Emelianov *et al.* [69]. They addressed their work to the improvement of the reversibility of Pc films operated near the room temperature region. Their two-component films of arachidic acid and copper tetra-tert-butyl Pc's showed good reversibility upon NO_2 exposure at 40°C.

Li *et al.* [70] investigated the properties of spin-coated Pc films. These films were found to have rapid response times, good recovery, and were able to detect concentrations of 1ppm NO_2 in air at room temperature. It was mentioned that illumination with laser light of 632.8nm enhanced the signal level of their devices. Further studies on soluble Pc's have been carried out by Kudo and co-workers [78]. Several Pc derivates were prepared and investigated which showed sensitivity down to the sub-ppm range and good reversibility towards the exposure to NO_2 at room temperature.

Water vapour is a strong electron donor and therefore, affects the performance of Pc gas sensors in the form of air humidity. Belghachi and Collins [79] investigated the effects of air humidity on NO_2 and NH_3 sensors. It is found that water vapour increases the performance of the sensor for donor gases such as NH_3 but overcompensates the behaviour of acceptor-like species such as NO_2.

They concluded that if their sensors are operated under atmospheric conditions at room temperature, the influence of humidity needs careful consideration.

Zhou *et al.* [80] addressed their work to the problem of oxygen doping. They pointed out that in α-CuPc the SCLC region is dominated by exponentially distributed trap levels whereas for heavily doped films this region has a discrete trap level.

DeHaan *et al.* [81] propose a very different approach to Pc-doping. It was claimed that traces of strongly oxidising gases such as NO_2 and O_3 in ambient air are the main doping agents rather than O_2. However, although a large amount of work has been done there is still conflicting evidence in this area.

Effects of crystal morphology and film thickness of PbPc were studied by Hsieh *et al.* [68]. They suggested that for electrical conductivity sensors the steady state current through the layer depends on the number of available adsorption sites in the conduction path. Therefore, amorphous films show the best response and recovery times because of higher porosity that allows faster gas diffusion. As the film becomes thicker their response speed reached a stationary value (limiting thickness). Dogo *et al.* [82] proposed an original way of identifying the crystalline phase of a phthalocyanine film by determining the temperature of maximum conductivity after exposing to NO_2, O_2 or Cl_2. It was found that several cycles of exposure were necessary to stabilise the response of their films to the gas. They suggest that this initialisation effect occurs due to the successive occupation of adsorption sites deeper and deeper into the bulk. It is claimed that for each exposure new adsorption sites inside the film can be reached by the gas molecules and made easily accessible for the next exposure.

The effect of electrode geometry on gas sensitivity of PbPc was investigated by Gardener *et al.* [83]. A model was proposed that predicts a linear relationship between film conductance and reciprocal electrode separation as well as a constant value in the steady state response. However, experimental results show that the former relationship does not increase linearly and the latter shows a gradual increase in steady state response. This suggests the presence of considerable film inhomogenities where electrical conductivity and the number of adsorption sites are significantly lower near the substrate surface than elsewhere.

Hu *et al.* [84] investigated the sensing characteristics of asymmetrical substituted Pc's exposed to NO_2. In their experiments they showed a linear relationship between log(resistance) and log(NO_2 concentration). Asymmetrically substituted Pc's have also been studied by Li *et al* [85]. Films were applied by spin coating as well as LB. They claim spin coated films are less ordered than LB films and seem to allow better gas diffusion into the bulk. The reverse process is in turn accelerated by the N_2 and O_2 molecules in the air to replace the test gas from the adsorption site resulting in a faster reversal time.

A further study by Ding *et al.* [86] of asymmetrically substituted Pc's shows that some derivates of this group applied as LB films do not lie flat on the substrate but rather subtend to a certain angle to the surface with the molecular plane of the molecules arranged cofacially. These films show a higher response current than LB films with flat lying molecules as well as a faster response time to NO_2 exposure in air.

Chloro-aluminium PC films were subject of investigation by Azim-Araghi *et al.* [87] where NO_2, Cl_2 and NH_3 were used as test gases. Being an electron donor NH_3 was found to cause the reverse effect to the film resistance than the other gases. A temperature of maximum sensitivity and a minimum temperature of good reversibility have been observed. These values could provide a characterisation of the test gas and thus better selectivity.

In conclusion, the nature of conduction and sorption mechanisms in organic semiconductors is still not fully understood and needs further investigation. However, this research could also be beneficial for other technologies which use phthalocyanine materials such as such as molecular electronics, and opto electronics [88].

2.5. Adsorption Kinetics of Gas Sensors

The gas kinetics of the response are an important factor in the investigation of gas sensors. An insight into the transient behaviour of the sensor upon gas exposure will allow a deeper understanding of the mechanisms involved in gas sensing. Consequently, this will open up a much wider basis for exploring sensor capabilities and the prediction of the sensor behaviour by mathematical models in order to optimise existing technology. A general treatment of the subject of adsorption kinetics can be found in surface chemistry books such as Adamson [89]. Many of the adsorption and desorption processes are believed to be governed by the Elovich equation. Aharoni and Tompkins [90] provide an extensive general overview of the various aspects of this model as well as examples of its application.

Langton and Day [91] studied the adsorption kinetics on FePc and found that it followed the Elovich adsorption model. Wright *et al.* [92] extended this work further to the kinetics of CuPc's. Archer *et al.* [93] studied kinetic factors in the response of organometallic semiconductor gas sensors with emphasis on oxygen adsorption and its replacement by a test gas such as NO_2. It was suggested that for a single crystal with a guarded earth ring applied there was no presence of gas absorption into the lattice. This implied, all conduction phenomena related Pc gas sensing may be attributed to currents on the crystal surface or at the grain boundaries. If the layer is exposed to NO_2 the gas is in strong competition with the pre-adsorbed oxygen which will be most easily replaced from the weak adsorption sites. Subsequently, lateral repulsions between the two species facilitate the displacement of the more strongly-bound oxygen.

Zhou *et al.* [94] studied the transient response behaviour of MPc films exposed to NO_2. Two minute exposures could be described by the Elovich adsorption model. Different levels of concentrations were found to have corresponding slopes of the Elovich plot. The method has the advantage that no steady state needs to be determined. Since the exposure time can be kept short there will only be a small amount of test gas adsorbed on the surface which in turn allows for a much quicker recovery of the system. Fedoruk *et al.* [95] investigated the kinetic response of CuPc and CuPc-polymer materials. From the Elovich plot they suggested a two-stage response process which they attributed to either different sorption processes on the surface or in the bulk or two types of sorption centres.

Based on the Langmuir adsorption model Liu *et al.* [96] proposed a surface adsorption/desorption model to describe the behaviour of NO_2 sensing for PbPc thin films and obtained an expression for the change in film current ΔI. The activation energies for adsorption and desorption could be extracted from the experimental data. Then, the model was extended by same group their taking into account bulk diffusion of NO_2 described by Fick's law [97]. From their study they concluded that the adsorption of nitrogen dioxide by lead phthalocyanine was controlled by the surface adsorption and desorption with negligible diffusion resistance.

2.6. Summary

Gas sensitive properties of phthalocyanines have received great attention from many researchers for their outstanding capability to respond to a variety of gases. However, despite extensive investigation there are still many problems to resolve in order to improve their gas sensing properties.The main issues for further research in this field are:

- Faster response to gas exposure and faster recovery
- Better reversibility of the signal
- Reduction of drift in sensitivity
- Better selectivity

Literature suggests that a sensor array needs a minimum number of four overlayer materials with different response characteristics to obtain sufficient selectivity to different analytes. Alternatively to overlayer materials from different chemical groups, a single core material could be used, which received different surface treatments and thus show different response characteristics. Additionally, a range of different sensing devices could be employed in combination with these films in order to provide additional information about the film - analyte interaction.

In this project copper phthalocyanine was chosen as gas sensitive overlayer material because of its easy availability at low cost, its non-toxic properties and its easy application by vacuum sublimation. NO_2 was used as test gas because of the well established response when exposed to CuPc and its great environmental importance. Sensor response was obtained from measuring the electrical conductivity of the Pc film but also from the response of acoustic wave devices.

The next chapter will provide the theoretical background of the work performed in this project.

References

[1] P.T.Moseley, Meas. Sci. Technol., (1997), 223

[2] G.C.Fox , J.F.Adler, Techniques and Mechanisms in Gas Sensing, Bristol: Hilger, (1991)

[3] D.S.Ballantine, R.M.White, S.J.Martin, A.J.Ricco, E.T.Zellers, G.C.Freye , H.Wohltjen, Acoustic Wave Sensors: Theory, Design, Physio-Chemical Applications, Academic Press, (1997)

[4] G.Sauerbrey, Z.Phys.**155**, (1959), 206

[5] A.W.Warner, C.D.Stockbridge, Symp. on Vac. Microbal. Tech., LA, Calif, (1962), 511

[6] S.Datta, Surface Acoustic Wave Devices, Prentice Hall, New Jersey, (1986), 40

[7] R.M.White, F.W.Voltmer, Appl. Phys. Lett., **7**,(1965), 314

[8] J.W.Grate, S.J.Martin, R.M.White, Anal.Chem., **65**, No.21, (1993), 940

[9] R.M.White, Proc.IEEE, **58**, No.8, (1970), 1238

[10] J.G.Gualtieri, IEEE Transact.Ultrason.Ferroel.Frequ.Contr., **41**, No.1, (1994), 53

[11] V.I.Anisimkin, R.G.Krystal, A.V.Medved, E.Verona, V.E.Zemlyakov, Electr.Letters, **34**, No.13, (1998), 1360

[12] A.A.Oliner, Acoustic Surface Waves, Springer-Verlag, New York, (1978), Chapter 2

[13] E.Gizeli, N.J.Goddard, C.R.Lowe, Sens.Actu.B, (1992), 293

[14] R.M.White, P.J.Wicher, S.W.Wenzel, E.T.Zellers, IEEE Transact.Ultrason.Ferroel.Frequ.Contr., **34**, (1987), 162

[15] Z.Ali, J.Therm.Anal.Calor., **55**, (1999), 371

[16] S.J.Martin, A.J.Ricco, Sens.Actu., **A21-A23**, (1990), 712

[17] G.McHale, M.I.Newton, M.K.Banerjee, S.M.Rowan, Faraday Disc. **107**, (1997), 107/2

[18] SAW-based touch screens, http://www.norteng.com

[19] H.Submaranian, V.K.Varadan, V.V.Varadan, M.J.Vellekoop, Smart Mat.Struct., **6**, (1997), 730

[20] F.Möller, J.Kuhn, Sens.Actu., **A30**, (1992), 73

[21] A.J.Ricco, S.J.Martin, Thin Solid Films, **206**, (1991), 94

[22] J.J.Caron, R.B.Haskell, J.C.Andle, J.F.Vetelino, Sens.Actu, **B35**, (1996), 141

[23] Z.P.Khlebarow, A.I.Stoyanova, D.I.Teplova, Sens.Actu., **B8**, (1992), 33

[24] A.J.Ricco, S.J.Martin, T.E.Zipperian, Sens.Actu., **8**, (1985), 319

[25] S.J.Martin, G.C.Frye, Appl.Phys.Lett., **57**, No.18, (1990), 1867

[26] A.McGill, J.W.Grate, M.R.Anderson, Interfacial Design and Chemical Sensing, Amer.Chem.Soc., (1994), Chapt.24,

[27] J.W.Grate, M.H.Abraham, C.M.Du, R.A.McGill,W.J.Shuely, Laingmuir, **11**, (1995), 2125

[28] D.Enguang, F.Guannping, H.Zenhua, C.Dafu, IEEE Transact.Ultrason.Ferroel.Frequ.Contr., **44**, No.2, (1997), 309

[29] A.J.Ricco, R.M.Crooks, G.C.Osbourne, Act.Chem.Res, **31**, (1998), 289

[30] M.Urbanczyk, W.Jakubik, S.Kochowski, Sens.Actu., **B22**, (1993), 133

[31] T.Wessa, S.Küppers, M.Rapp, J.Reibel, U.Stahl, Fresenius J.Anal.Chem., **363**, (1999), 744

[32] A.Rügemer, S.Reiss, A.Geyer, M.v.Schickfuss, S.Hunklinger, Sens.Actu., **B56**, (1999), 45

[33] D.Rebiere, G.Duchamp, J.Pistre, M.Hommady, D.Hauden, R.Planade, Sens.Actu., **B13-14**, (1993), 642

[34] V.I.Anisimkin, I.M.Kotelyanskii, V.I.Fedosov, C.Caliendo, P.Verardi, E.Verona, IEEE Ultrason.Symp., (1996), 293

[35] A.Ahuja, D.L.James, R.Narayan, Sens.Actu., **72**, (1999),234

[36] Y.J.Lee, H.B.Kim, Y.R.Roh, H.M.Cho, S.Baik, Sens.Actu., **A64**, (1998), 173

---

[37] J.D.Galipeau, L.J.LeGore, K.Snow, J.J.Caron, J.F.Vetelino, J.C.Andle, Sens.Act., **B35-36**, (1996), 159

[38] A.A.Shul'ga, B.K.Zuev, V.V.Lontsov, J.Anal.Chem., **54**, No.5, (1999), 513

[39] M.Penza, E.Millela, V.I.Anisimkin, Sens.Actu., **B47**, (1998), 218

[40] A.E.Hoyt, A.J.Ricco, M.Bartolomew, G.C.Osbourn, Anal.Chem., **70**, (1998), 2137

[41] M.S.Nieuwenhuizen, J.L.N.Harteveld, Sens.Actu., **A44**, (1994), 219

[42] J.Hechner, T.Wrobel, IEEE Symp., **543**, (1995), 543

[43] A.J.Ricco, R.M.Crooks, C.Xu, R.E.Allred, Interfacial Design and Chemical Sensing, Amer.Chem.Soc., (1994), Chapt.23

[44] W.D.Bowers, R.L.Chuang, T.M.Duong, Rev.Sci.Instr., **62**, No.6, (1991), 1624

[45] H.Becker, C.Rupp, M.v.Schickfuss, S.Hucklinger, IEEE Transact.Ultrason.Ferroel.Frequ.Contr., **43**, No.4, (1996), 527

[46] F.L.Dickert, P.Forth, W.E.Fischerauer, U.Knauer, Sens.Actu., **B46**, (1998), 120

[47] V.I.Anisimkin, I.M.Kotelanskii, V.I.Fedosov, IEEE Ultrason.Symp., (1995), 515

[48] V.I.Anisimkin, E.Verona, IEEE Transact.Ultrason.Ferroel.Frequ.Contr., **45**, No.5, (1998), 1347

[49] R.G.Kryshtal, A.V.Medved, V.V.Shemet, V.E.Zemlyakov, Electronics Letters, **35**, No.8, (1999),676

[50] M.Penza, V.I.Anisimkin, L.Vasanelli, IEEE Transact.Ultrason.Ferroel.Frequ.Contr., **43**, No.2, (1996), 218

[51] A.Pohl, R.Steindl, L.Reindl, IEEE Transact.Ultrason.Ferroel.Frequ.Contr., **46**, No.4, (1999), 1728

[52] D.S.Ballantine, S.L.Rose, J.W.Grate, H.Wohltjen, Anal.Chem., **58**, (1986), 3058

[53] S.M.Chuang, H.Maramatsu, I.Karube, Sens.Mater., **7**, No.1, (1995), 13

[54] H.K.Hong , W.S.Shin, H.S.Park, D.H.Yun, C.H.Kwon, K.Lee, S.T.Kim, T.Moriizumi, Sens.Actu., **B33**, (1996), 68

[55] Z.Deng, D.C.Stone, M.Thompson, Analyst, **121**, (1996), 671

[56] V.Sommer, P.Tobias, D.Kohl, Sens. Actu. **B12**, (1993), 147

[57] Y.Kungi, K.Nigorikawa, Y.Harima, K.Yamashita, J.Chem.Soc., Chem.Comm., (1994), 873

[58] R.P.Linstead, Rep.Brit.Adv.Sci., **465**, 1933

[59] A.Braun, J.Tscherniac, Ann.Ber. **40**, (1907), 2709

[60] Nandini Institute of Chem. Ind., Copper Phtalocyanine blue, http://www.sourceindia.com/nandini/copper.htm

[61] T.Aola, K.Namba, IEEE Tokio Section, Donshi Tokyo, **31**, (1992), 231

[62] G.McHale, M.I.Newton, P.D.Hooper, M.R.Willis, Opt.Mat., **6**, (1996), 98

[63] C.C.Leznoff, C.Clifford, A.B.P.Lever, Phthalocyanines: Properties and applications, New York, Weinheim : VCH, (1989)

[64] F.H.Moser, A.L.Thomas, The Phtalocyanines, Vol. I and II, CRC Press, Florida, (1983)

[65] Neil B McKeown, Phthalocyanine Materials Synthesis Structure and Function, Chemistry of Solid State Materials 6, (1998)

[66] T.Parr, An Investigation into the Structural, Optical and Electrical Properties of Phtalocyanines with Regard to their Feasibility as Commercial Gas Sensors, PhD-thesis, Univ. of Lancaster, (1995), 19

[67] M.K.Engel, Report Kawamura, Inst.Chem.Res., (1997), 11

[68] J.C.Hsieh, C.J.Lu, Y.H.Ju, Thin Solid Films, **322**, (1998), 98

[69] I.Emilianov, V.Khatko, A.Tomochenko, Sens.Actu., **B47**, (1998), 158

[70] X.Li, S.Shen, Q.Zhou, D.Jiang, A.Lu, Thin Solid Films, **324**, (1998), 274

[71] A.W.J.Cranny, J.K.Atkinson, P.M.Burr, D.Mack, Sens.Actu., **B4**, (1991), 115

[72] M.A.Lampert, A.Rose, R.W.Smith, Phys.Chem.Solids, **8**, (1959), 464
[73] Q.Zhou, R.D.Gould, Thin Solid Films, **317**, (1998), 432
[74] T.A.Jones, B.Bott, Sens.Actu., **303**, (1986), 11
[75] R.Zhou, F.Josse, W.Gölpel, Z.Z.Ötztürk, Ö.Bekaroglu, Appl.Organomet.Chem., **10**, (1996), 557
[76] G.Guillaud, J.Simon, J.P.Germain, Coord.Chem.Rev., **178**, (1998), 1433
[77] P.K.Clifford, D.T.Tuma, Sens.Actu., **3**, (1983),233
[78] T.Kudo, M.Kimura, K.Hanabusa, H.Shirai, T.Sakaguchi, J.Porph.Phthal., **3**, (1999), 6995
[79] A.Belghachi, R.A.Collins, J.Phys.D, **23**, (1990), 223
[80] G.Zhou, R.Gould, Thin Solid Films, **317**, (1998), 432
[81] A.DeHaan, M.Debliquy, A.Decroly, Chem.Sens., **I**, (1998), 183
[82] S.Dogo, J.-P.Germain, C.Maleysson, A.Pauly, Thin Solid Films, **219**, (1992), 257
[83] J.W.Gardener, M.Z.Iskandarani, B.Bott, Sens.Actu., **B9**, (1992), 133
[84] W.Hu, S.Liu, D.Zhu, Thin solid films, **324**, (1998), 285
[85] X.Li, H.Xu, Q.Zhou, D.Jiang, L.Zang, A.Lu, Thin Solid Films, **324**, (1998), 277
[86] X.Ding, S.Shen, Q.Zhou, H.Xu, Dyes and Pigments, **40**, (1999), 187
[87] M.E.Azim-Araghi, A.Krier, Appl.Surf.Sci., **119**, (1997), 260
[88] Y.G.Krieger, J.Struct.Chem., **34**, No.6, (1993), 896
[89] A.W.Adamson, Physical Chemistry of Surfaces, J.Wiley and Sons Inc., USA (1990)
[90] C.Aharoni, F.C.Tompkins, Adv.Catal., **21**, (1970), 1
[91] J.Langton, P.Day, J.Chem.Soc.,Faraday Trans., **2**, (1982), 1675
[92] J.D.Wright, A.V.Chdadwick, B.Meadows, J.J.Miasik, Mol.Cryst.Liq.Cryst., **93**, (1983), 315
[93] P.B.M.Archer, A.V.Chadwick, J.J.Miasik, M.Tamizi, J.D.Wright, Sens.Actu., **16**, (1989), 379
[94] G.Zhou, R.Gould, Thin Solid Films, **317**, (1998), 436
[95] G.G.Fedoruk, D.I.Sagadiak, A.V.Misevich, A.E.Pochtenny, Sens.Actu., **B9**, (1992), 133
[96] C.J.Liu, J.C.Hsieh, Y.H.Ju, J.Vac.Sci.Technol., **A14(3)**, (1996), 753
[97] Y.H.Ju, C.Hsieh, C.J.Liu, Thin Solid Films, **342**, (1999), 238

Chapter 3: Theoretical Background

This chapter presents an overview of the theoretical background required for a practical understanding of the work in this thesis. First, structure and electrical properties of Pc's are explained, which are the basis for the application of Pc based gas sensitive devices. For laser illumination of the Pc film to improve its sensing properties an understanding of the underlying photochemical processes is necessary. To investigate the process of gas adsorption on Pc layers this chapter also provides an introduction to adsorption kinetics. Finally, an overview of the field of surface acoustic wave devices for gas sensing applications is given.

3.1. Phthalocyanines

The properties of copper phthalocyanine are explained in the following section. Copper phthalocyanine was used because of its non-toxic properties, easy availability and its known response to oxidising gases.

3.1.1. Structure of Copper Phthalocyanine

Copper phthalocyanine (CuPc) is a planar molecule and regarded as a type 1 phthalocyanine because of its symmetrical structure with respect to the molecular plane. Its macrocycle usually exists as a dianion (Pc^{2-}) although it can be oxidised or reduced to different oxidation states. The copper ion (Cu^{2+}) is held so tightly that it cannot be chemically removed without the destruction of the macrocycle. CuPc is an aromatic molecule with a planar conjugated array of π-electrons [1]. The term conjugated refers to the alternation of single and double chemical bonds in the molecule and 'aromatic' denotes the delocalised electrons in the ring structure of the molecule. Figure 3.1 shows the structure of the CuPc molecule and a scanning tunneling microscope image of these molecules.

3.1.2. Conduction in Phthalocyanines

Phthalocyanine materials are known as organic semiconductors. Although their dark conductivity is very low and close to that of insulators they are called semiconductors because their conductivity increases exponentially with temperature, hence:

$$\sigma = \sigma_0 e^{\left(\frac{-\Delta E}{2kT}\right)} \tag{3.1}$$

with *ΔE* being the energy to produce an electron-hole pair, *k* the Boltzmann constant and *T* the absolute temperature.

In contrast to the strong covalent or ionic bonds in their inorganic counterparts, the bonding in organic semiconductors is mainly due to van der Waals or London forces and is therefore rather weak. In addition, this structure is not favourable for charge transport because, both the overlap of the orbitals as well as the intermolecular electron exchange are small.

Electron orbitals which overlap with those from the neighbouring atoms to form a bond are called σ-bonds. However, the remaining π-orbitals in each of the C and N atoms do not participate in any bonds. Their axes are aligned perpendicular to the molecular plane and these orbitals overlap to form a π-orbital. The charge density in the π-orbital appears in two layers stretching around the ring, one above and one below the molecular plane. The π-electrons are delocalised over all the carbon and nitrogen atoms so that they move freely inside the molecule. They form an electric current flowing around the ring with opposite directions on the both sides of the molecular plane [2].

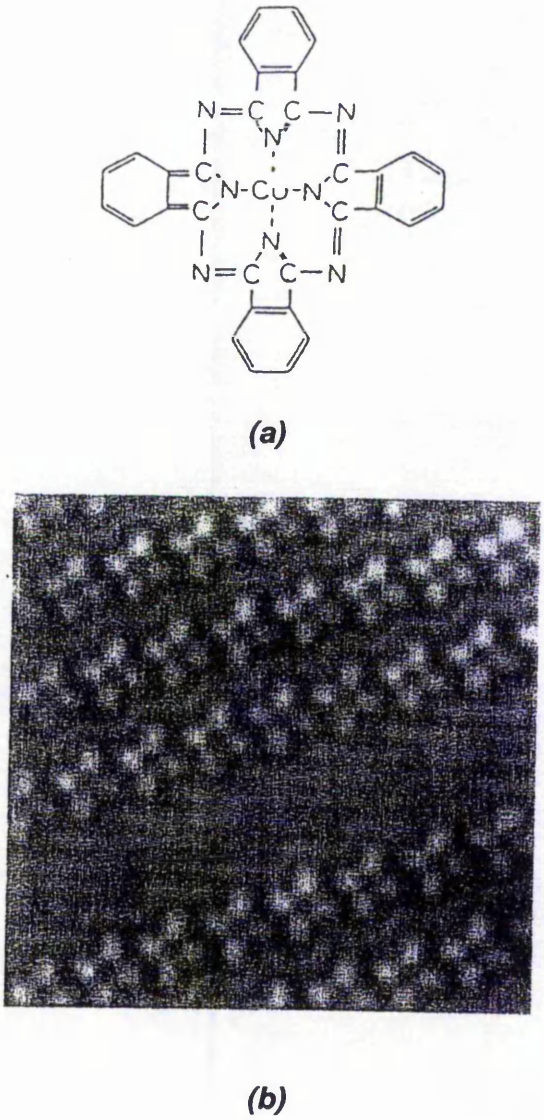

Figure 3.1:* *(a) chemical structure of CuPc [3] and (b) STM image of these molecules on a MoS_2 surface [4]

A more recent explanation for the electrical properties of Pc's by Maitrot *et al.* states that these materials are heavily doped insulators rather than semiconductors. Some of the criteria that discriminate a doped insulator from a true semiconductor would assign CuPc to the group of doped insulators. These criteria are [5]:

- it should have an intrinsic conductivity of 10^{-6} to 10^{-1} mho cm^{-1}
- it should be capable of being doped as either p or n-type.

Conduction in phthalocyanines requires the presence of mobile charge carriers. The conductivity of a material is defined as:

$$\sigma = \sum en\mu \qquad (3.2)$$

with e the electronic charge, n the density of carriers per unit volume and μ the mobility of the charge carriers [1].

When the charge carriers acquire sufficient energy to cross the energy gap between valence and conduction band they become free carriers and intrinsic conduction occurs. Extrinsic conduction, on the other hand, arises from lattice anomalies such as imperfections in the crystal structure, dopand atoms in the material or impurities [1].

If the temperature of an organic semiconductor is increased there is a point where the dominating conduction mechanism will change from extrinsic to intrinsic. That is because more and more charge carriers are thermally generated whereas the extrinsic mechanism cannot provide any more carriers. In a plot of

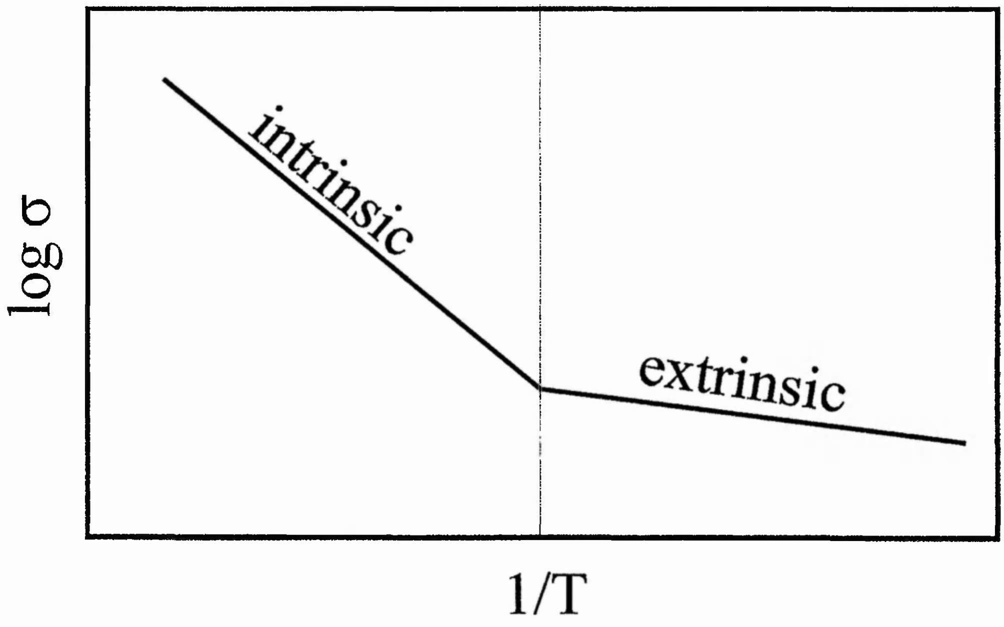

Figure 3.2: Arrhenius plot of the conductivity in an extrinsic semiconductor

1/T versus *log* σ (Arrhenius plot) this transition is reflected in a distinct change of slope (Figure 3.2).

3.1.3. Photo Excitation of Phthalocyanine

Phthalocyanines are photosensitive materials. Illumination with light may bring the molecule into an excited state. Photoconductivity in Pc materials may be regarded as the formation and destruction of photo-generated excited states known as *Frenkel excitons* [6]. It results from the molecular absorption of a photon of light causing the promotion of an electron from an occupied molecular orbital to an unoccupied orbital of higher energy (HOMO-LUMO transition). This excitation produces a short-lived singlet exciton state of the molecule. Excitons can be transported from one molecule to the next along the whole material. The efficiency of the photo conduction process at a certain wavelength correlates well with the absorption spectrum of the material.

Oxygen plays an important role in the charge carrier formation by photo excitation. This associated so-called *type I mechanism*, results in a large increase in conductivity in the presence of pre-adsorbed oxygen (Figure 3.3).

$$Pc + O_2 \xrightarrow{h\nu} {}^1Pc^+ + O_2^- \tag{3.3}$$

where ^{3}Pc and ^{1}Pc represents the Pc molecule in its first excited triplet or singlet state respectively. The transition from the first excited singlet to the first excited triplet state is forbidden by all selection rules and is called intersystem crossing (ISC). For macrocyclic materials, however, these rules cannot exactly be applied which is the reason for large ISC rates in these molecules. The high population of the triplet state is the result of its relatively long life time in the range of μs.

Since oxygen exists in a triplet ground state, energy can be transferred from ${}^3Pc$ to O_2 which may result in an excitation of O_2 into its first excited singlet state ${}^1O_2$. This energy transfer is called *type II mechanism*:

$$Pc + O_2 \xrightarrow{h\nu} {}^1Pc \xrightarrow{ISC} {}^3Pc + {}^1O_2 \qquad (3.4)$$

Singlet oxygen is a highly reactive species and has been extensively investigated in photodynamic cancer therapy. However, the generation of singlet oxygen has so far only been reported for photochemical reactions in solution [7].

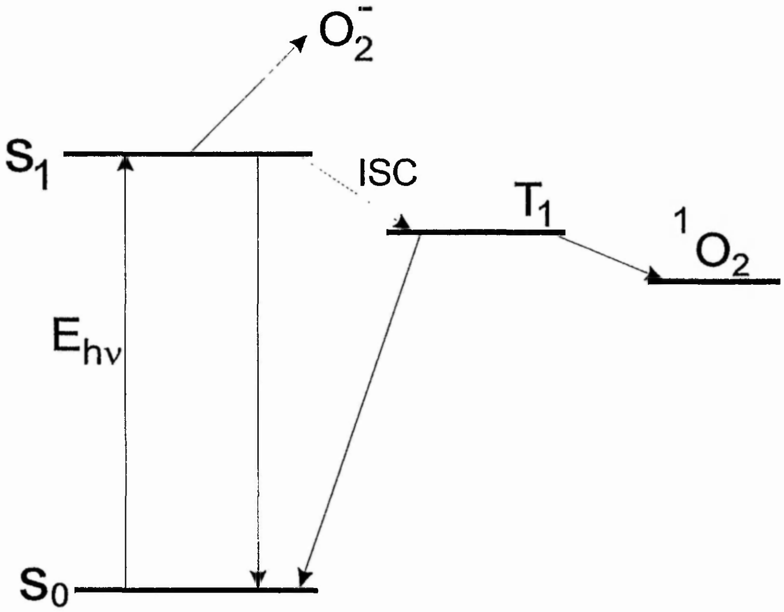

Figure 3.3: Photoexcitation of phthalocyanine in the presence of molecular oxygen

3.1.4. Gas Adsorption on Phthalocyanines

A description of the gas adsorption on phthalocyanines in air has to take into account a number of physio-chemical processes. In most cases there will be a surface coverage already, usually O_2, which has to be replaced by the new molecules. There will also be adsorption effects on structural and chemical defects of the material as well as intercrystallite diffusion (Figure 3.4) [8].

It is believed that the adsorbed molecules may interact with the π-electron system of the phthalocyanine. Hence, good electron donors such as CuPc with a large, planar, delocalised π-orbital interact relatively strongly with acceptor molecules like O_2 resulting in a relatively slow displacement. On the other hand, non-planar PbPc has a less delocalised electron system with a weaker donor power which leads to faster displacement of the adsorbed molecules, generally resulting in a quicker response of the film [9].

Figure 3.4 shows that there is a heterogenity in the binding energy of the gas molecules to the Pc's due to imperfections in the molecular structure which may cause a variation of the activation energies for adsorption. However, even on a perfectly uniform surface the activation energy of adsorption can decrease with higher surface coverage due to a change in lateral repulsion between the adsorbed molecules [10, 11].

Apart from the surface adsorption there will be a diffusion of the gas molecules into the bulk of the Pc layer. The diffusion rate of this process depends on the morphology of the Pc film and was found to be constant for varying thicknesses [12]. In contrast to surface adsorption, bulk diffusion is a much slower process and therefore contributes in a different way to the overall adsorption of gas molecules [12].

Adsorption on phthalocyanines is a complex mechanism, which involves a number of different processes simultaneously. However, under certain conditions it may be possible to eliminate either surface adsorption or bulk diffusion. As isolated processes it may be easier to apply adsorption models to them.

In this work two models have been applied to the adsorption of NO_2 on CuPc. One assumes a constant activation energy of adsorption and the other a variation of the adsorption energy with changing surface coverage. These models, the Langmuir and the Elovich models, will be described in the next section.

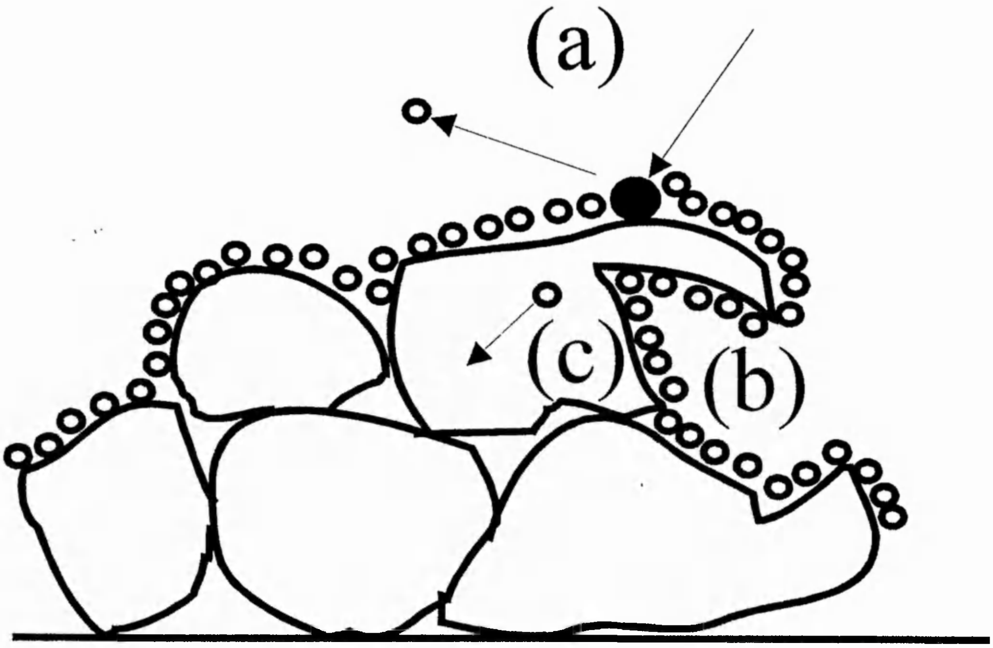

Figure 3.4: Interaction of gas with polycrystalline thin molecular film: (a) displacement, (b) defects (structural and chemical), (c) intercrystallite diffusion

3.2. Kinetics of Adsorption

3.2.1. The Langmuir Model

An adsorption process based on the replacement of one molecule by another, which is more strongly bound was first proposed by Langmuir [8]. His model states that the number of available adsorption sites is proportional to the rate of change of this number. It also takes into account a simultaneous desorption of molecules, thus:

$$\frac{d\theta}{dt} = k_a p(1-\theta) - k_d\theta \qquad (3.5)$$

with p being the partial pressure of the gas, k_a and k_d the rate constant of adsorption and desorption respectively and θ the ratio of the number of adsorbed molecules to the total number of available adsorption sites. Assuming a constant temperature of the process the constants k_a and k_d only depend on the activation energy of adsorption (E_a) and desorption (E_d) respectively;

$$k_a = e^{\left(-\frac{E_a}{RT}\right)} \qquad (3.6)$$

$$k_d = e^{\left(-\frac{E_d}{RT}\right)} \qquad (3.7)$$

where R is the gas constant. These equations assume a constant activation energy but they will also be a good approximation for processes where the activation energy may change slightly.

With the boundary condition $\theta = 0$ at $t = 0$, Equation (3.5) yields a solution of the form:

$$\theta = \theta_{\infty}\left(1 - e^{-(k_a p + k_d)t}\right) \tag{3.8}$$

The constant θ_{∞} is the steady-state condition after a sufficiently long adsorption time has lapsed and adsorption and desorption of the gas on the surface are in equilibrium i.e. $d\theta/dt = 0$. Hence, from Equation (3.5) θ_{∞} is related to the partial pressure and the adsorption and desorption constants,

$$k_a p(1 - \theta_{\infty}) = k_d \theta_{\infty} \tag{3.9}$$

Thus, the steady state condition of adsorption only depends on the partial pressure of the gas and is called the Langmuir isotherm:

$$\theta_{\infty} = \frac{k_a p}{k_d + k_a p} \tag{3.10}$$

For low partial pressures a linear relationship with the steady state value of surface coverage ($\theta = k_a p/k_d$) is obtained (Figure 3.5). In many gas sensing applications the steady state value is used to determine the partial pressure of the test gas. Gas adsorption on phthalocyanines however, usually takes a very long time to reach this steady state. Therefore, another special case of Equation

3.5 is of interest, which expresses the initial rate of change in surface coverage at the beginning of an exposure. Equation 3.5 becomes:

$$\left(\frac{d\theta}{dt}\right)_{\theta=0} = k_a p \qquad (3.11)$$

This expression shows that the initial rate of adsorption will be proportional to the partial pressure of the adsorbing gas [13,14].

However, this model does not take a variation in activation energies with increasing surface coverage into account, which often occurs in adsorption processes on phthalocyanines. In order to describe such a process more accurately the Langmuir model is extended to account for a changing *Ea*.

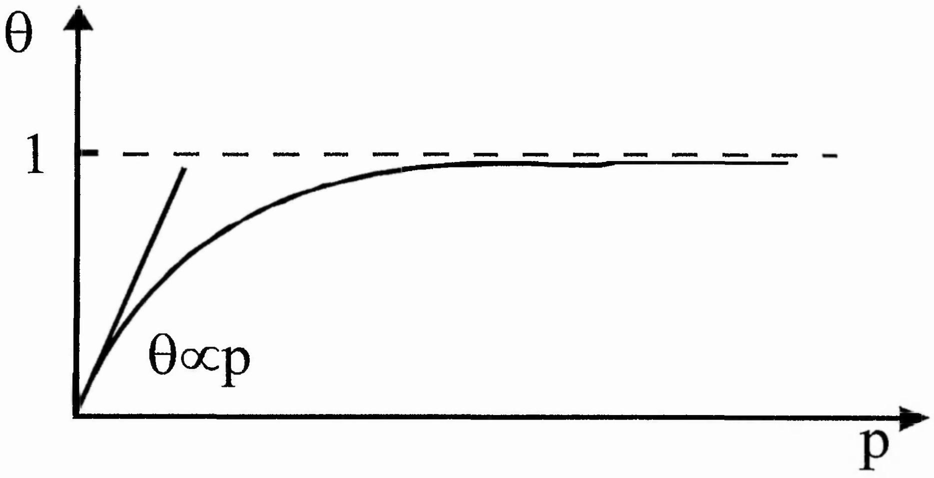

Figure 3.5: Percentage of occupied sites as a function of the pressure [8]

3.2.2. The Elovich Model

The Elovich model describes adsorption of gas molecules on surfaces for a process with varying activation energy of adsorption. For the empirical description of adsorption processes under the condition of low surface coverage the desorption term is usually neglected.

Lateral repulsion between the adsorbed molecules often changes with higher surface coverage. This variation is often described by the empirical relation $E_a = E_o + \alpha\theta$ which changes the adsorption rate constant k_a to:

$$k_a = Ae^{\left(\frac{-E_0 + \alpha\theta}{RT}\right)} \tag{3.12}$$

The rate of adsorption then changes to:

$$\frac{d\theta}{dt} = Ap(1-\theta)e^{\left(-\frac{E_0 + \alpha\theta}{RT}\right)} \tag{3.13}$$

which is known as the Elovich equation [15] and often found in the literature in the form:

$$\frac{d\theta}{dt} = ape^{-b\theta} \tag{3.14}$$

for the case of low surface coverage [16] with a and b being constants. If a gas adsorption process on phthalocyanines follows this relationship, a plot of $\log [d\theta/dt]$ vs. θ should be linear. From the slope of these plots the values for a and

b can be extracted. Under the condition of low surface coverage it is found that there is an approximately proportional relationship between a and the gas pressure p [17].

For phthalocyanine gas sensors the value θ for surface coverage has to be replaced by an expression suitable to a particular type of sensor such as change in current ΔI for conductivity sensors or change in frequency Δf for surface acoustic wave sensors. This conversion from a value of surface coverage into a measurable quantity from the sensor output is discussed in the next section.

3.2.3. Gas Sensing Models

It has been experimentally found that the current of Pc conductivity sensors is proportional to the nth power of the adsorbed surface concentration θ, i.e., $I \propto \theta^n$ [18]. With the solution of the Langmuir equation one obtains an expression for the film current dependent on the surface coverage:

$$I = I_{ss}\left[1 - e^{-\left(k_a p + k_d\right)t}\right]^n \tag{3.15}$$

with I_{ss} being the steady-state current of the sensor. This equation was shown to closely approximate surface adsorption of NO_2 on PbPc [12].

However, the Langmuir model is not always applicable to the description of the adsorption processes on phthalocyanine conductivity sensors. When applying the Elovich equation for measuring concentrations in a range within one order of magnitude, the conductivity change can be regarded as proportional to the surface coverage [19]. Hence, θ can be replaced by I with the inclusion of new constants *a'* and *b'* proportional to *a* and *b* respectively. We obtain the modified Elovich equation:

$$\frac{dI}{dt} = a'e^{-b'I} \tag{3.16}$$

The value for the conductivity σ_s for a thin Pc film applied to an array of interdigitated electrodes can then be calculated with the equation

$$\sigma_s = \frac{I}{V}\frac{d}{(2N-1)l} \tag{3.17}$$

with *d* being the electrode spacing and *l* the overlap length of the electrode finger [20].

Surface adsorption can change both electrical conductivity and mass loading of the phthalocyanine film on a SAW device and therefore its resonance frequency. For room temperature Pc gas sensors this change can be a direct measure of the mass loading if the contributions of the film conductivity can be neglected. Changes in film conductivity are measured with surface acoustic wave devices indirectly via a change in SAW attenuation Δa and can be converted into a value for conductivity σ_s (Section 3.3.4). The operation principles of SAW devices are described in the next section.

3.3. Surface Acoustic Waves

Surface acoustic wave devices are a useful tool to monitor gas adsorption on phthalocyanine layers. The measurement has a more physical character since there are no electrodes in direct contact with the sensitive films applied to the SAW path. Under certain conditions, associated with the conductivity of the sensitising layer, the change in resonance frequency of the SAW device can be a direct measure of the change in mass loading due to gas adsorption on the film.

3.3.1. Wave Propagation in Piezoelectric Solids

Since Lord Rayleigh's investigation in 1885 [21], it has been known that elastic waves can propagate along the surface of a solid. With the wave travelling along the stress free boundary of the surface, the particles of the wave are less restrained than their counterparts deep in the interior (which are surrounded by the medium at all sides). Therefore, the surface wave has a lower velocity than the bulk wave in that medium. (Figure 3.6) [22]. Through the microwave range the surface wave velocity is independent of its frequency.

A Rayleigh wave has most of its energy confined to a depth of the order of one wavelength. The motion of the particles can be both perpendicular to the depth and along the direction of wave propagation. Hence, the wave has shear and a compressional component respectively [23]. The particle displacements $u_{x,y,z}$ of the acoustic wave are accompanied by a surface electrical potential ϕ. The potential is related to the displacement components through the constants $c_{x,y,z}$ thus:

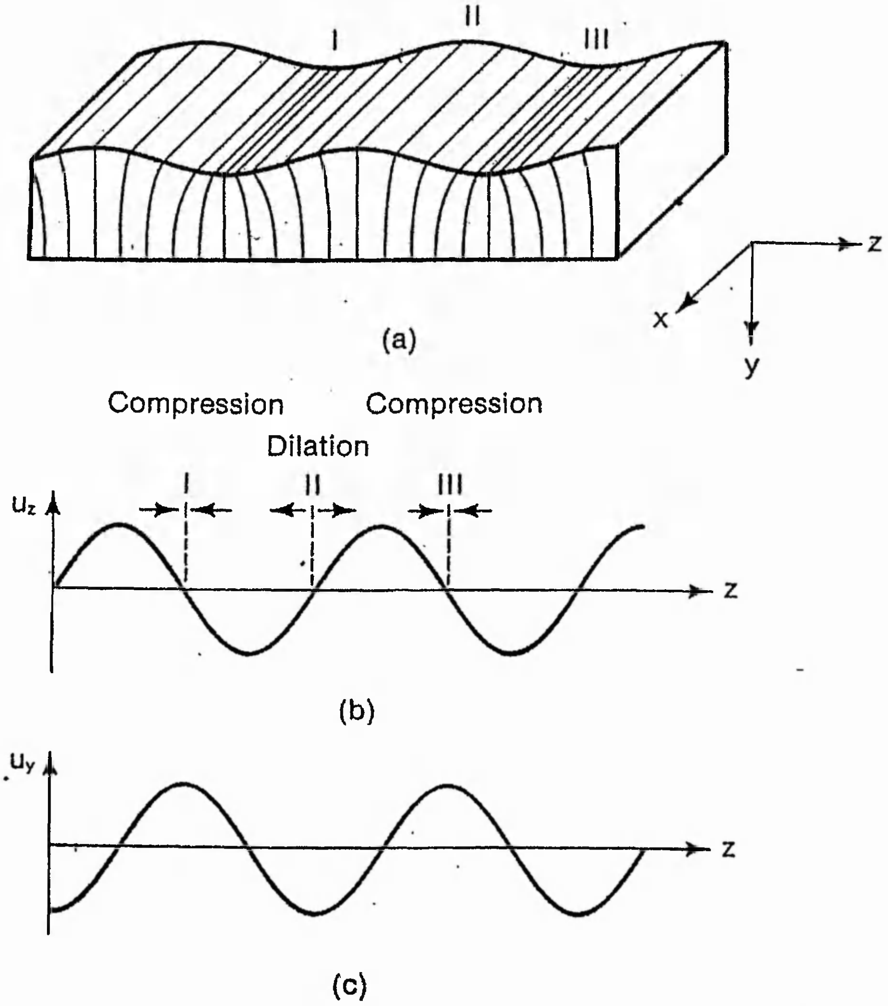

Figure 3.6: (a) Surface wave in a semi-infinite solid, (b) u_z versus z at the surface, (c) u_y versus z at the surface [24]

$$c_{x,y,z} = \frac{u_{x,y,z}}{\phi} \tag{3.18}$$

In the case of the displacement component u_x (perpendicular to the wave propagation and parallel to the surface) being zero ($u_x = 0$) and the other two components being non-zero, particles will move in an elliptical path (Figure 3.8). This *Rayleigh wave* is the most common wave type used for gas sensor applications. Other wave types exist such as the *Gulayev-Bleustein wave* (shear-horizontal wave), which has a displacement component only in the plane of the material. A detailed description of surface wave types can be found in [23].

The coupling between the acoustic wave and its accompanying electric field is usually described by the piezoelectric coupling constant K^2. This constant is the ratio between constants associated with the electrical and mechanical properties of a solid, hence:

$$K^2 = \frac{e^2}{\varepsilon c} \tag{3.19}$$

with ε being the dielectric constant, e the piezoelectric constant and c the stiffness constant. It should be noted that for the general case e and ε are both matrices whilst c is an element of the stiffness tensor [24].

If a conducting layer is applied on top of a surface acoustic wave the electric field will be shorted out which causes a reduction in the wave velocity dependent on the piezoelectric coupling constant:

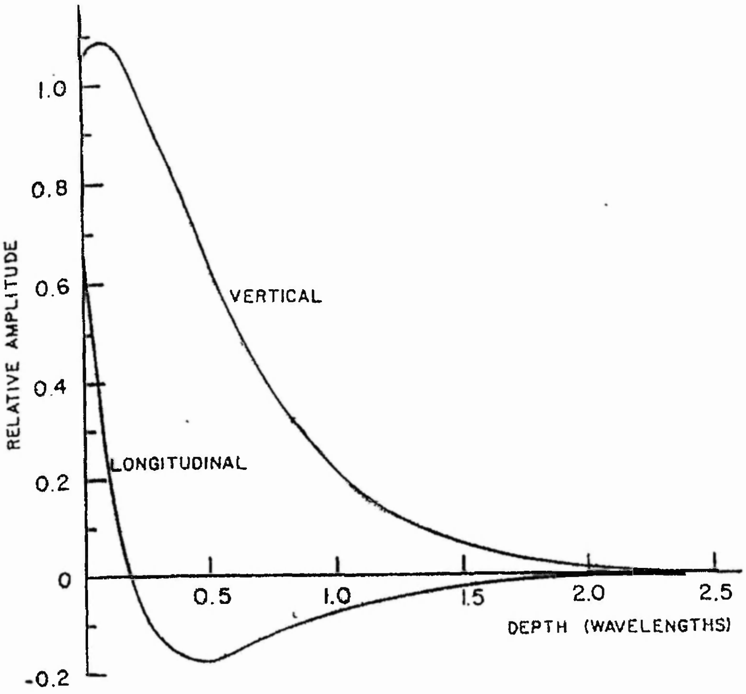

Figure 3.7: Displacement components as a function of penetration depth [23]

$$K^2 = 2\left|\frac{\Delta v_0}{v_0}\right| \qquad (3.20)$$

with v_0 being the unperturbed wave velocity.

The generation of surface acoustic waves by using flat metal electrodes applied to the surface is described in the following section.

3.3.2. Surface Acoustic Wave Generation

Optical, acoustic and mechanical excitation techniques can all be used to produce waves on the surface of a solid [22]. The most common method however, is the generation of surface waves using interdigital transducers (IDT's) on a piezoelectric substrate. An interdigital transducer consists of a metallic pattern of interdigitated electrodes on the top polished surface of a piezoelectric substrate (Figure 3.9). The interdigital transducer is the most important component of a SAW device. It acts as the interface between the electrical circuit and the acoustic transmission path. The advantages of IDT's are their low cost and ease of fabrication by photolithography.

An interdigital transducer transforms electrical signals into an acoustic wave. If a RF electrical field is applied to the IDT's the alternating potential on the electrodes causes a mechanical strain in the piezoelectric material according to the polarity of the transducers. If the electrical field alternates with a high frequency that matches the resonance frequency of the device an acoustic wave is radiated from the transducer in both directions and propagates along the surface of the substrate (Figure 3.10).

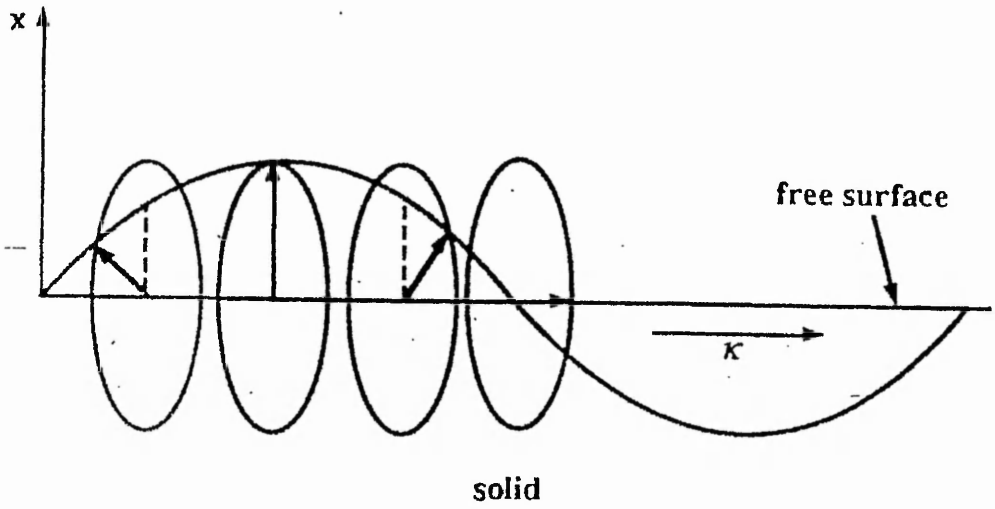

Figure 3.8: Particle displacment in an elliptical path [25]

The reverse effect is used to transform the acoustic wave back into an electrical signal. As the wave arrives at the receiving transducer, the electric field associated with the wave will be picked up by the metal electrodes (Figure 3.10).

For a simple single-finger transducer design as it is used in many gas sensor applications the wavelength λ is determined by the distance between the centres of two electrodes of the same polarity. This distance is equal to one wavelength. As the wave velocity v is constant for an unperturbed polished surface the frequency f of the acoustic wave will be:

$$f = \frac{v}{\lambda} \tag{3.21}$$

In the simplest configuration the metallisation ratio is equal to one i.e. the widths of the transducers are of the same size as the distance between them. Applications that deviate from this simple pattern are described by Datta [24]. Considerations on the design of interdigital transducers are discussed in section 3.3.5.

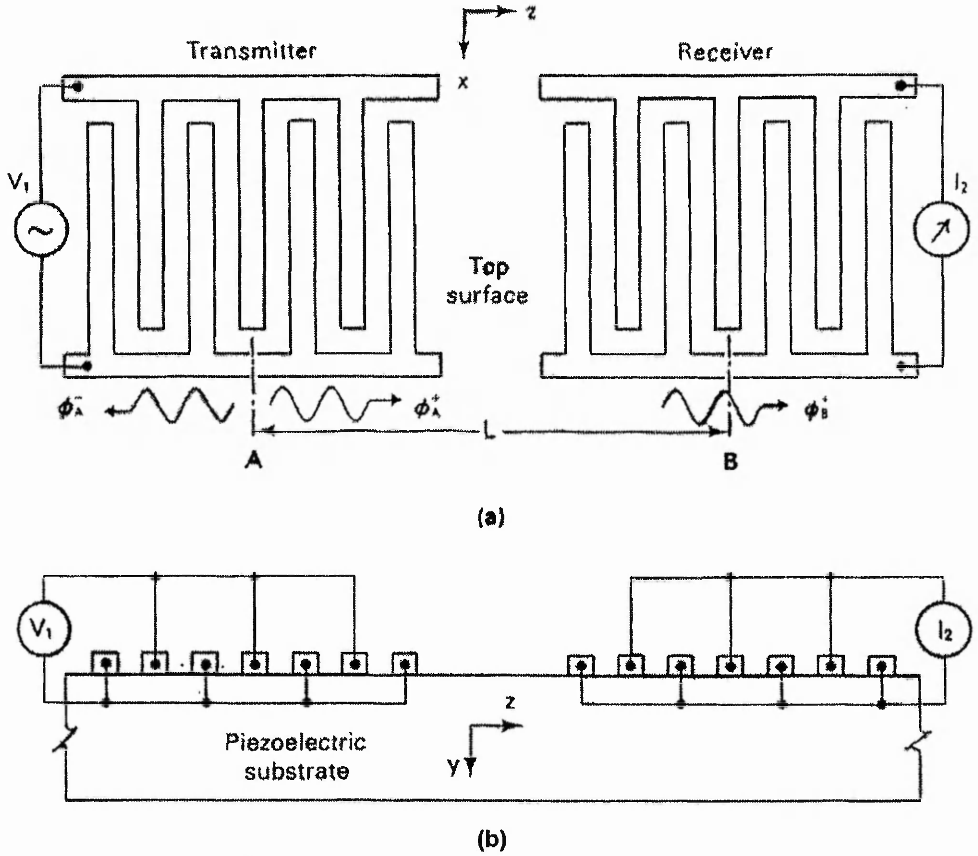

Figure 3.9: SAW delay line: (a) physical structure, top view; (b) end view [24].

3.3.3. Piezoelectric Materials

There exist a whole range of materials with piezoelectric properties for SAW applications. The most commonly used are quartz, lithium niobate and lithium tantalate. Normally, these materials are supplied in precisely cut wafers from syntetic single crystals. The type of surface wave on such a material is determined by the cut direction of the crystal and the direction of wave propagation (Figure 3.11). The cut direction may also promote certain properties of the material such as temperature stability or stress compensation [26].

To determine the physical properties of a surface wave on the crystal plane the cut direction of the crystal and the propagation direction of the wave with respect to the *xyz*-axis have to be known. For example, 128° rotated *YZ-lithium niobate* is a crystal cut where the surface of the wafer is normal to a direction of 128° rotated from the *y*-axis, through the *z*-axis and about the *x*-axis. This common arrangement would result in a Rayleigh wave type device with the Rayleigh wave propagating along the *x*-axis [27].

Surface acoustic wave sensors exploit the fact that the surface wave velocity changes upon perturbations of the acoustic transmission path. The physical mechanisms of this phenomenon are described in the following section.

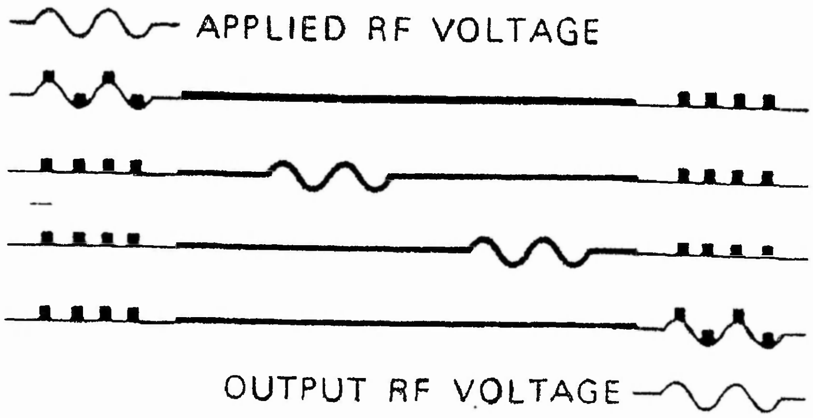

Figure 3.10: Generating and receiving surface waves with IDT's [20]

3.3.4. Perturbation Mechanisms of Surface Acoustic Waves

SAW sensors rely on changes in wave propagation along the surface or the near surface region of the sensor. The complex SAW propagation factor (γ) which expresses the fractional change of the wave number $\Delta k/k$, (Δk being a complex number $\alpha+j\beta$) with α/k being the acoustoelectric attenuation per wavenumber and $\Delta v/v_0$ the fractional change in wave velocity [28],

$$\frac{\Delta k}{k} = \Delta\gamma = \Delta\alpha / k - j(\Delta v / v_0) \tag{3.22}$$

is altered by any change in the physical properties of the surface [29]:

$$\Delta\gamma = \frac{\partial\gamma}{\partial m}\Delta m + \frac{\partial\gamma}{\partial\mu}\Delta\gamma + \frac{\partial\gamma}{\partial\eta}\Delta\eta + \frac{\partial\gamma}{\partial\sigma}\Delta\sigma + \frac{\partial\gamma}{\partial\varepsilon}\Delta\varepsilon + \frac{\partial\gamma}{\partial p}\Delta p + \frac{\partial\gamma}{\partial T}\Delta T + \cdots \tag{3.23}$$

with the unperturbed wave velocity (v_0), the mass (m), electrical conductivity (σ), stiffness (c), dielectric coefficient (ε), temperature (T), pressure (p), shear elastic modulus (μ) and the viscosity (η).

A SAW gas sensor will usually have a chemically selective overlayer like CuPc applied to the surface. If exposed to a gas the physical properties of the overlayer may change and thus, the propagation parameters attenuation α or velocity v or both.

For gas sensing technology, the perturbation mechanisms due to mass loading and electrical conductivity are of special interest. Assuming these are the dominant components to the change their influence to the SAW velocity is described by Equation 3.24:

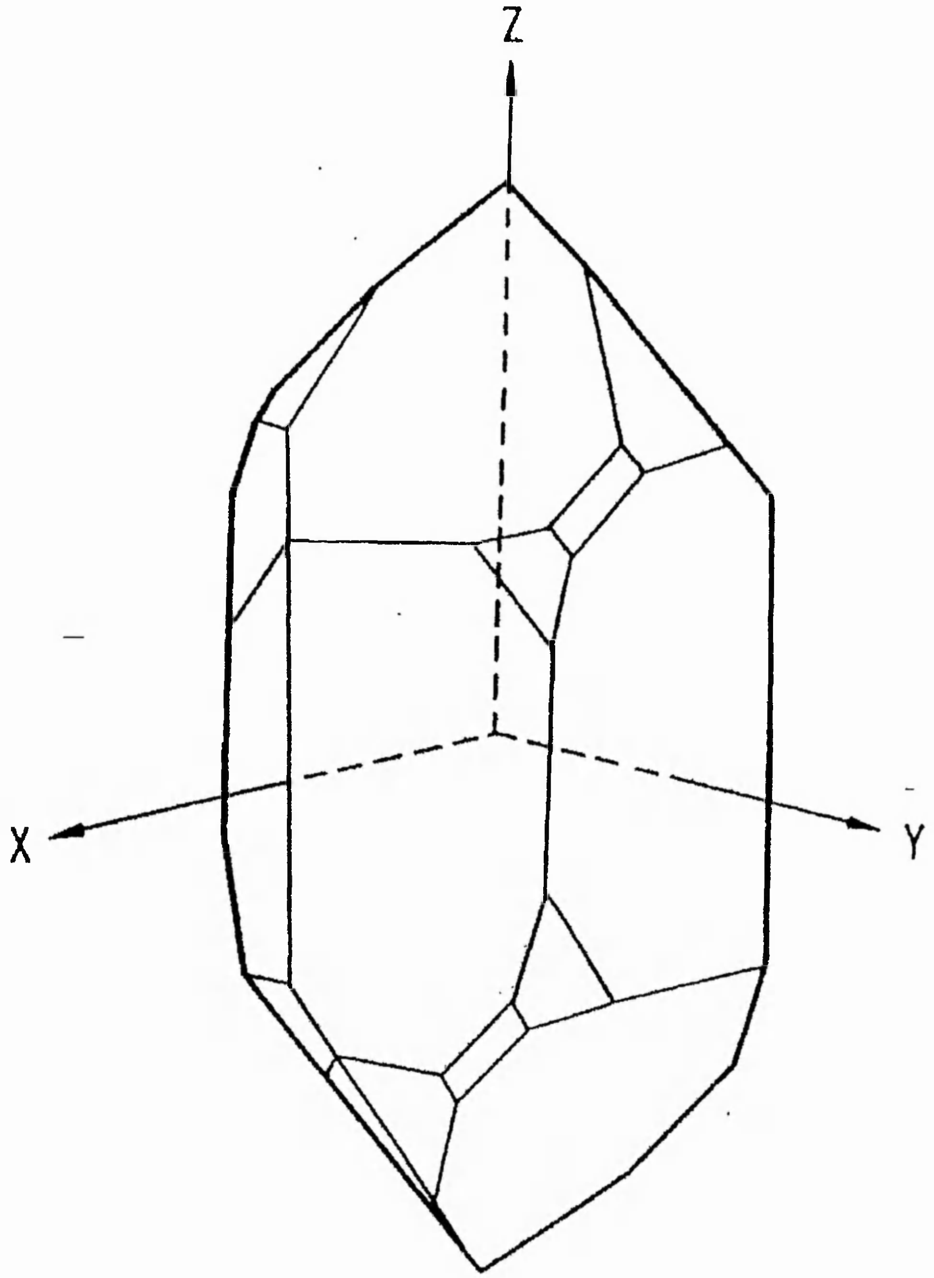

Figure 3.11: The assignment of axis to a quartz crystal [27]

$$\frac{\Delta v}{v_0} = -c_m f_0 \Delta \rho_s - \frac{K^2}{2} \Delta \left[\frac{\sigma_s^2}{\sigma_s^2 + v_0^2 \varepsilon_s^2} \right] \tag{3.24}$$

with the electromechanical coupling coefficient (K^2), sheet conductivity of the film (σ_s), capacitance per unit length of the surface (ε_s), mass per area (ρ_s), frequency of the unperturbed wave (f_0), and the sensitivity coefficient (c_m). The right side of Equation 3.24 is an approximation for acoustically thin films (film thickness<<λ) and represents the change in wave velocity due to mass loading and conductivity respectively. Table 1 summarises the material constants for $LiNbO_3$ and ST-cut quartz used in Equation 3.24.

Substrate	K^2 (%)	c_m ($cm^2g^{-1}MHz^{-1}$)	c_e (cm^2sg^{-1})	v_0 (kms^{-1})	ε_s ($pFcm^{-1}$)
ST-cut Quartz	0.11	1.28	3.86×10^{-7}	3.16	0.5
128° rotated YZ-$LiNbO_3$	4.80	0.55	1.73×10^{-7}	3.49	4.6

Table 1: Material constants for widely used piezoelectric materials

For a system that operates at the natural frequency of the SAW device such as a resonator circuit, the changes in velocity are proportional to the frequency shift, hence:

$$\frac{\Delta f}{f_0} = \kappa \frac{\Delta v}{v_0} \tag{3.25}$$

with κ being the fraction of the distance between the transducers that is affected by the perturbation. These systems usually provide a high stability which, for well controlled conditions, is typically better than 1Hzs^{-1}. Therefore, for a 35MHz SAW device changes in wave velocity of less than 1ppm should be measurable.

If mass in the form of a thin film or of adsorbing molecules is applied to the surface, the wave velocity v_O will decrease. The change in frequency due to mass loading is then proportional to the square of the resonance frequency:

$$\Delta f \propto f_0^2 \Delta\rho_s \tag{3.26}$$

This equation indicates that the frequency response due to changes in mass loading can be greatly improved by increasing the resonating frequency of the SAW device. For the detection of conductivity changes on the surface the value of the resonating frequency is not of such great significance since Δf is only proportional to f_O.

Perturbations can also affect the attenuation of the amplitude of the acoustic wave. Equation 3.27 shows the mechanism for thin non-viscoelastic films:

$$\frac{\Delta\alpha}{k} = \frac{K^2}{2}\Delta\left[\frac{v_0 C_s \sigma_s}{\sigma_s^2 + v_0^2 \varepsilon_s^2}\right] \tag{3.27}$$

with k being the wavenumber ($k=2\pi/\lambda$) and C_s being the capacitance per length of the SAW substrate material.

From Equation 3.27 it can be shown that all changes of attenuation in thin non-viscoelastic films are merely a result of acoustoelectric coupling: higher conductivity of the film shorts out the electrical field associated with the acoustic wave. Other perturbations are usually so small that they will not cause changes

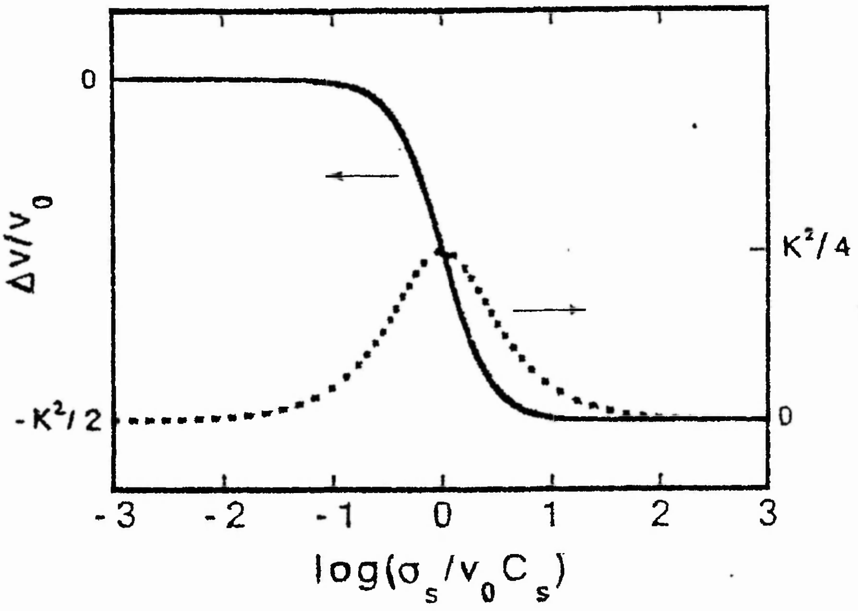

Figure 3.12:Theoretical form of the acoustoelectric effect with wave velocity (solid line) and attenuation (squares) [29]

in the wave amplitude. Figure 3.12 shows the theoretical form of the acoustoelectric effect for surface acoustic waves as a function of sheet conductivity derived from Equation 3.24 and Equation 3.27.

This effect has its maximum at $\sigma_S = v_O \varepsilon_s$ and ranges over ±2 orders of magnitude around this value. Hence, in order to achieve a high sensitivity with respect to changes due to the acoustoelectric effect there has to be a careful consideration of the initial value of sheet conductivity.

Ricco *et al.* [29] derived an approximate relationship between the velocity shift and attenuation change for the case of non-viscoelastic thin films:

$$\left(\frac{\Delta v}{v_0}+\frac{K^2}{4}\right)^2+\left(\frac{\Delta\alpha}{k}\right)^2=\left(\frac{K^2}{4}\right)^2 \qquad (3.28)$$

This equation is particularly useful in distinguishing the contributions of mass loading and conductivity by measuring their attenuation and velocity contributions.

The next section will describe the operation of interdigital transducers in electronic terms and provide design considerations for simple single-finger IDT's.

3.3.5. Interdigital Transducer Design

An IDT is essentially a capacitor with the parallel plates rotated away from each other until they are horizontal (Figure 3.13) [24].

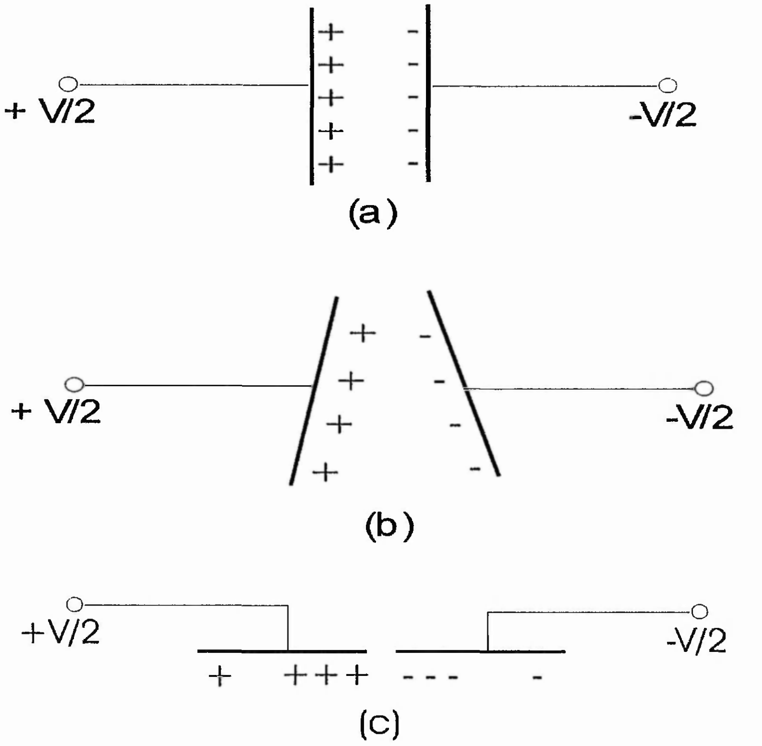

Figure 3.13: (a) Parallel-plate capacitor; (b) plates rotated away from each other; (c) two electrodes of an IDT

The capacitance (C) of a single finger pair is calculated with:

$$C = (M\lambda)\varepsilon_s \tag{3.29}$$

with ε_s being the permittivity of the substrate.

Section 3.3.2. outlined the dimensioning of the finger width of the IDT's in order to obtain a certain wavelength. However, two more parameters have to be considered in a single finger transducer design: the aperture M (overlap of the fingers) and the number of finger pairs N (Figure 3.14).

In order to determine these parameters the limiting factors of the transducer performance have to be taken into account [30]. The bandwidth of a SAW device is restricted by three quality factors from which expressions for M and N will be derived:

Electrical/Radiative:

$$Q_r = \frac{\pi}{4K^2 N} \tag{3.30}$$

LCR Resonant:

$$Q = \frac{1}{\omega_0 NCR_a} \tag{3.31}$$

Acoustic:

$$Q_a = N \tag{3.32}$$

with $\omega_0 = 2\pi f$ and R_a being the radiation resistance which determines how well the transducers are matched to the 50Ω peripheral system.

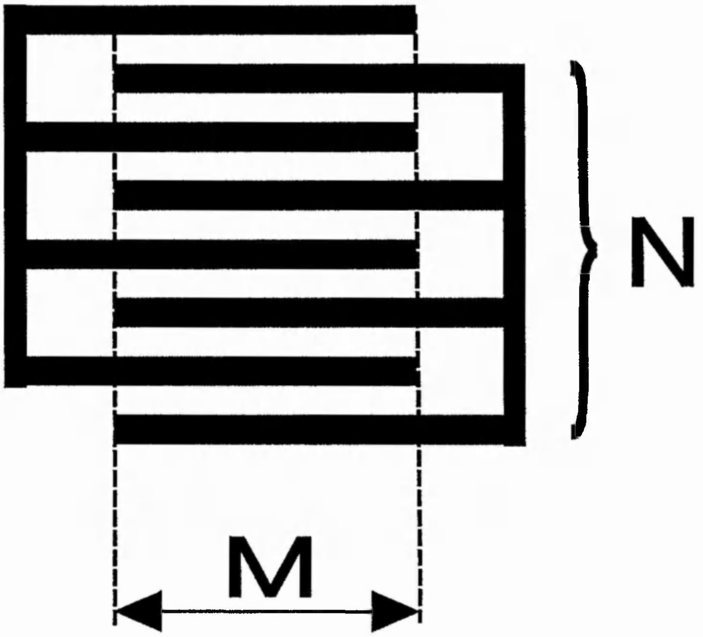

Figure 3.14: Aperture M and number of finger pairs N of an IDT

To find the number of finger pairs N for the optimum bandwidth of the transducer Equation 3.30 and Equation 3.32 are combined to:

$$N_{opt} = \sqrt{\frac{\pi}{4K^2}} \tag{2.33}$$

The aperture related to N_{opt} is obtained by combining equation (2.29) and (2.31):

$$M_{max} = \frac{1}{N^2(2\pi\nu\varepsilon_s R_a)} \tag{2.34}$$

For a given R_a the factor MN^2 should be a constant. With

$$\frac{1}{Q} = \frac{\Delta f}{f} = N^{-1} \tag{3.35}$$

the number of finger pairs for the actually desired bandwidth $\Delta f/f$ can be calculated. Finally, $MN^2 = const.$ provides the relationship to calculate the optimum value for the aperture.

In this design consideration many effects such as reflections and mass contribution are neglected. For more complicated electrode structures (such as double finger IDT's), designing transducers becomes an increasingly complex task and may be accomplished by numerical methods and computation.

In the following chapter experimental methods and development of the measurement system are discussed. The second part of this chapter includes preliminary experiments carried out to develop and understand the experimental system and its properties.

References

[1] T.Parr, An Investigation into the Structural, Optical and Electrical Properties of Phtalocyanines with Regard to their Feasibility as Commercial Gas Sensors, PhD-thesis, Univ. of Lancaster, (1995), 10

[2] H.Meier, Organic Semiconductors, Chemie (Weinheim), (1974), 72

[3] A.Fejfar, G.Takaoka, I.Jamada, Czech.J.Phys., **43**, No.9/10, (1993),453

[4] C.Ludwig, R.Strohmeier, B.Gompf, W.Eisenmenger, J.Vac.Sci.Technol., **B12**, No.3, (1994), 892

[5] M.Maitrot, G.Guillaud, B.Boudjema, J.J.Andre, H.Simon, R.Even, Chem.Phys.Letts., **133**, No.1, (1987), 112

[6] N.B.McKewon, Phthalocyanine Materials: Synthesis, Structure and Function, Cambr.Univ.Press, (1998), 129

[7] J .G.Moser, Photodynamic Tumor Therapy, Gordon and Breach (1998), 10

[8] G.Guillaud, J.Simon, J.P.Germain, Coord.Chem.Rev., **178-180**, (1998), 1433

[9] P.B.M.Archer, A.V.Chadwick, J.J.Miasik, M.Tamizi, J.D.Wright, Sens.Actu., **16**, (1989), 379

[10] R.L.van Ewyk, A.V.Chadwick, J.D.Wright, JCS Faraday I, **76**, (1980), 2194

[11] J.D.Wright, A.V.Chadwick, B.Meadows, J.J.Miasik, Mol.Cryst.Liq.Cryst., **93**, (1983), 315

[12] Y.H.Ju, C.Hsieh, C.J.Liu, Thin Solid Films, **342**, (1999), 238

[13] C.J.Liu, J.C.Hsieh, Y.H.Ju, J.Vac.Sci.Technol., **A14**, No.3, (1996), 753

[14] H.E.Avery, Basic Reaction Kinetics and Mechanisms, MacMillan, (1974), 123

[15] A.W.Adamson, Physical Chemistry of Surfaces, J.Wiley and Sons Inc., USA, (1990), 700

[16] C.Aharoni, F.C.Tompkins, Adv.Catal., **21**, (1970), 1

[17] D.O.Hayward, B.M.W.Trapnell, Chemisorption, Butterworths. London, (1963), 93

[18] M.Passard, A.Pauly, J.P.Blanc, S.Dogo, J.P.Germain, C.Maleysson, Sens.Actu., **B 18-19**, (1994)

[19] J.W.Gardener, M.Z.Iskandarani, B.Bott, Sens.Actu., **B9**, (1992), 133

[20] C.C.Leznoff, A.B.P.Lever, Phthalocyanines: Properties and Applications, VCH Publishers Inc., (1989)

[21] Lord Rayleigh, Proc.London Math.Soc., **17**, 4-11

[22] R.M.White, Proc. IEEE, **58**, No.8, (1970)

[23] A.A.Oliner, *Acoustic Surface Waves*, Springer Verlag, New York, (1977)

[24] S.Datta, Surface Acoustic Wave Devices, Prentice Hall, New Jersey, (1986)

[25] E.Gizeli, New Acoustic Wave Sensor Geometries, PhD Thesis, Cambridge, (1992)

[26] J.G.Gualtieri, J.A.Kosinski, A.Ballato, IEEE Trans.Ultras.Ferroel.Freq.Contr., **41**, No.1, (1994)

[27] C.Lu, Theory and Practice of the Quartz Crystal Microbalance, Braun-Schweig, (1984)

[28] S.Datta, Surface Acoustic Wave Devices, Prentice Hall, New Jersey, (1986), 181

[29] A.J.Ricco, S.J.Martin, Thin Solid Films, **206**, (1991), 94

[30] K.B.McEnaney, Magneto-absorption of Surface Acoustic Waves by a 2-dimensional Electron Gas, PhD Thesis, University of Nottingham, (1991), 56

Chapter 4: Experimental Methods and Development

4.1. Overview

This chapter outlines the development of experimental methods equipement used in this work. The first section describes the design, fabrication and preparation of the electrical conductivity, surface acoustic wave and QCM sensors. This is followed by a general overview of the gas sensing apparatus as well as a detailed description of its components.

In the second part of this chapter a description of preliminary experiments, which served as the basis for the phthalocyanine gas sensing experiments at room temperature, is presented. The vacuum chamber experiments described in this section looked at responses of the different sensor types to evaporation of Pc layers and oxygen doping. Subsequently, the results of gas sensing experiments at elevated temperatures are shown, which were carried out in order to repeat previously published work by other researchers and to characterise the gas sensing apparatus.

4.2. Gas Sensor Design and Fabrication

4.2.1. Photolithography

Both conductivity and SAW sensors required a set of interdigitated electrodes applied to the substrate surface. These electrodes were produced in-house with a photolithographic process [1]. The photolithographic process used a lift-off technique and was the same for both conductivity and SAW sensors.

Initially the substrates were immersed and cleaned in ethyl lactate, acetone, methanol and iso-propanol for ten minutes each in an ultrasonic bath. After cleaning the substrates were blow dried with N_2. A layer of *Microposit SP-25* positive photoresist [2] was then applied to the substrate surface by spin coating. The speed of the spin coater was 4000rpm, which gave a film thickness of approximately 1.2μm.

The layer of photoresist was then soft baked for 2.5 minutes on a temperature controlled hot plate at 130°C. The baked layer was then exposed to UV-light for 60 seconds. An in-house produced lithographic mask covered the areas, which needed to remain unexposed. After exposure the sample was immersed in a developer to remove the exposed parts of the photoresist.

After the sample had been cleaned with deionised water and blow dried in dried N_2 an approximately 80nm thick gold film was applied to the surface using a DC sputtering unit. Subsequently, the sample was immersed in acetone to remove the remaining photoresist with the gold layer on top. This left a gold pattern in the form of interdigitated electrodes on the surface of the substrate in the regions corresponding to the exposed parts of the photoresist as determined by the mask.

Before applying the phthalocyanine layer to the substrate the samples were cleaned again in acetone and baked for 2 hours on a hot plate at 140°C.

4.2.2. Fabrication of Conductivity Sensors

Conductivity sensors consisted of a set of gold interdigitated electrodes on glass substrates. The electrodes had equal finger width and spaces of 25μm and consisted of 20 finger pairs with an overlap of 2mm.

The CuPc was obtained from Fluka and purified twice by train sublimation [3]. The films were deposited on top of the electrodes by thermal evaporation at a rate of 0.1nm/s at a pressure of 5 x 10^{-6} Torr. The substrate was held at room temperature during evaporation producing films in an α-phase [4] with a thickness of approximately 160nm.

For the conductivity sensors copper phthalocyanine was deposited directly onto top of the gold electrodes. Gold electrodes are known to provide ohmic contact with the CuPc material [5].

4.2.3. Preparation of QCM Devices

For the quartz crystal microbalance measurements temperature and pressure compensated AT-cut quartz crystal resonators (2.458MHz fundamental frequency) purchased from *RS* were used. The active surface area of one side of the crystal, which was covered by the electrode, was $0.25cm^2$. To fabricate a phthalocyanine sensor, the metal case around the crystal was removed and the open crystal was then coated with a CuPc layer on one side. The coating process was carried out at a rate of 0.1nm/s to a thickness of 160nm using phthalocyanine material, which had previously been purified twice by train sublimation.

4.2.4. Fabrication of SAW Sensors and SAW Device Design

The interdigital electrodes of the SAW devices were produced with the same photolithographic process as the conductivity sensors. The substrate material was 128° rotated YZ-cut lithium niobate with a surface wave propagating along the X-direction. Each interdigital transducer consisted of 10 finger pairs with equal widths and spaces of 24.9μm and an aperture of 2mm. These devices gave a resonant frequency of 35MHz and a bandwidth of 10%. Figure 4.1 shows a typical frequency spectrum of the SAW devices used in this work.

For the SAW devices a configuration was chosen where two surface acoustic wave paths are located side by side on the same substrate. The Pc layer is applied to one of the paths and the other path serves as a reference. This configuration is believed to compensate, in the first approximation, for environmental changes such as temperature and pressure [6].

The separation of the IDT's on the SAW device was 7.5mm. The sensitising layer between one pair of transducers had a width of 5mm and was deposited under the same conditions as the films for conductivity and QCM sensors.

In simple IDT designs surface waves are launched from the transmitting transducer equally in both directions perpendicular to the fingers. This is normally considered as undesirable since the SAW energy radiated in the opposite direction of the receiving transducer provides an additional 6dB of attenuation to be overcome by the amplifier.

In this work a novel design was used which employs a separate set of transducers for detection of the oscillatory frequency using this 'unwanted' SAW component (Figure 4.2). This configuration removed the usual requirement for a power splitter to be provided in the oscillator circuit, reduced the gain requirements of the amplifier and provided greater stability.

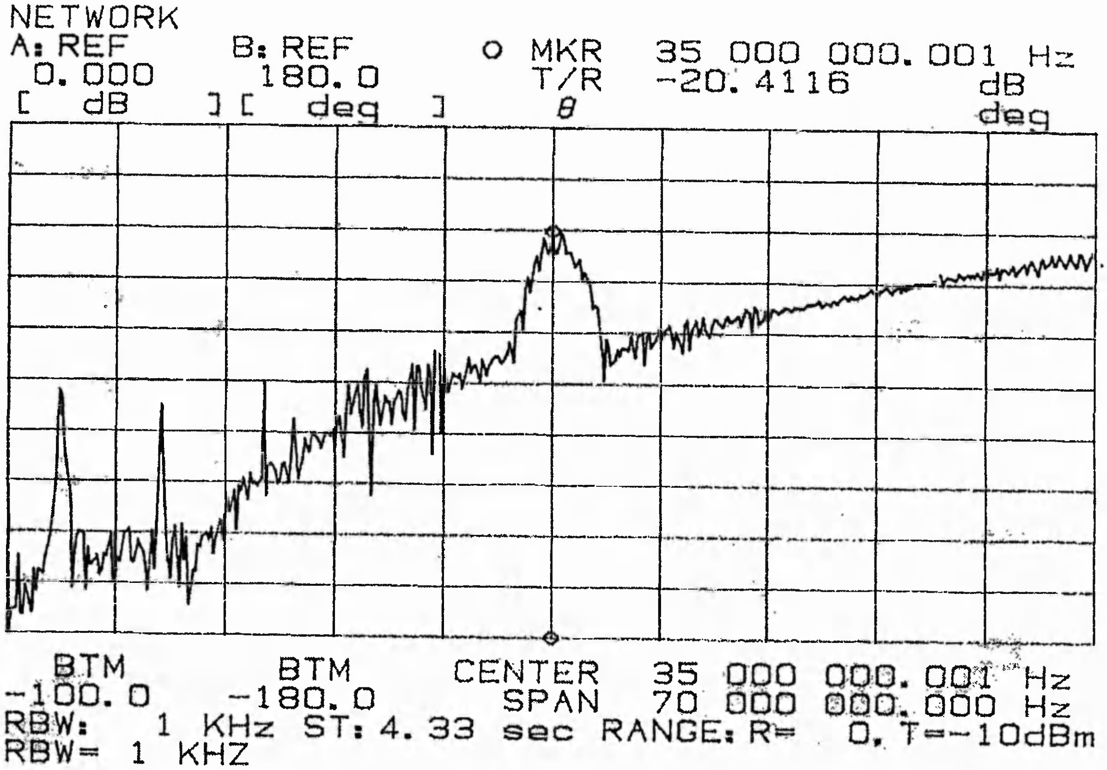

```
NETWORK
A: REF        B: REF          ○ MKR    35 000 000.001 Hz
 0.000         180.0            T/R    -20.4116        dB
[  dB    ][   deg    ]           θ                     deg

   BTM          BTM        CENTER    35 000 000.001 Hz
-100.0       -180.0          SPAN    70 000 000.000 Hz
RBW:    1 KHz  ST: 4.33  sec  RANGE: R=   0, T=-10dBm
RBW=  1 KHZ
```

Figure 4.1: Typical frequency spectrum of a SAW device

The stability of the SAW signal improved significantly with this design because of the electronic decoupling of resonator and detection circuit [7].

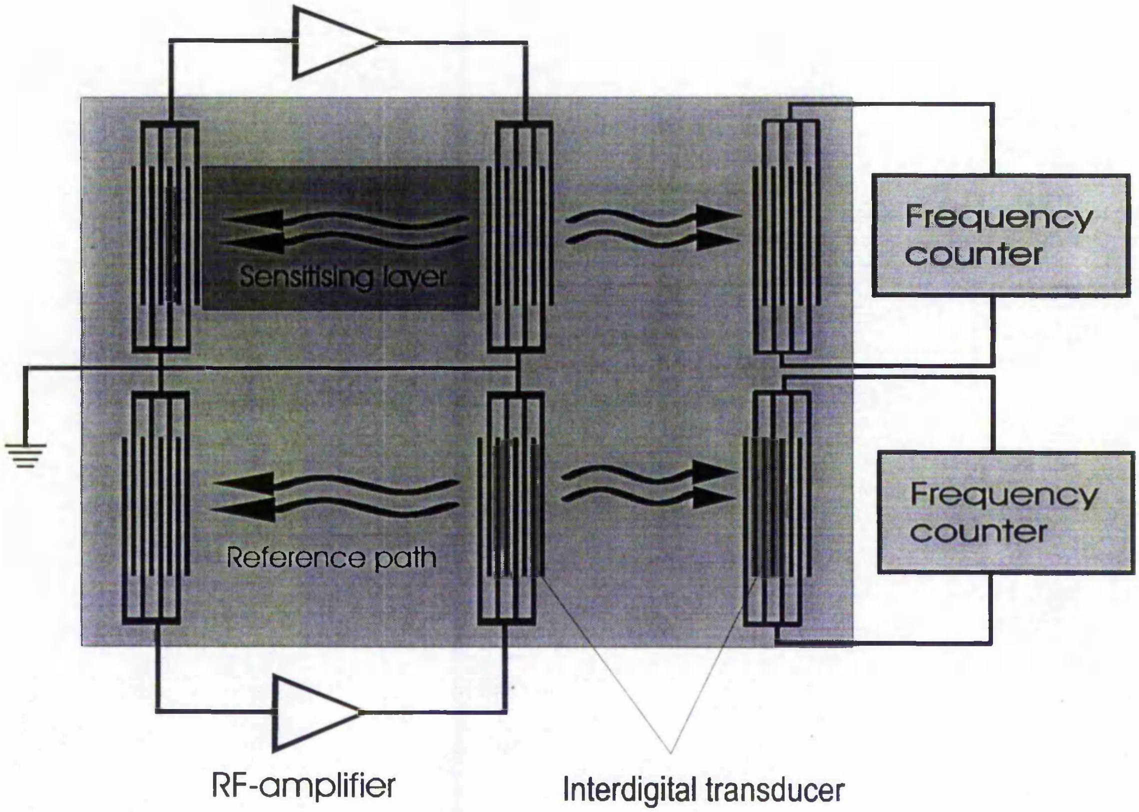

Figure 4.2: Schematic diagram of SAW device design

4.3. Experimental Apparatus

This section describes the experimental set-up of the vacuum evaporation chamber experiments and subsequently the experimental details of the gas sensing system.

4.3.1. The Vacuum System

The preliminary evaporation and oxygen doping experiments described in Section 4.6.1. were performed using an *NGN* vacuum sublimation unit model 12 HG-2.

Figure 4.3 shows the schematic diagram of the system. The vacuum in the *NGN* sublimation unit is generated using a rotary pump for the rough vacuum and a diffusion pump for the high vacuum. For evaporation the unit was usually operated at pressures of 10^{-6} Torr. Pressures were monitored for rough and high vacuum with a Pirani and a Penning gauge, respectively.

The vacuum chamber consisted of a glass bell jar with feed through's for data cable to the measurement devices. Apart from the standard air admission valve the *NGN* unit also provides a needle valve for controlled inlet of test gases.

For the evaporation of phthalocyanines the material was kept in a crucible held by a tungsten basket. By applying a power of approximately 10V/30A the basket was heated up and resulted in sublimation of the Pc material in the crucible.

Substrates were held by a metal construction directly above the crucible. This construction also supported the sensor for the film thickness monitor *Edwards FTM 5* based on a quartz crystal oscillator. The film thickness sensor was positioned next to the substrate at the same height.

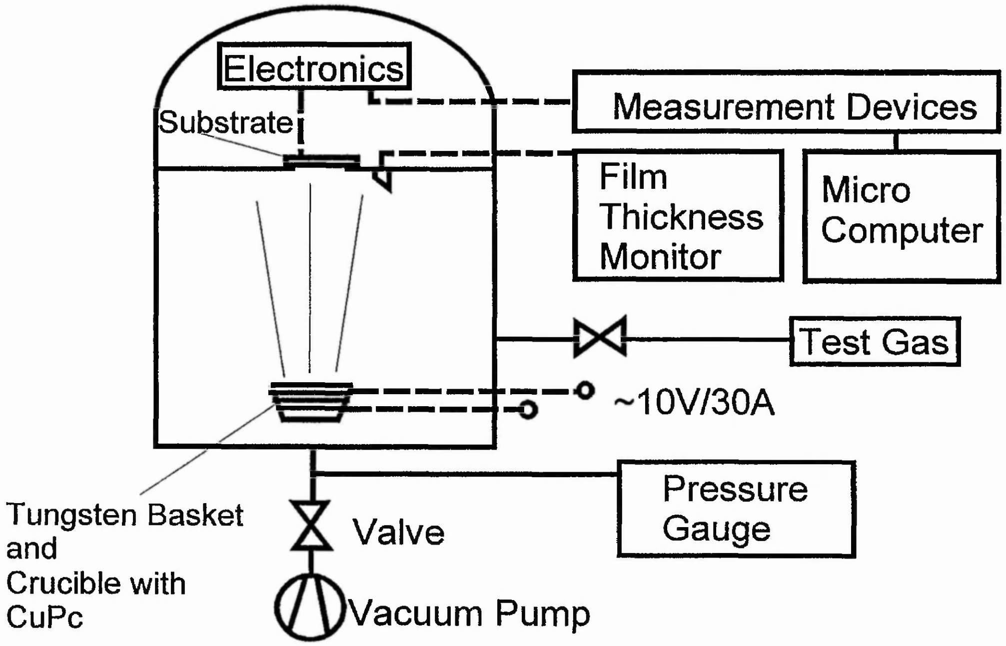

Figure 4.3: Schematic diagram of the vacuum system for oxygen doping and vacuum evaporation experiments

The electronic circuits for the gas sensors were directly connected to the substrates within the vacuum chamber. Data lines and power supplies were provided via the feed through's of the bell jar.

Electrical connections between electronic circuits and the electrodes of the gas sensors were made by copper wires using silver conducting paste. The gas sensors with the conducting paste were left under vacuum for at least 24 hours to ensure full evaporation of the solvent [8].

4.4. The Gas Sensing System

4.4.1. General Overview

All gas sensing experiments for conductivity and SAW phthalocyanine sensors were performed with the system shown in Figure 4.4., which was purpose built for the project. The system consists of a flow cell with a gas flow chamber containing the gas sensors. The electronic circuits for the sensors were directly attached to the cell via electrical connectors suitable for elevated temperature application. Flow cell and connectors were built in a modular way that made it possible to change the mode of operation from SAW to conductivity sensors by changing the electronic modules connected to the flow cell.

The whole flow cell was enclosed in a box containing glass fiber material for thermal insulation. BNC connectors on the box allowed the connection of the electronics at the test cell with peripheral devices and power supplies. Feed through's provided the connection of the flow cell to a gas delivery system with the mass flow controllers (MFC's) and the exhaust to enable the safe disposal of the gas. The box also contained a holder for laser diodes and optics as well as a cooling system for the laser diodes.

4.4.2. The Flow Cell

Figure 4.5 shows the flow cell used for gas sensing experiments. This consisted of an aluminium block with a relatively large thermal mass to reduce the variations in temperature. An electrical heater element was inserted into the bulk of the cell. Together with a thermocouple and an external computerised PID controller a temperature stability of ±0.1°C was achieved (Figure 4.6).

The flow chamber had a depth of 5mm and a width of 25.4mm. Its length of 70mm allowed the operation of two sensors at the same time. The contact pads of the sensor were connected with copper wires using silver conducting paste.

After sealing the edges with PTFE tape a PTFE lid was bolted to the top of the flow chamber. The lid also contained a 10mm glass window for laser illumination.

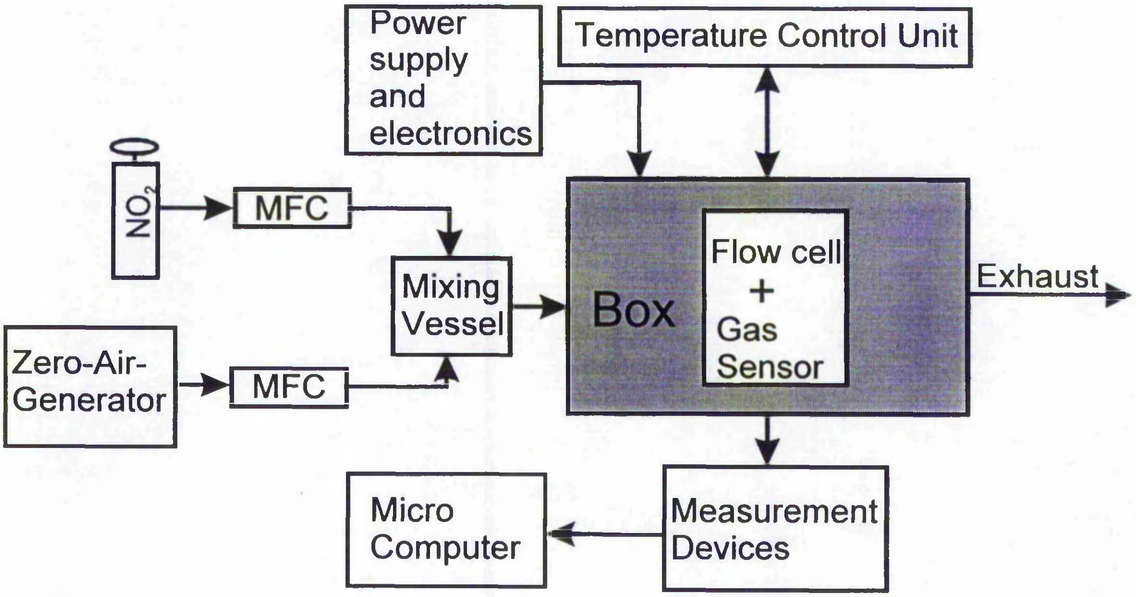

Figure 4.4: Schematic diagram of the gas sensing system

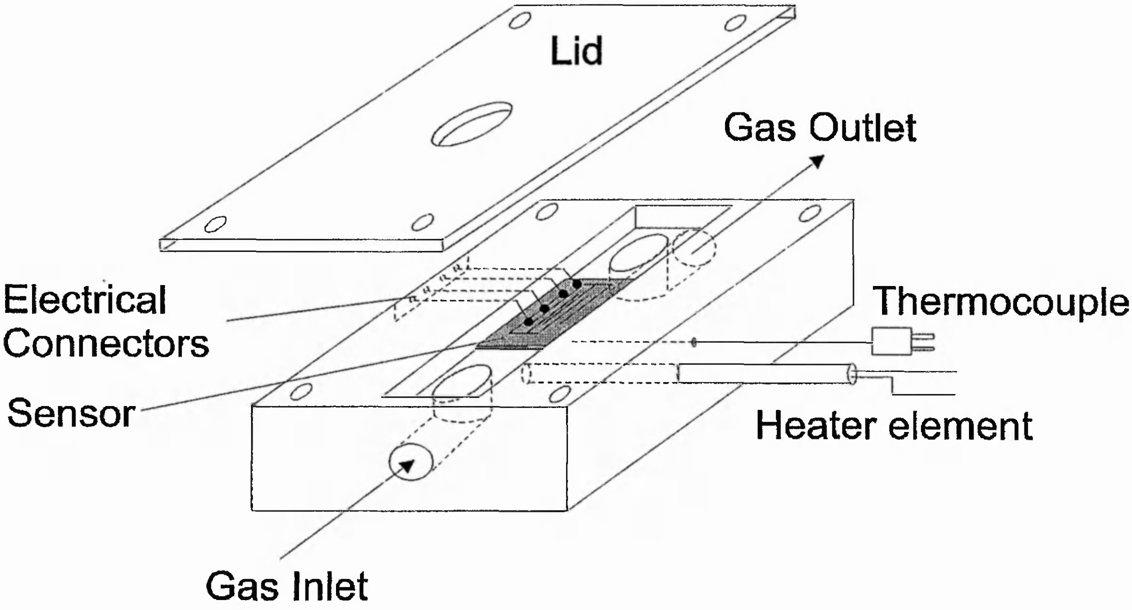

Figure 4.5: Schematic drawing of the flow cell used for gas sensing experiments

4.4.3. The Gas Delivery System

Figure 4.6 shows a schematic diagram of the gas delivery system, which provided the test gas for the sensing experiments. The flow rate of the gas was set to 1l/min for all experiments.

The test gas consisted of a mixture of 100ppm NO_2 in N_2. The mixture was contained in a standard gas cylinder from *Air Products*. The carrier gas was supplied by a *Bambi 35/20* air compressor and catalytically purified by a zero air generator (*Air Products 2500*). The concentration of the test gas was determined by computer controlled mass flow controllers (Cole-Parmer). Computer control allowed a pre-programmed set of exposure cycles with different exposure times and concentrations.

The requirements for a gas going through the flow chamber were: stable flowrate, stable concentration, and stable temperature. Despite the high accuracy of the mass flow controllers (MFC's) it was not possible to fully compensate the pressure differences from the compressor by the use of MFC's. In order to stabilise the flow before reaching the mass flow controller the gas was therefore led through a vessel with a flexible membrane. The fluctuation of the pressure from the compressor was thus partially compensated by a change in volume of the vessel.

After passing the mass flow controllers the gas was then mixed in a mixing vessel which had a volume of approximately 1.5l and consisted of a sealed box with two inlets and one outlet. From there the gas was guided through a coiled tube of 4m length within a thermally insulated water vessel containing water at room temperature. From this temperature stabilisation unit the gas was directly led into the flow cell.

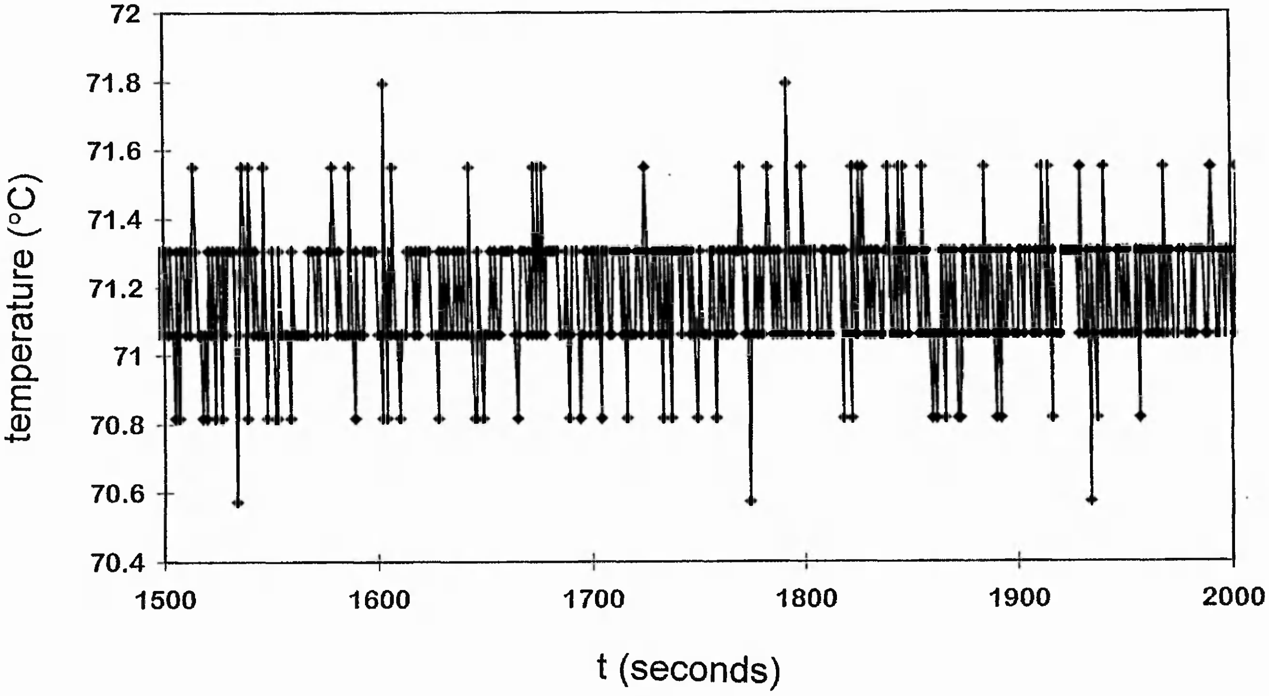

Figure 4.6: Typical stability of the PID temperature control

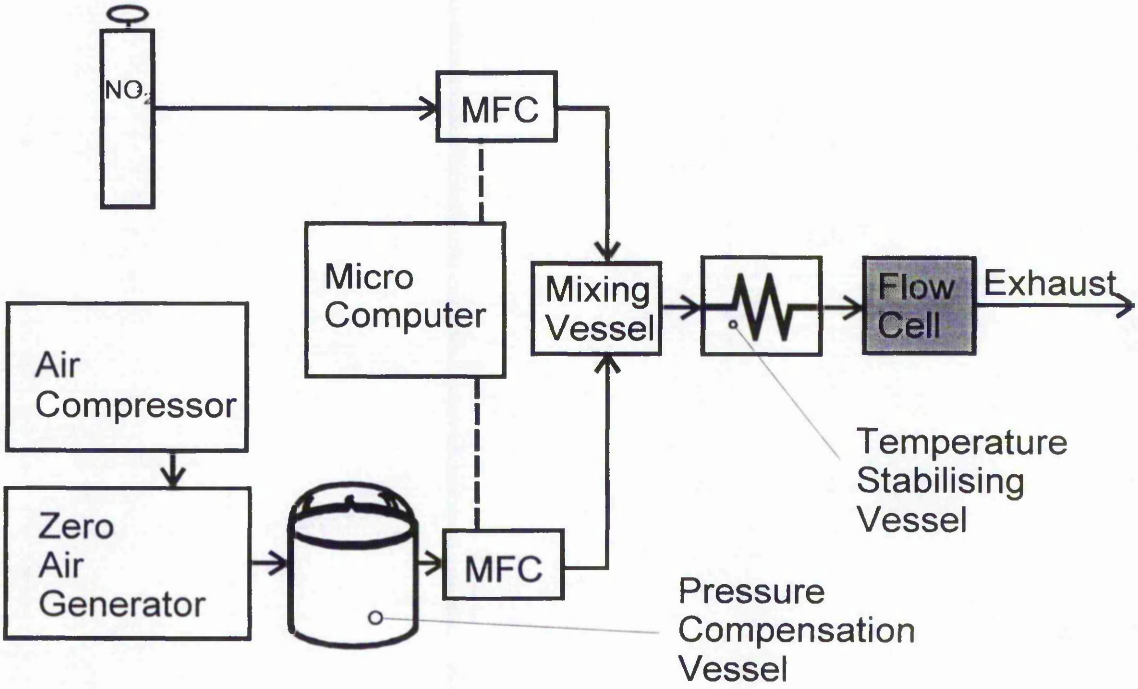

Figure 4.7: Schematic diagram of the gas delivery system

After leaving the flow cell the gas went through an exhaust tube directly into a fume cupboard for safe disposal.

4.4.4. The Laser System

A high power laser diode was used to illuminate the CuPc layers of the gas sensors during the experiments. It was suggested that the strong illumination of the phthlocyanine layer may initiate photochemical reactions which could influence the sensing properties of the gas sensors.

Illumination of the sensitising layer was carried out using a *Philips CQL806/30* diode laser with a output power of 30mW and a wavelength of 675nm. This wavelength corresponds to the light absorption maximum of CuPc at around 680nm. The laser diode was mounted in a collimator tube with lens supplied by *Thorlabs.* To gain a high stability of the output power the laser was cooled with a continuous flow of water through a pipe coiled around the collimator tube. The laser tube was fixed by a holder directly on top of the window of the lid of the flow cell.

The operating power for the laser was supplied by a *Thorlabs LDC 500* laser diode controller. To avoid direct laser exposure which can damage the eyes the box around the flow cell was equipped with a safety interlock to interrupt the supply power for the laser as soon as the box is opened.

For operation in pulsed mode the laser diode controller was connected to a *Thurlby TGD 110* pulse generator. Pulse lengths of more than 1s or controlled change of laser power the laser diode controller were realised by using the output of an analog-digital conversion card of the micro computer.

4.5. Electronics Circuits

In order to operate the phthalocyanine gas sensors electronic circuits had to be implemented to either amplify the signals of the conductivity sensors or generate a resonance for the SAW sensors. These circuits are described in this section.

4.5.1. Circuits for Conductivity Sensors

Conductivity sensors consisted of two interdigitated electrodes with a CuPc layer on top of them (in-plane configuration). If a potential is applied to the electrodes a current will flow from one electrode to the other through the Pc film. The film current depends on the conductivity of the film and may change due to the adsorption of gas molecules such as NO_2 on the Pc layer. To measure the conductivity of a Pc sensor and a fixed potential can be applied across the electrodes and a current measurement made through the film.

Due to the low conductivity of the Pc sensors the current in this circuit is very small requiring a Keithley 485 picoammeter to be employed. The input impedance of this device is very low to avoid a disturbance of the current flow in the circuit.

Alternatively, conductivity measurements were carried out using a voltage divider circuit where the voltage across a reference resistor is measured. For effective operation the reference resistor should have a resistance which is within one order of magnitude of the resistance of the sensor [9].

A measurement of the voltage across the sensor can be carried out with the circuit shown in Figure 4.8. An integrated electrometer circuit with a very high input impedance in the range of GΩ is used to measure the voltage V_R across the reference resistor with the resistivity R_R. Since the overall voltage V applied to the sensor and resistor is known the resistivity of the sensor R_s can easily be determined with:

$$R_S = R_R\left(\frac{V}{V_R} - 1\right) \tag{4.1}$$

This voltage divider circuit was found to be more sensitive than the direct current measurement. However, the simple ammeter circuit was more robust in terms of signal stability and operation and did not require a calibration of the signal. It was therefore chosen for the experiments in this work.

It should be noted that throughout all the experiments batteries were used as the power sources for the electronic circuits because of their independence from the mains electricity allowing improved stability of the signals.

4.5.2. Differentiator Circuit

In this work two ways were used to obtain a derivative plot of the sensor signal: (a) the reading of the meter can be digitally processed by a computer program or (b) the output signal of the measurement circuit can be fed into a differentiator circuit which gives an analogue voltage output that is proportional to the rate of change of the signal.

Figure 4.9 shows the diagram of an operational amplifier circuit that carries out a continuous analogue derivation of the output of the sensor circuit [10]. Figure 4.10 shows a comparison between the derivative signals obtained from this circuit and from computation of the output signal. The two signals show a good agreement. To obtain absolute values for the differentiator circuit a calibration of the analogue signal would be necessary.

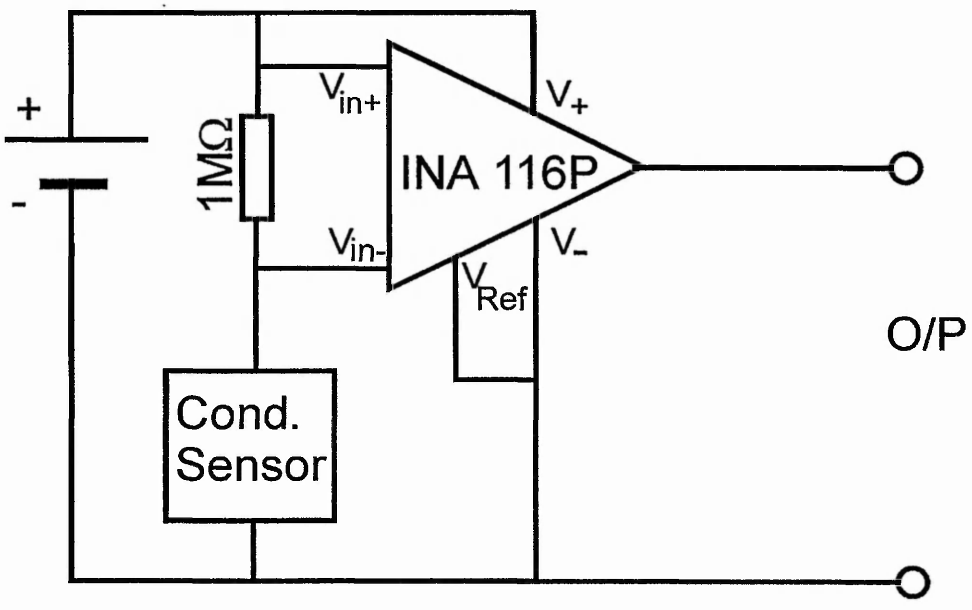

Figure 4.8: Voltage divider circuit for measuring the conductivity across the Pc sensor

In combination with the electrometer circuit described in the previous section this circuit has the potential to work as a cheap, portable and effective processing element for a phthalocyanine based conductivity gas sensor.

4.5.3. SAW Resonator Circuit

A surface acoustic wave resonator circuit consists of an acoustic wave device and an amplifier operating at radio frequencies. The gain of the amplifier has to be at least as high as the insertion loss of the SAW device and the phase of the loop close to 0° to establish an oscillation. A wave that loses energy during its passage across the surface of the SAW device is converted by the receiving transducer into an electrical signal, amplified and sent back to the transmitting transducer where it is converted back into an acoustic wave.

Figure 4.11 shows the resonator circuit that is used in this work. It consists of a RF amplifier with a gain of 25dB at a frequency of 35MHz. Input and output of the circuit are connected to the IDT's. A network of resistors and capacitors matches the impedances of the SAW device and the amplifier [11].

High frequency circuits generate electromagnetic radiation, which leads to cross talk with the other circuits of the experiment. This may disturb the operation of these devices. It is therefore crucial to provide proper grounding, sufficient shielding and to apply decoupling capacitors for all electronic elements. All electrical connections in this work were made with *BNC* connectors and coax cables.

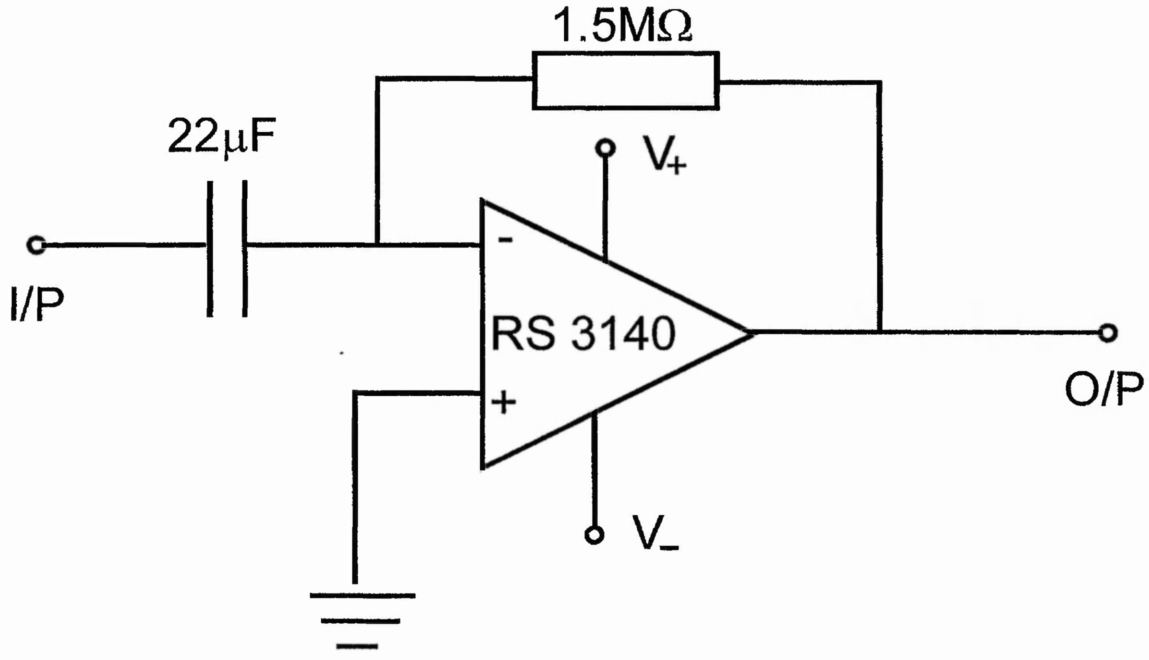

Figure 4.9: Differentiator circuit

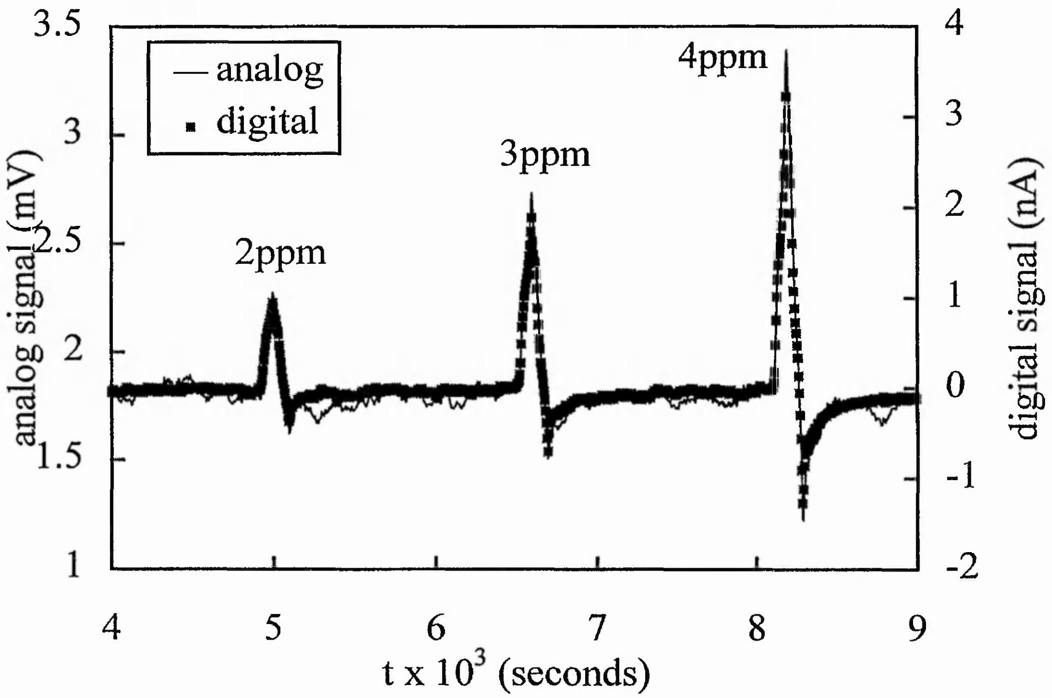

Figure 4.10: Comparison of the derivative plots obtained from the digitally processed signal and from the analogue differentiator circuit for 100s exposures of NO_2 in air at 100°C

Frequency measurements were carried out using a *Feedback S-230* frequency counter. The frequency counter was remotely controlled by a *RS 232* serial bus and set to a measurement period of one second which gave an accuracy of 1Hz. All frequency data were stored on a micro computer.

A continuous monitoring of the temperature was achieved by converting the voltage output of the thermocouple amplifier into a digital value using a 16 bit analog-digital conversion card. This temperature monitoring system was part of the PID temperature control.

4.5.4. Data Acquisition

The current of the conductivity sensors was measured with a Keithley 485 Picoammeter. Other voltage or current values such as the laser current were measured with a Keithley 175A Multimeter. Both Keithley meters were connected to a micro computer for data storage via an *IEEE 488* interface. The data acquisition program of the computer was set to a rate of one measurement per second.

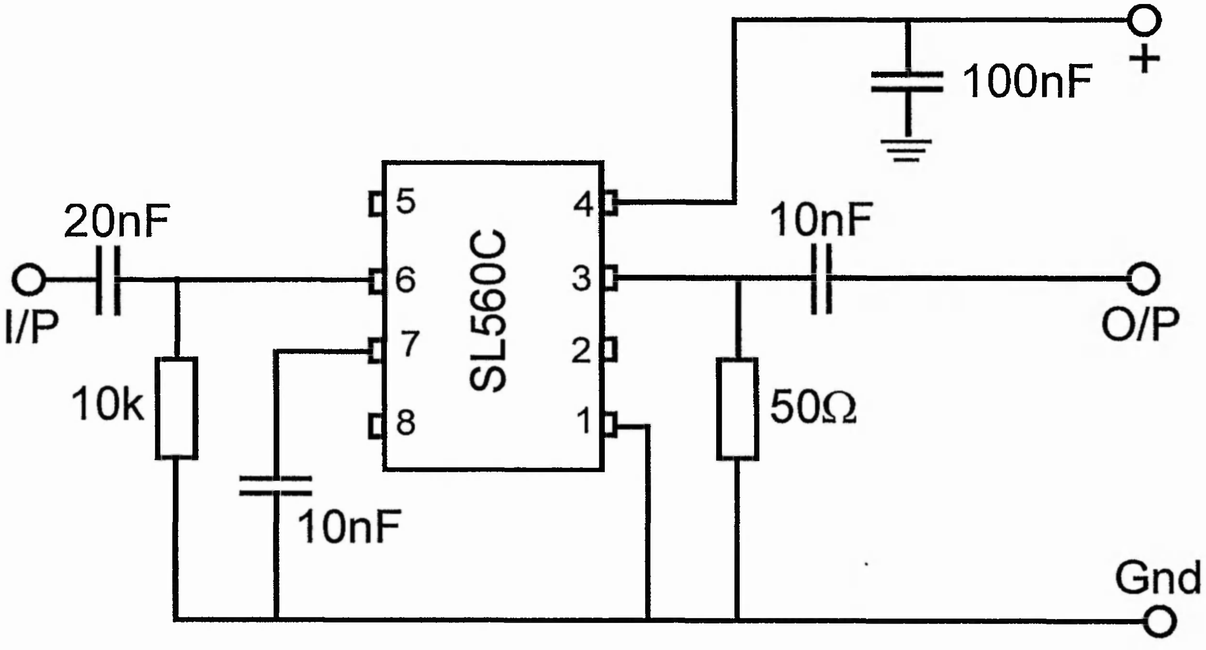

Figure 4.11: SAW resonator circuit

4.6. Evaluation of Sensor Properties

The second part of this chapter describes preliminary experiments with the conductivity, SAW and QCM sensors. These were carried out to gain a better understanding of sensor properties such as stability, sensitivity, and response characteristics and to gain insight into the behavior of the experimental set up in terms of temperature stability, signal stability, reproducibility, operation and robustness.

The gas sensing experiments at elevated temperature which are described at the end of this chapter were carried out following the experimental procedures of existing work by other research groups such as Bott and Jones [12, 13], Zhou and Gould [14], Hsieh *et al* [15, 16] and Wright *et al.* [17]. Phthalocyanine gas sensors operated at elevated temperature have the advantage of eliminating any sensor response due to humidity. They also found a faster and more sensitive response than sensors operated at room temperature. However, for a gas sensor working at elevated temperature a considerable operating power is required which can be a limiting factor for field and remote gas sensing applications where a long operation time without operator intervention is required.

4.6.1. Film and Sensor Characterisation

This first part of this section describes the monitoring of film evaporation and oxygen doping with conductivity, SAW and QCM sensors. These experiments were carried out using the vacuum evaporator unit. The data from these experiments provided insight into the response behavior and the operation range of the gas sensors and supported the implementation of the gas sensing system.

In the second part gas sensor responses to changes in flow rate as well as the interaction between Pc sensor and laser are discussed; both of these factors can lead to unwanted responses.

4.6.1.1 Sensor Response to Film Evaporation

The application of thin, chemically sensitive films to the substrate of the sensor is known to be an important step in the determination of the sensor properties [18]. It is suggested in the literature that a slow evaporation with a rate of 0.1nm/s onto room temperature substrate gives smooth, highly ordered α-phase copper phthalocyanine films [4, 18, 19]. As it is often found difficult to obtain films with consistent properties [19] a close control of the evaporation parameters is crucial to meet the requirements of a reproducible and meaningful investigation.

Figure 4.12 shows the response to an evaporation of a CuPc film at a rate of 0.1nm/s measured with a conductivity sensor and a quartz crystal microbalance simultaneously. After the evaporation was finished the thickness monitor displayed a film thickness of 160nm which was then used for all subsequent phthalocyanine evaporations in this work. Figure 4.12 shows that during the evaporation the change in frequency of the QCM is relatively small and undergoes a steep rise after the process is finished.

This behavior may be attributed to the subsequent change in film properties such as temperature of the film and stiffness. As the temperature of the film shortly after evaporation is still high the particles have good mobility leading to a rearrangement effect within the film. The behavior of the conductivity seems closely related to these processes since it follows the same trend as the QCM. The frequency and the conductivity reach a steady state only after several hours.

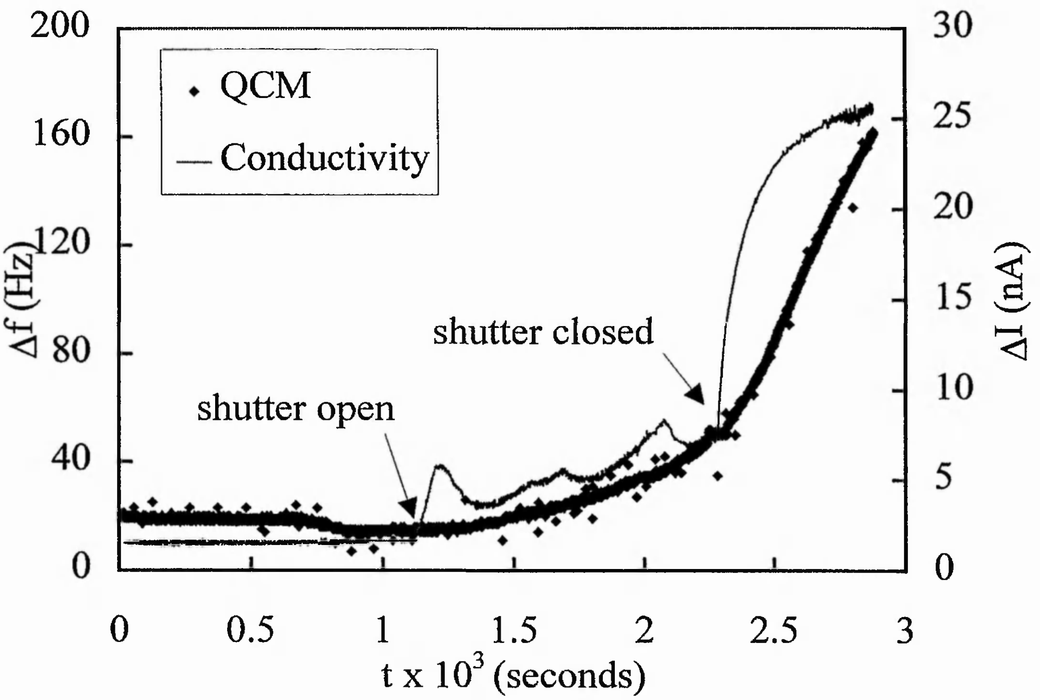

Figure 4.12: QCM and conductivity sensor response to evaporation of a CuPc film at a rate of 0.1nm/s

4.6.1.2. Oxygen Doping

The results presented in this section investigate the doping process of freshly evaporated Pc films with oxygen in air. These experiments provided a better understanding of the response behavior of the different sensor types used in this work and the general sensing capabilities of the phthalocyanine sensors.

Experiments were carried out within the evacuated chamber of the evaporator after Pc films were vacuum sublimed onto the substrates and left to stabilise for several hours. All films were applied under the same experimental conditions with consistent thicknesses measured with the *FTM 5* thickness monitor. After evaporation of the Pc films zero grade air was admitted into the vacuum chamber causing an increase in pressure from 5 x 10^{-6} Torr to atmospheric pressure within the period of a few seconds.

In NO_2 gas sensing phthalocyanine sensors are usually operated in air. O_2 is believed to be a main doping agent which enhances the gas sensing properties of the sensor. Oxygen incorporated in the films of phthalocyanine sensors affects the conductivity of the film [20] and moderates the gas sensing properties to other gases [21].

Figure 4.13 shows the initial conductivity response upon oxygen doping measured with a conductivity sensor and a SAW device during two different experiments. The conductivity change of the CuPc film on the SAW device was measured by monitoring the change in attenuation $\Delta\alpha$ of the amplitude. In both cases a strong initial increase in conductivity is followed by a slow and steady rise that can continue for several days.

The behavior of the conductivity and the SAW-attenuation sensor is generally similar. The conductivity sensor shows a steep initial response time followed by a slight drop in conductivity whereas the SAW response follows a steady rise. These differences may arise from the fact that the latter uses a more physical method to measure the conductivity whereas the former employs metal electrodes, which, within a certain range, may not follow ohmic behavior. Although a purely physical measurement of the conductivity in the form of surface wave attenuation $\Delta\alpha$ would certainly be the preferable measurement mechanism the signal to noise ratio is poor. The conductivity sensor was therefore chosen for measuring the film conductivity in the gas sensing experiments.

Figure 4.14 shows the response to oxygen doping of a QCM sensor (a) and a SAW sensor (b) both coated with copper phthalocyanine during two different experiments. The QCM shows a steady rise in Δf following a similar behavior as the SAW attenuation measurement in Figure 4.13(a). The similarity of these purely physical measurements indicates that the conductivity change of the Pc film correlates with the adsorbation of molecules on the surface of the film.

Surface acoustic wave sensors are pressure sensitive devices when Δf is used for measurements. In the oxygen doping experiments the SAW sensor configuration with a Pc coated and an uncoated reference path could not fully compensate the drastic pressure change of many orders of magnitude. Figure 4.14(b) shows an initial steep decrease in frequency during the admission of zero grade air into the vacuum chamber. This process is soon replaced by the response due to oxygen doping. This response shows similar characteristics for the QCM and SAW attenuation measurements to oxygen doping.

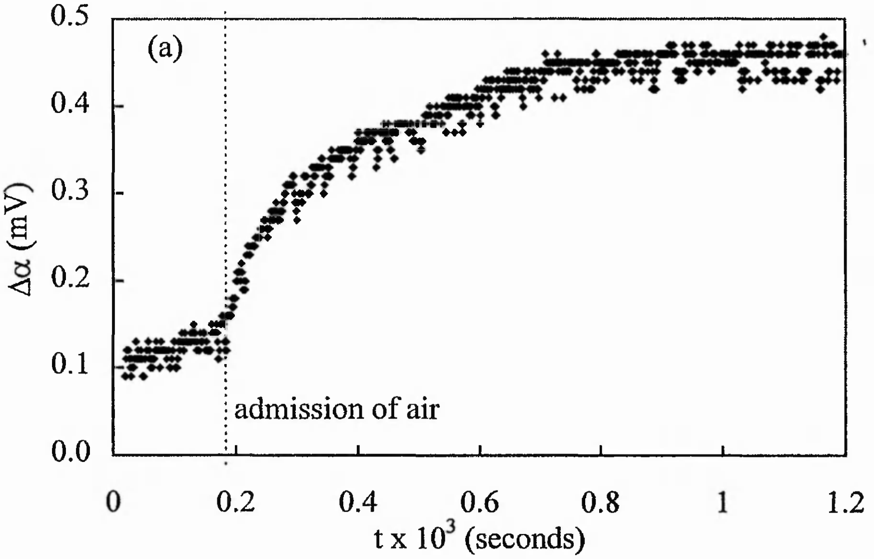

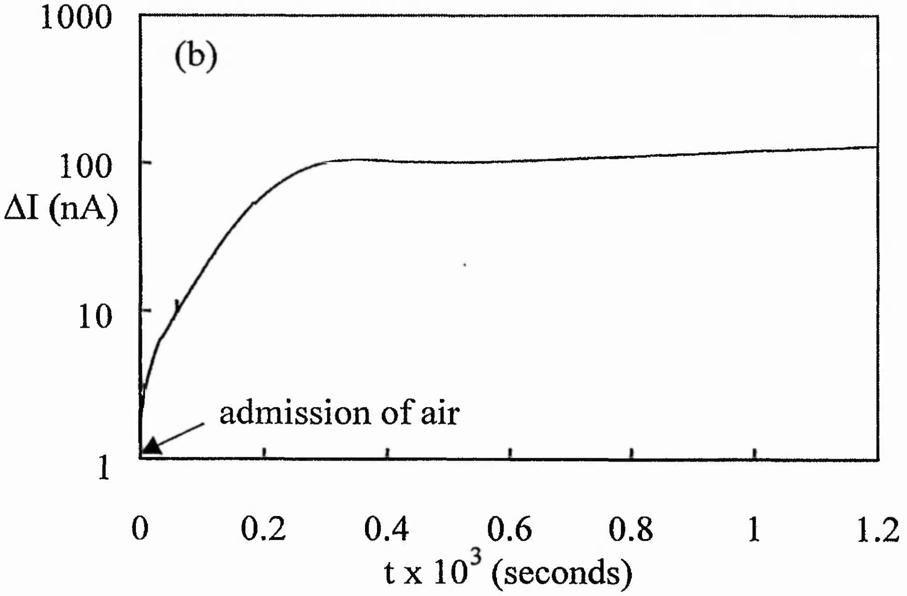

Figure 4.13: Initial response of (a) the conductivity sensor and (b) the SAW attenuation to oxygen doping

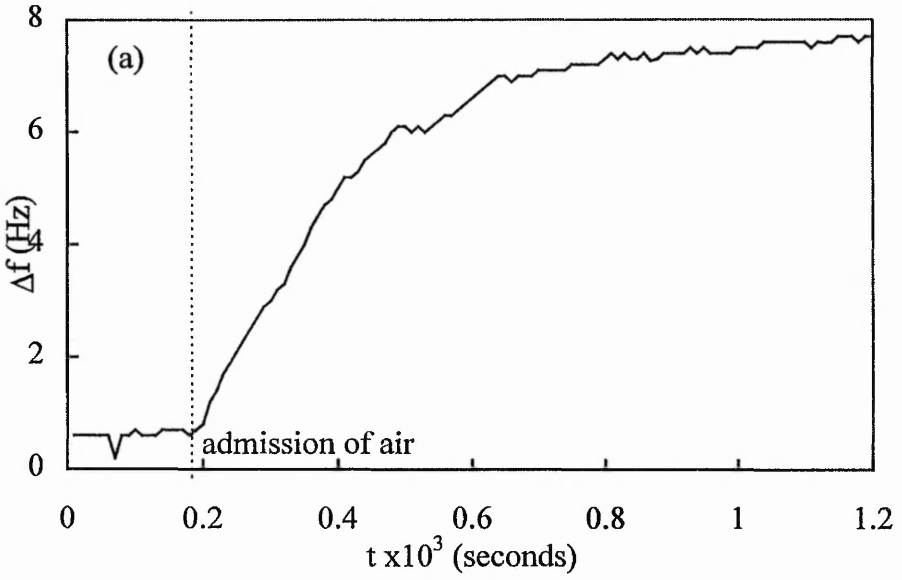

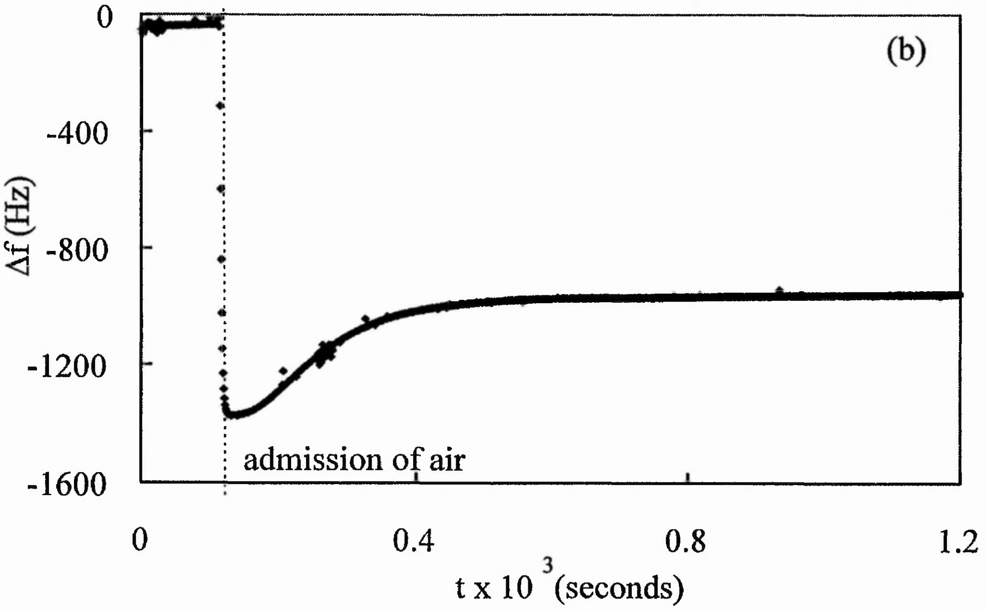

Figure 4.14: Response of (a) QCM sensor and (b) SAW sensor to oxygen doping

However, comparing the frequency responses of the SAW sensor and the QCM sensor to oxygen doping shows a change in frequency of approximately 400Hz and 8Hz respectively. This is a result of the higher resonance frequency of the SAW device (35MHz), in contrast to 2.458MHz of the QCM, which gives a significantly higher sensitivity of the SAW sensor despite the 2.5 times larger active surface area of the QCM. In gas sensing experiments under atmospheric conditions it is thought that pre-adsorbed oxygen is only replaced by NO_2 molecules. It can be concluded that, if a large change in mass loading (as in the oxygen doping experiments where O_2 adsorbs to a clean Pc layer) produces a frequency shift of only 8Hz on the QCM sensor, the change in frequency due to replacement of oxygen with NO_2 will be negligible for this QCM device. All gas sensing experiments in this work therefore used the more sensitive SAW sensors.

To verify that the response of the SAW sensor was genuinely due to oxygen doping a reference experiment was carried out exposing a Pc coated SAW device to pure nitrogen instead of air. Figure 4.15(a) shows the response of a SAW device to N_2 admission onto a freshly evaporated Pc layer. After the initial change in resonance frequency due to the admission of nitrogen there is no further response of the SAW sensor as in the case for oxygen doping.

In Figure 4.15(b) a freshly prepared layer was exposed to a mixture of nitrogen with 100ppm of nitrogen dioxide. The response of the Pc coated SAW device is less distinct but follows the same pattern as the oxygen doping, suggesting that oxidising gases adsorbing on the copper phthalocyanine film produce a change in mass loading which can be detected with a SAW device. An non-oxidising gas such as nitrogen does not significantly adsorb to the Pc layer and therefore does not produce a measurable change in resonance frequency of the SAW device.

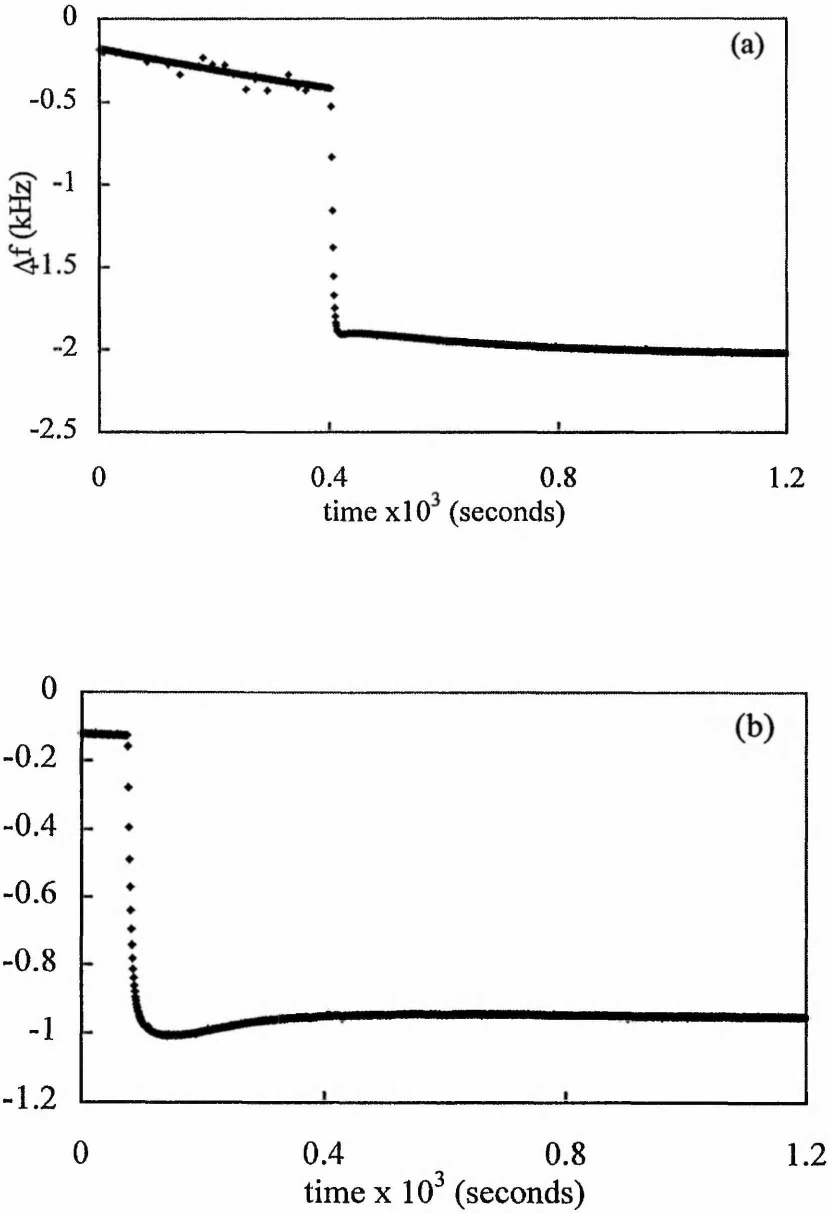

Figure 4.15: SAW response to (a) admission of pure nitrogen and (b) mixture of 100ppm NO_2 in N_2

4.6.1.3. Phthalocyanine Sensor Response to Different Flow Rates

All of the following experiments were performed with the phthalocyanine gas sensors implemented in the flow cell of the gas sensing system rather than in the evaporation system used for earlier preliminary work. The experiments in this section were carried out at room temperature conditions using phthalocyanine conductivity sensors.

Due to the dynamic nature of the equilibrium at the steady state of adsorption, the response of the sensor is also influenced by the gas flow rate. A higher flowrate will result in a cooling effect of the surface of the Pc film and will change the rate constants for adsorption and desorption. The desorption rate constant k_d can also be related directly to the flow rate F and the test chamber volume V:

$$k_d = \left(\frac{\alpha F}{V} + \beta \right) \tag{4.2}$$

with α and β being constants [16].

Figure 4.16 shows the response of the conductivity sensor to a flow rate of 1l/min, which was periodically increased for a time of 15s and the decreased down to the original flow rate. The sensor responds immediately to these changes. The change in film current after a short period of time is approximately proportional to the change of flow rate (Figure 4.16(b)).

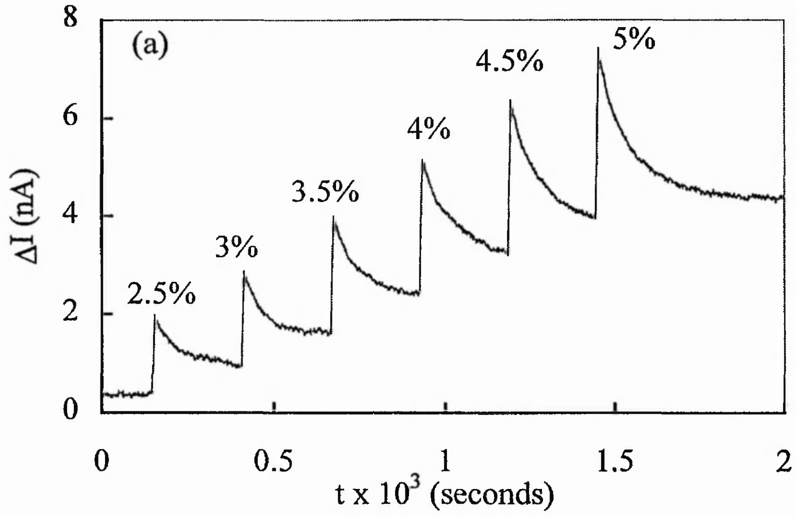

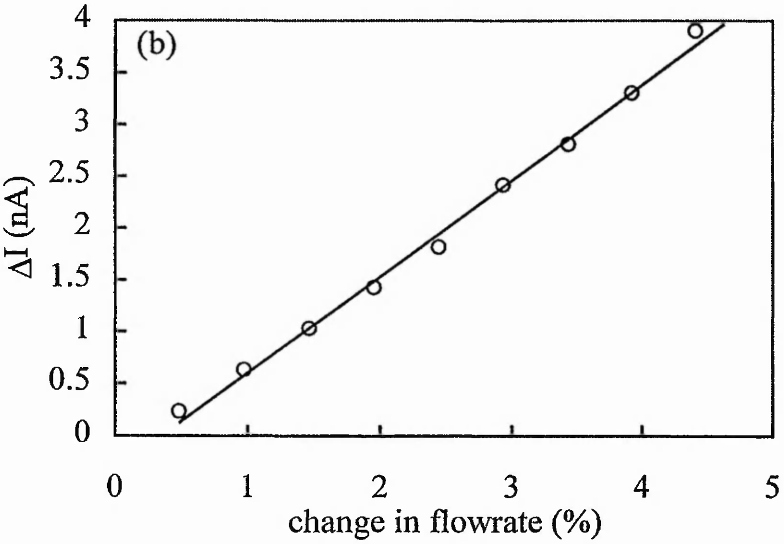

Figure 4.16: (a) Sensor response to a 15s increase in flow rate air followed by a decrease back to the basic flow rate of 1l/min and (b) relationship between sensor response and flow rate change

Figure 4.17 shows the response of the conductivity sensor to a 3.5ppm NO_2 exposure, which resulted in a 3.5% change in flow rate. In Figure 4.17(a) two consecutive response features can be distinguished. The initial rise can be ascribed to the change in flow rate to which the sensor responds immediately. After approximately 80 seconds the NO_2 gas has reached the conductivity sensor which results in drastic change in the sensor response. Both of these changes are illustrated even more distinct in the derivative plot of this experiment (Figure 4.17(b)) as two consecutive peaks.

These experiments clearly show that even slight changes in flow rate have to be taken into consideration for gas sensing experiments. Simple injection of the test gas, changing the flow rate, will initially produce a response which is a mere artifact from the change of the rate constants of adsorption and desorption. Therefore, a close control of the flowrate is crucial for gas sensing experiments with CuPc films to prevent unwanted responses. In order to maintain a constant flow rate in the gas sensing experiments, an increase in flow rate with test gas injection was balanced by a decrease in flow rate of the carrier gas and vice versa. This was done automatically by the computerised flow rate control system.

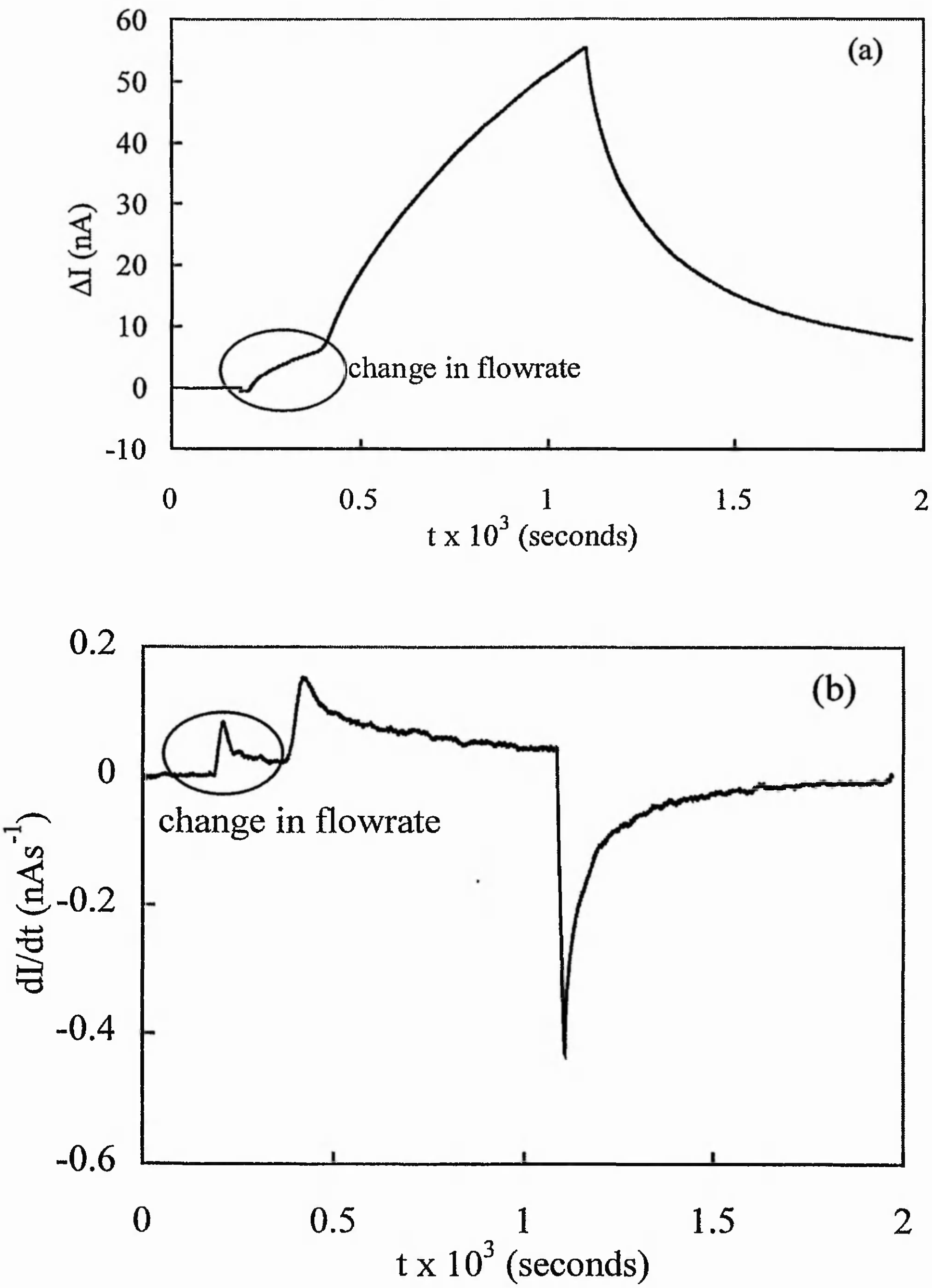

Figure 4.17: Exposure to 3.5ppm NO_2 for 700s with a change in flow rate of 3.5% (a) normal response and (b) derivative

4.6.1.4. Phthalocyanine Sensor-Laser Interaction

This section describes NO_2 sensing experiments using CuPc gas sensors which were illuminated by a high power laser diode to try to improve the interaction of the phthalocyanine layer with the test gas. Initial experiments describe the interaction of the laser with the conductivity and the SAW sensor.This section focuses on the interaction of the laser and the sensor without exposure to a test gas in order to rule out unwanted side effects, spurious signals and artifacts.

Initially the effect of laser illumination on the temperature of the SAW and conductivity sensors was measured with a thermocouple fixed to the surface of the sensor substrates opposite the Pc layer. There was no increase in temperature recognised, however, there may be heat lost along the thickness of the substrate. Figure 4.18 shows the response of a conductivity sensor to laser illumination. A possible increase in temperature of the sensor after the laser is switched on should reflect in a slow increase in film current. However, after the initial steep increase due to the photoelectric effect the current settles at a constant value within a few seconds. It is thought that an increase in temperature of the film would be a slower process, which could be distinguished from the photoelectric response. The sensor response to laser illumination at different temperatures is shown in Figure 4.19. ΔI has a maximum at around 90°C and decreases again at higher temperatures.

Figure 4.19 indicates that the current response of the sensor to laser illumination should increase significantly at higher temperature. The sensor response to laser illumination at room temperature in Figure 4.18 reaches a stable value after a few seconds which is similar to that for the current response at room temperature in Figure 4.19. Therefore, the temperature change of the Pc film due to laser illumination was regarded as insignificant.

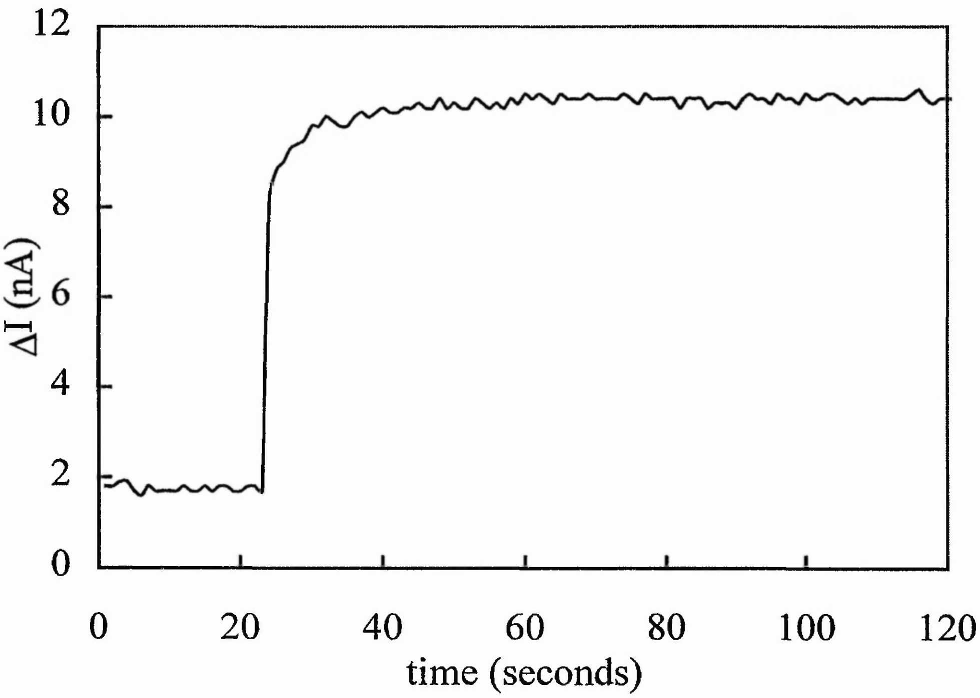

Figure 4.18: Sensor response to switching on the laser

Figure 4.20 shows the response of the SAW and conductivity sensor to a gradual increase in laser current. The data sheet for the laser diode gives a linear relationship between the current and the output power of the laser after the threshold current for laser generation of the diode of 33mA is reached [22]. Soon after exceeding the threshold current both sensors show an increase of conductivity and frequency respectively. The response of the conductivity sensor may be attributable to the photoelectric effect.

The change in SAW frequency however, may be dominated by acoustic wave - laser interaction. That is, because the change of frequency, which is in the range of kHz would otherwise correspond to a much larger change in conductivity than is actually observed (Figure 4.20(a)).

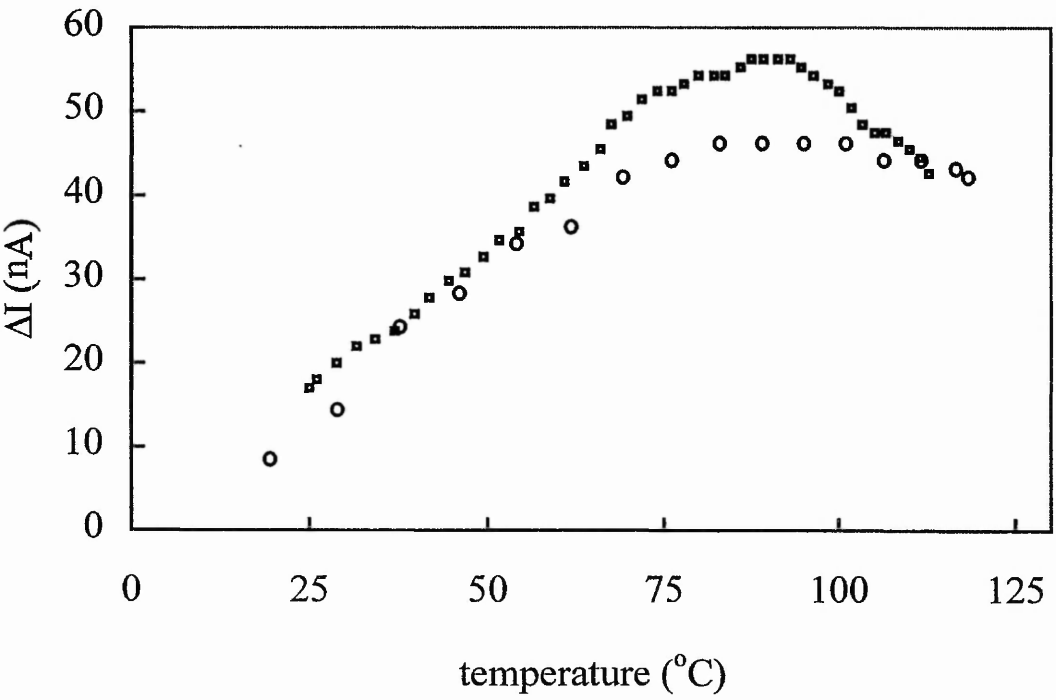

Figure 4.19: Photoelectric effect of the PC conductivity sensor at different temperatures in nitrogen (circles) and air (squares)

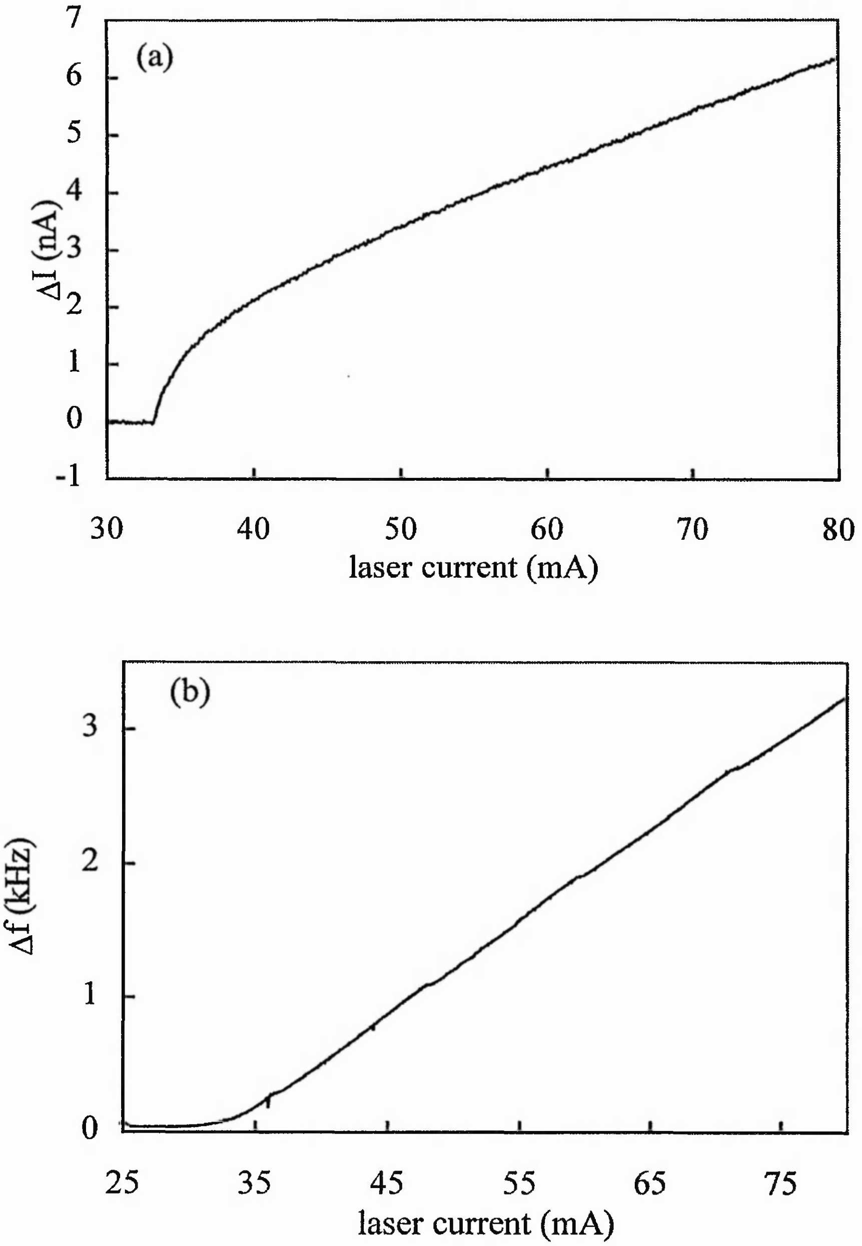

Figure 4.20: Photoelectric response of (a) the conductivity and (b) the SAW sensor to a gradual increase in laser current

4.6.2. Gas Sensing Experiments at Elevated Temperatures

Gas sensing experiments with vacuum sublimed phthalocyanine films are usually carried out at elevated temperatures to improve the sensitivity of the sensor and eliminate unwanted sensor responses due to humidity. The gas sensing experiments at elevated temperature presented in this section were carried out to confirm that the measurement system produced consistent results with other researchers in this field. All elevated gas sensing experiments in this section were carried out at a temperature of 102°C.

4.6.2.1. Exposures of the Conductivity Sensor to NO_2 with Different Concentrations

It is common to test the gas sensing capabilities of phthalocyanine sensors by exposing them to range of different concentration for a certain time with a fixed amount of time between consecutive exposures [23]. Figure 4.21 shows the response of a conductivity sensor upon NO_2 exposure to different concentrations in air. The exposure time in this experiment was 500s and the time between the exposures was 1500s – this period was just sufficient for the conductivity sensor to reach a stable baseline.

In Figure 4.21(b) the maximum peak height of the current response of the sensor compared to its baseline is plotted against the concentration of each cycle. The slope of this plot obeys a power law. This can be based on the assumption that the partial pressure of the test gas is proportional to the surface coverage $\theta \propto p$ (Figure 3.5) which was empirically found to reflect in a change in film current following the power relationship $\Delta I \propto \theta^n$ [14].

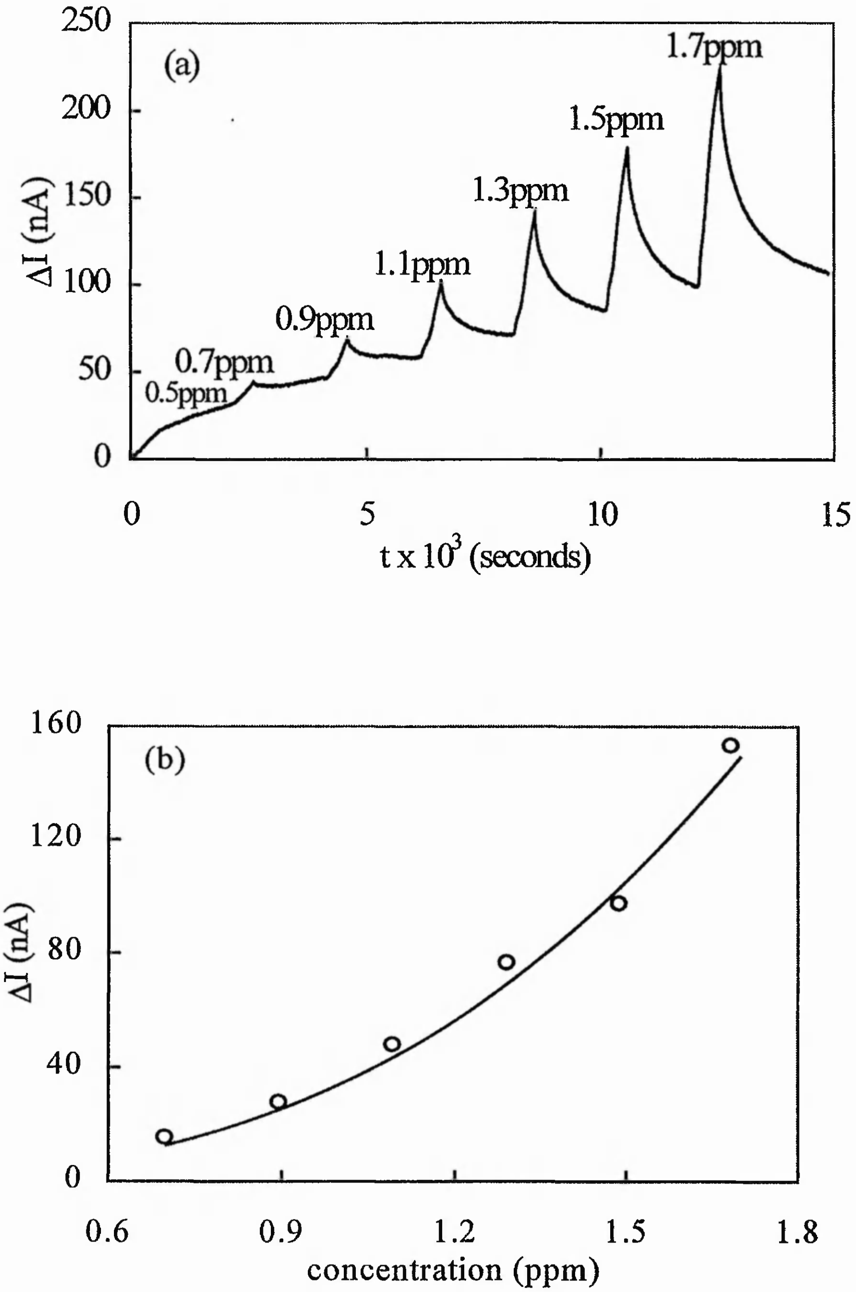

Figure 4.21: 500s exposures to NO_2 in air with different concentrations (a) sensor current vs. time (b) maximum peak height vs. concentration

Figure 4.21(a) also shows two of the problems one encountered in the field of gas sensing with phthalocyanine materials: a drift of the baseline and incomplete recovery of the signal which suggests that only a fraction of the adsorbed NO_2 molecules have desorbed again. Pre-adsorbed NO_2 molecules however, change the sensitivity of the conductivity sensor. This effect is the major draw back for a commercial implementation of Pc gas sensors since it causes a dependence of the sensitivity on the exposure history of the film. Electronic support systems such as electronic slope subtraction of the base line and resetting of the signal prior to each exposure may be used but these are expensive or inefficient.

The adsorption models suggest that initially there will be a maximum for the rate of adsorption of gas on the surface of the phthalocyanine film which is proportional to the partial pressure of the test gas. Figure 4.22(a) shows a derivative plot of the data in Figure 4.21(a). This way of plotting eliminates the offset of the baseline. The drift of the baseline may produce an offset in the derivative plot, which is usually negligible. Most importantly, however, is that one can obtain a definite value for the maximum slope after a very short period of time. This value is a direct representation of the concentration and appears to be linear for the given concentration range (Figure 4.22(b)). As well as the steady state value the initial rate is independent of the exposure time given a sufficiently long exposure for the maximum to occur.

4.6.2.2. NO_2 Exposures with a Fixed Concentration and Varying Exposure Times

To investigate the time independence and reproducibility of the derivative method, conductivity sensors were exposed to a concentration of 1ppm for a period from 50 to 350 seconds (Figure 4.23).

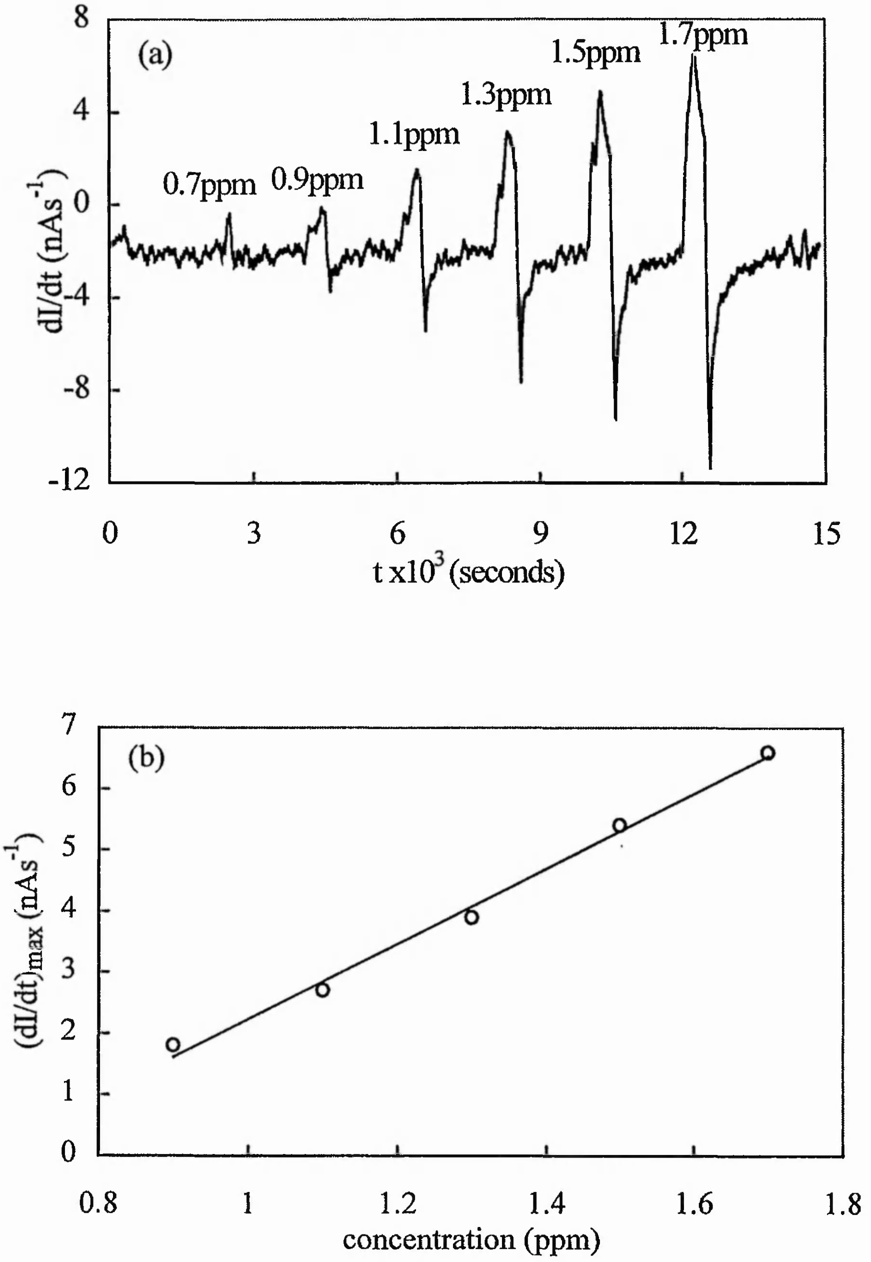

Figure 4.22: (a) derivative of the response of Figure 4.22 and (b) plot of the maximum value of the derivative for each exposure cycle versus concentration

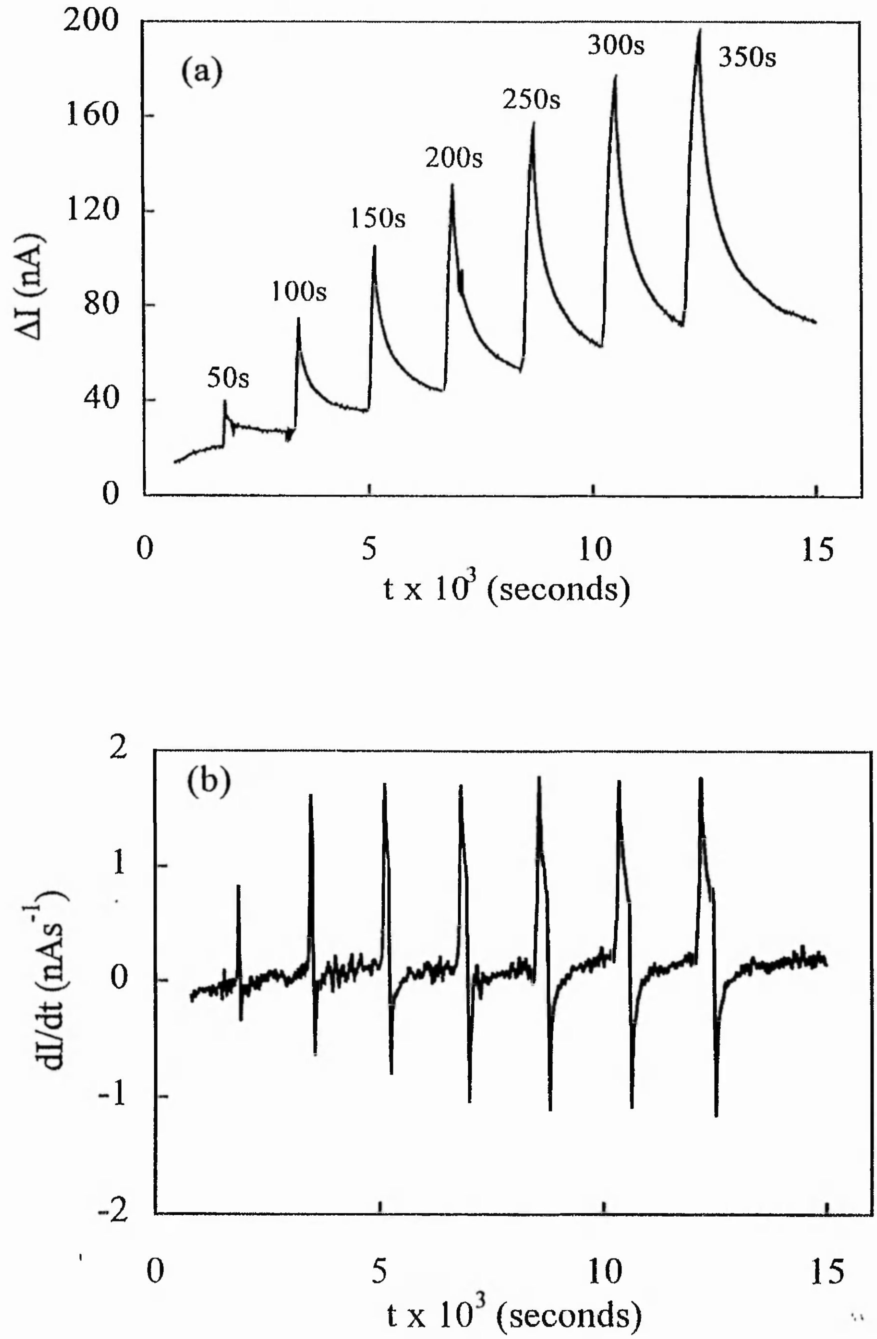

Figure 4.23:Exposure to 1ppm NO_2 in air for varying periods of time (a) plot of current vs. time and (b) derivative plot

From Figure 4.23(a) it is clear that a simple plot of the film current of the conductivity sensor against time does not provide sufficient information about the concentration of the test gas unless the exposure time is long enough for the process to reach equilibrium. The plot of *dI/dt* versus time, on the other hand, provides a maximum value, which is consistent for each of the 1ppm exposures longer than 200s.

Figure 4.24(a) shows a plot of the maximum derivative value of Figure 4.23(b) versus the time duration from the beginning of the exposure cycle to the moment at which the maximum derivative value is reached. In the case of a concentration of 1ppm this maximum is obtained after 200s. The exposure time to reach the maximum rate of adsorption will decrease with increasing concentration. Figure 4.24(b) shows a plot of the time between the beginning of the gas exposure to that moment when the maximum derivative value occurs for the different concentrations in the experiment of Figure 4.22. This graph shows that the response time of the sensor becomes significantly faster with higher concentrations.

4.6.2.3. Continuous Monitoring of Gas Concentration

In many applications a continuous monitoring of the environment is necessary. In order to achieve this a gas sensor is required which works equally well at low and high surface coverage and reaches a steady state in a reasonably short time. CuPc is not well suitable since its steady state response time is usually too long.

However, Figure 4.25(a) shows the response of a conductivity sensor to a stepwise increase of the concentration of 0.2ppm every 200 seconds followed by a decrease with the same increment. For the plot of ΔI versus t this is reflected in a stepwise increase or decrease in slope. The derivative plot shows peaks for

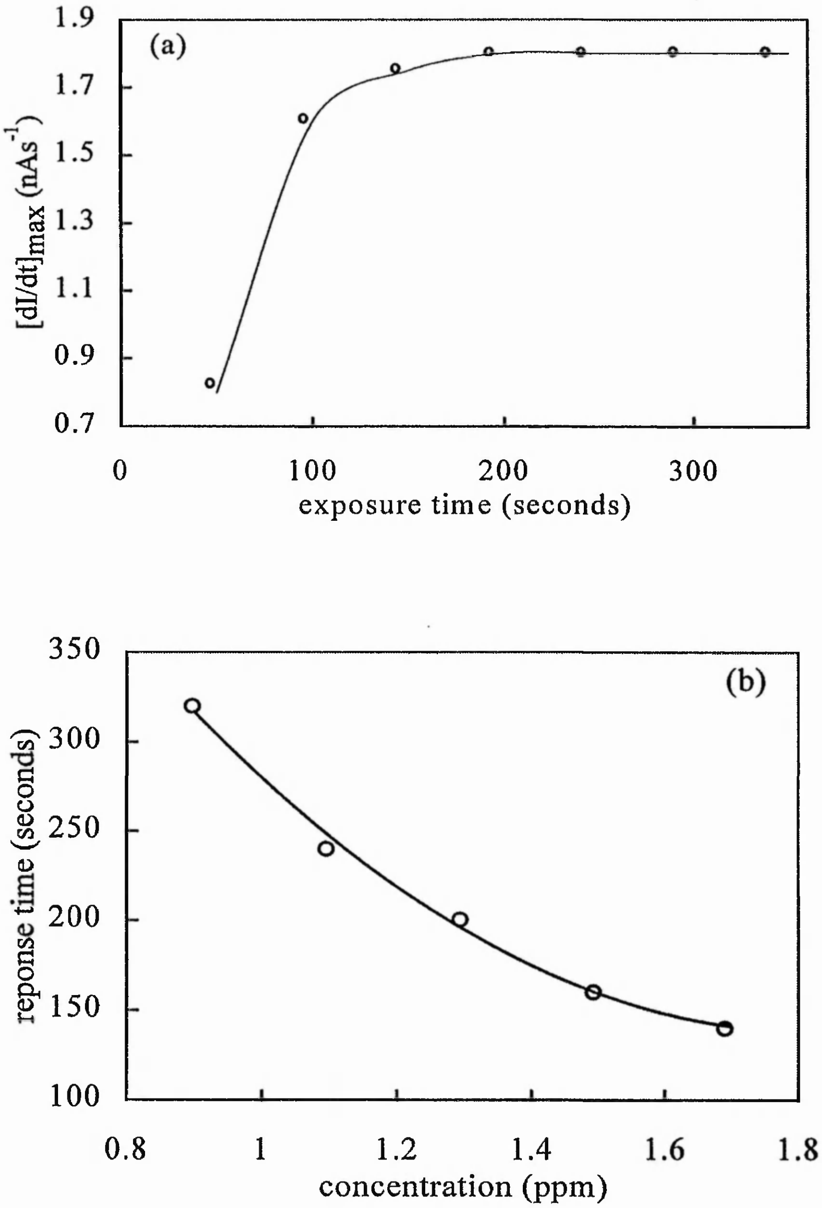

Figure 4.24: (a) The value of $[dI/dt]_{max}$ which correlates to the concentration of the test gas is obtained for 1ppm NO_2 in air after only 200s exposure time and has a constant value for any other exposure time. (b) time duration from the beginning of the exposure until $[dI/dt]_{max}$ is obtained for the experiment in Figure 4.22

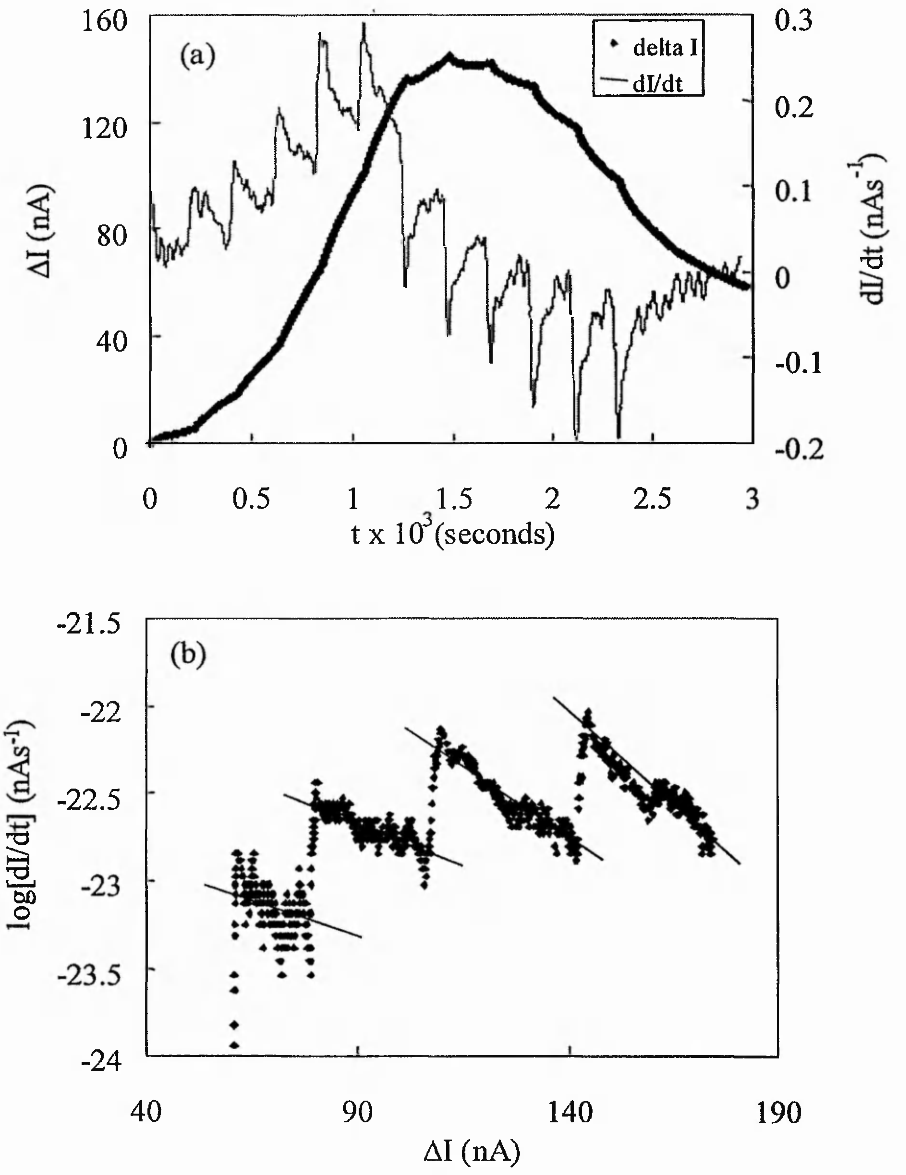

***Figure 4.25:** (a) Step exposure to NO_2 from 0.5ppm to 1.5ppm in steps of 0.2ppm and down to 0.5ppm again. (b) Elovich plot of the same experiment from 400s to 1250s.*

each change in concentration. Although these plots give an indication of the concentration changes they do not provide a definite value for the state of the system i.e. the concentration at any point in time.

A plot of *dI/dt* versus *ΔI* (Elovich plot) is thought to follow a linear relationship upon adsorption of a constant concentration of NO_2. Figure 4.25(b) shows such a plot for the concentrations 0.9, 1.1, 1.3 and 1.5ppm. Every concentration has a corresponding slope. Each of these slopes is a representation of the current state of the system i.e. the concentration of NO_2 in air.

This chapter has shown some preliminary experiments with CuPc coated sensors and detailed a number of gas sensing experiments at elevated temperature. Despite the advantages of maintaining a temperature above 100°C the operation of phthalocyanine gas sensors has a high power consumption and needs a close control of the temperature. For many gas sensing applications it would be an advantage to have a sensing system which can operate at room temperature with comparable properties as elevated temperature sensing systems. In the next chapter approaches are investigated to building a viable phthalocyanine gas sensor which can operate at room temperature with properties comparable to those of their high temperature counterparts.

References

[1] A.A.Oliner, Acoustic Surface Waves, Springer-Verlag, New York, (1977), 305

[2] W.S.Deforest, Photoresist: Materials and Processes, McGraw-Hill, New York, (1975)

[3] P.D.Hooper, Electrical Properties of Thin Film Devices, PhD Thesis, Nottigham Trent Univ., (1996), 29

[4] A.K.Hassan, R.D.Gould, Phys.Stat.Sol.(a), **132**, (1992), 91

[5] A.Sussmann, J.Appl.Phys., **38**, (1967), 2738

[6] S.J.Martin, A.J.Ricco, Sens.Actu., **A21-A23**, (1990), 712

[7] M.I.Newton, T.K.H.Starke, G.McHale, M.R.Willis, A.Krier, Elect.Lett., **34**, No.17, (1998)

[8] A.K.Ray, S.M.Tracy, A.K.Hassan, IEE Proc.-Sci.Meas.Technol., **146**, (1999), 205

[9] G.B.Clayton, Operational Amplifiers-2nd ed., Butterworths, (1979), 388

[10] G.B.Clayton, Operational Amplifiers-2nd ed., Butterworths, (1979), 244

[11] D.S.Ballantine, R.M.White, S.J.Martin, A.J.Ricco, E.T.Zellers, G.C.Freye, H.Wohltien, Acoustic Wave Sensors: Theory, Design, Physio-Chemical Applications, Academic Press, (1997)

[12] B.Bott, T.A.Jones, Sens.Actu., **5**, (1984), 43

[13] B.Bott, T.A.Jones, Sens.Actu., **9**, (1986), 19

[14] Q.Zhou, R.D.Gould, Thin Solid Films, **317**, (1998), 436

[15] J.C.Hsieh, C.J.Lu, Y.H.Ju, Thin Solid Films, **322**, (1998), 98-103

[16] C.J.Liu, J.C.Hsieh, Y.H.Ju, JVac.Sci.Technol., **A14**, No.3, (1996)

[17] J.D.Wright, A.V.Chadwick, B.Meadows, J.J.Miasik, Mol.Cryst.Liq.Cryst., **93**, (1983), 315

[18] Neil B McKeown, Phthalocyanine Materials Synthesis Structure and Function, Chemistry of Solid State Materials 6, (1998)

[19] T.Parr, An Investigation into the Structural, Optical and Electrical Properties of Phthalocyanines with Regard to their Feasibility as Commercial Gas Sensors, PhD-thesis, Univ. of Lancaster, (1995)

[20] A.Ahmad, R.A.Collins, Thin Solid Films, **217**, (1992), 75

[21] A.V.Chadwick, P.B.M.Dunning, J.D.Wright, Mol.Cryst.Liq.Cryst., **134**, (1986), 137

[22] Data Sheet: Phillips CQL806/30 visible light laser diode, (1998)

[23] A.K.Ray, M.J.Cook, S.C.Thorpe, S.Mukhopadhyay, Phys.Stat.Sol., **140**, (1993), K85

Chapter 5: Results and Discussion

5.1. Overview

In the previous chapter a gas sensing system was developed and tested for conductivity sensors with CuPc sensitising layers at elevated temperature. This chapter describes gas sensing experiments with copper phthalocyanine conductivity and SAW sensors at room temperature using the previously developed system. Subsequently it investigates the response kinetics of these room temperature sensing experiments.

Operating phthalocyanine gas sensors at room temperature has the advantage of a relatively low power consumption since there is no heater required [1]. This would be a great advantage for the implementation of portable and remote gas sensing devices. The sensor should also be able to respond in an appropriate time to changes in gas concentration.

This chapter describes the development of phthalocyanine gas sensor, which can be operated at room temperature with comparable properties as in elevated temperature sensing experiments. Initially it shows the response of copper phthalocyanine coated conductivity and SAW sensors to NO_2. Changes in the sensing capabilities of these sensors are then investigated by using a diode laser illuminating the sensitising layer to cause photo excitation of the Pc molecules. The findings of these experiments lead to the introduction of NO_2 doping of the Pc layer, which significantly improved the room temperature sensing properties of the conductivity sensors. A cooling of the phthalocyanine layer to liquid nitrogen temperature prior to the gas sensing work was found to give conductivity as well as SAW sensors some interesting properties.

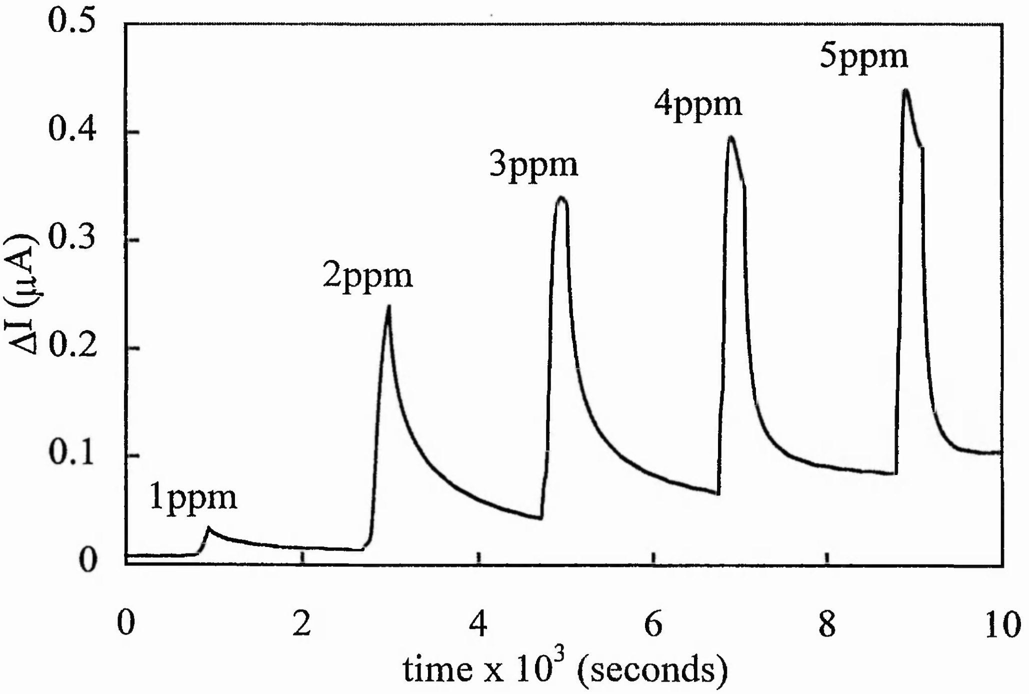

Figure 5.1: Response of conductivity sensor to 300 seconds NO_2 exposure at room temperature

Since the steady state response of Pc gas sensors occurs only after a relatively long period of time [2] the following section investigated kinetic responses of the NO_2 doped and the cooled Pc gas sensors in order to quantify the concentration of the test gas within the first, few minutes of exposure [3]. The proposed system using kinetic responses of doped and cooled Pc gas sensors is shown to allow a determination of the gas concentration which is faster than using the steady state response and independent of the exposure history of the phthalocyanine film.

5.2. Gas Sensing with an Untreated Phthalocyanine Layer

Initially the response of Pc sensors at room temperature with untreated films was investigated. Although the conductivity and SAW sensors responded to NO_2 exposure their performance in terms of sensitivity and reversibility was not as good as in elevated temperature experiments [4]. This motivated further investigations to enhance the properties of the gas sensors. The different response patterns of the conductivity and the SAW sensor indicate that there could be two separate dominating mechanisms involved in the adsorption of NO_2 on the Pc layer.

5.2.1. Response of the Conductivity Sensor Operated at Room Temperature to NO_2 Exposure

Figure 5.1 shows a typical response of a conductivity sensor exposed to NO_2 and operated at room temperature. Although there is a clear response for each of the concentrations the reversibility of the signal could be improved. The magnitude of the signal varies significantly even within this small concentration range. Below 2ppm the signal is small whereas at concentrations above 3ppm

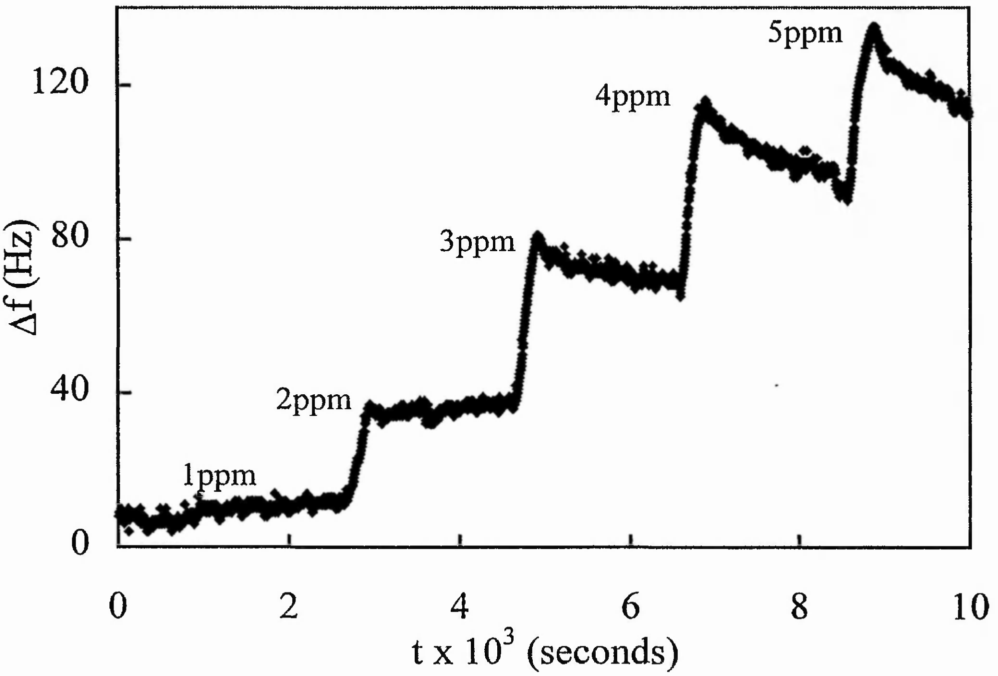

Figure 5.2: Response of SAW sensor to 300 seconds NO_2 exposure at room temperature

the current saturates after a relatively short time. As the exposure continues the current decreases before the test gas is turned off.

This behaviour is not desirable for gas detection since it allows sensible measurements only within a very narrow concentration range. The signal is also very dependent on the exposure history and therefore, has poor reproducibility. Thus, a correlation of the signal with the gas concentration is only valid if all parameters as well as the exposure history of the Pc film are known precisely [5].

5.2.2. Response of Surface Acoustic Wave Sensors to NO_2 Exposure at Room Temperature

A SAW sensor was installed next to the conductivity sensor and simultaneous measurements were carried out. The sensitising layers of both sensors were applied during the same evaporation [6].

Unlike the conductivity sensor the SAW sensor (Figure 5.2) does not show a significant recovery of the signal. At 5ppm the response is even lower than at the 4ppm exposure. Together with the lack of recovery this indicates a saturation of the film with gas molecules which is not fully reversible.

5.2.3. Discussion of Conductivity and SAW Response of Untreated Room Temperature Pc Sensors

The obvious difference between the data from the conductivity and the SAW sensor is the lack of signal recovery of the latter. SAW sensors respond to changes in mass loading and film conductivity. Ricco *et al.* [7] suggested that the contribution of mass loading for Pc-SAW sensors is several orders of magnitude smaller than the contribution due to the change in conductivity and can therefore

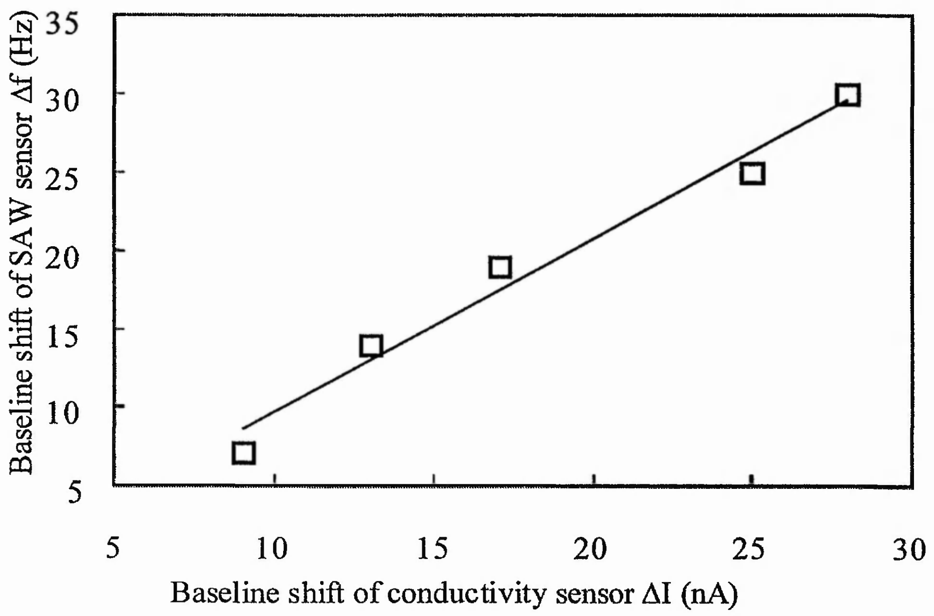

Figure 5.3: Correlation between the shift in baseline of the conductivity sensor and the SAW sensor before and after NO_2 exposures during the experiment in Figure 5.1 and Figure 5.2

be neglected. However, there will only be a distinct change in frequency of the SAW device if the conductivity of the Pc film σ_S has a value which lies within two orders of magnitude of v_0C_s which is a constant for the SAW devices used in this work and has a value of $1.6x10^{-6}$mhos.

The phthalocyanine films in these experiments have a conductivity in the order of 10^{-10}mhos which is significantly lower than the value for v_0C_s. This means that a 2ppm exposure as in Figure 5.1 would therefore be equivalent to a change in frequency of $2x10^{-4}$Hz, which is too small to be detected by the frequency counter. The actual value for Δf obtained from the SAW device is 35Hz suggesting that the dominating contribution to the change in resonance frequency must be mass loading.

Figure 5.1 and Figure 5.2 suggest that the shift in baseline of the SAW sensor and of the conductivity sensor before and after each exposure shows a correlation (Figure 5.3) indicating that the response of the SAW sensor may be a representation of the baseline shift of the conductivity sensor.

This indicates that the SAW gas sensing device monitors a process which is indirectly reflected by the conductivity sensor as a change of baseline. It suggests the presence of two different components for the adsorption, which contribute differently to conductivity and mass loading.

Archer *et al.* [8] have proposed a heterogeneous surface site model for gas adsorption on Pc's. This model provides for a fast initial response of the sensor on easily accessible, weakly binding adsorption sites and a slow response caused by the replacement of O_2 by NO_2 on strong adsorption sites. On the basis of experimental results, Wang *et al.* [9] proposed a theoretical model for gas sensing on Pc films, which considers gas adsorption and desorption on the film surface and gas diffusion through the film. Yu *et al.* [10] argue that the conductivity change due to the adsorption of molecules on the surface will be

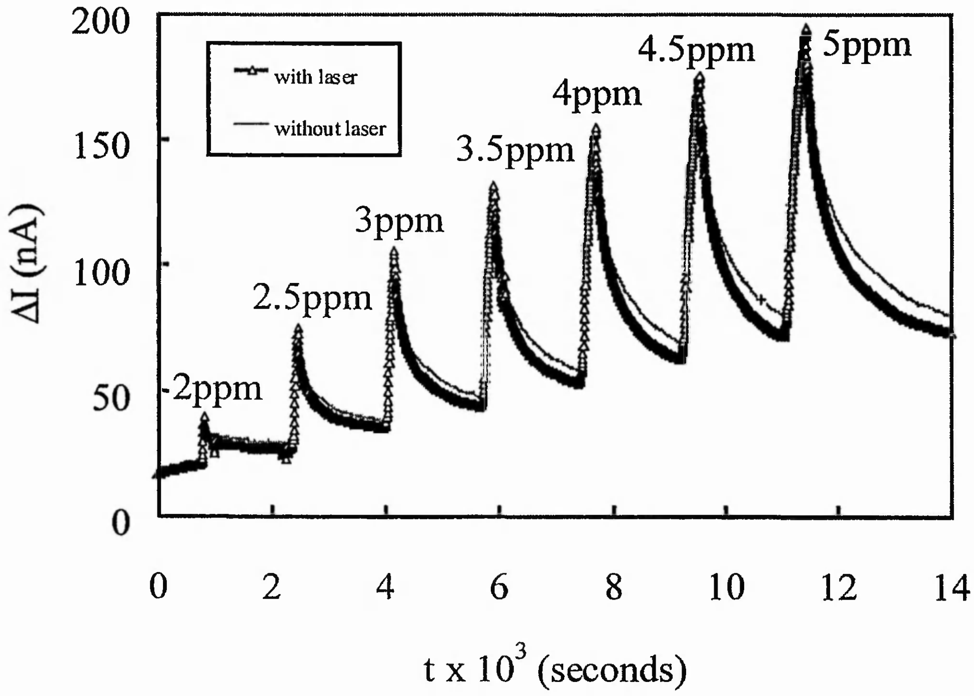

Figure 5.4: Response of illuminated and unilluminated conductivity sensors exposed to different concentrations of NO_2 for 300s

much larger than that due to bulk effects. On the other hand bulk adsorption involves a much larger amount of molecules and mainly contributes to the mass loading whereas the comparatively small number of molecules from surface adsorption contributes very little to the mass loading.

A possible explanation for the response of the surface acoustic wave device to gas exposure is, that the SAW sensor operated at room temperature mainly detects the slow component of gas adsorption which involves higher activation energies of adsorption and desorption. This would result in a less reversible response. The correlation between the irreversible changes in baseline (Figure 5.3) indicate that it could be a bulk diffusion process which causes the irreversible change in baseline of the conductivity sensor.

Hsieh *et al.* described in their work [11] with lead phthaloclyanine the presence of simultaneous bulk diffusion and surface adsorption effects. For the CuPc material used in this work a similar mechanism may exist.

One possible way to improve the sensing properties of phthalocyanines would be to alter the chemical compound by substituting new chemical groups to the molecule. Derivates of phthalocyanine materials which show better gas sensing properties than the basic molecules can be very difficult to synthesise and may be expensive [12,13]. Laser illumination leads to photo excitation of the phthalocyanine molecules and, in the presence of molecular oxygen, to the generation of oxygen superoxide (O_2^-) and perhaps singlet oxygen($^1O_2$) [14]. These species are highly reactive and may improve the interaction of the phthalocyanine layer with the test gas [15].

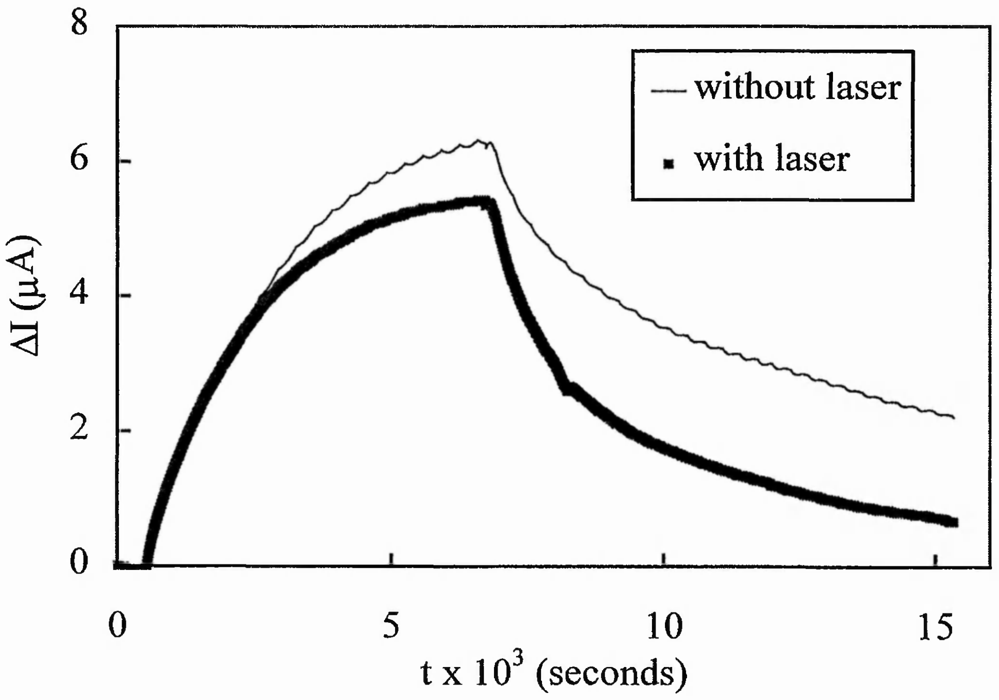

Figure 5.5: Response of illuminated and unilluminated conductivity sensors exposed to 2ppm NO_2 for 6500s

5.3. Laser Illumination of Pc Gas Sensors

This section explains gas sensing experiments where sensors were illuminated with a 30mW laser diode in order to improve the gas sensing properties of the sensor [16]. Conductivity sensors did not show a great difference in response to NO_2 exposure between illuminated and unilluminated devices. However, illuminated SAW sensors showed remarkably different response patterns than their unilluminated counterparts. The responses of both conductivity and SAW sensors provide further indication of the existence of two separate adsorption mechanisms (surface adsorption and bulk diffusion). It is suggested that the laser mainly effects the bulk diffusion mechanism.

5.3.1. Gas Response of Illuminated Conductivity Sensor

The following set of experiments employed an illuminated conductivity sensor as well as an unilluminated sensor for reference. The sensors were located side by side on the same substrate.

During the first experiment the sensors were exposed to different concentrations of NO_2 for 300s. Figure 5.4 shows that, for these short exposures there is little difference between the response of the illuminated sensor and the reference sensor. However, it should be noted that the overall current for the illuminated conductivity sensor is approximately 10nA higher than the overall current for the unilluminated conductivity sensor.

The difference between the two becomes more distinct for longer exposure times (Figure 5.5). Although the response of the illuminated sensor saturates at a lower current than that of the reference device it shows much better recovery. The

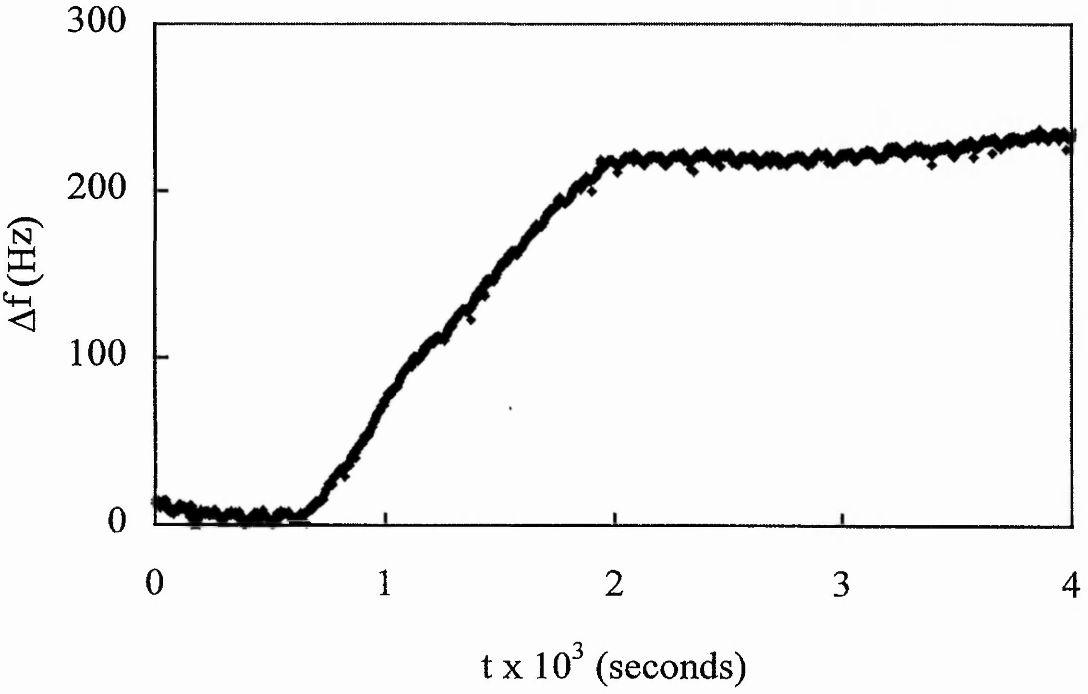

Figure 5.6: Response of the SAW sensor to 10ppm NO_2 for 300s without laser illumination

former recovers to nearly 90% of the maximum value whereas the latter reaches only a 65% recovery. However, this effect becomes only significant at exposure times above 2000s. For steady state gas sensing the better recovery of the illuminated sensor would certainly provide a more controllable exposure history.

The same set of experiments as above was carried out using the laser in different pulsed modes. The mark-space ratio of the pulses was set to 0.1, 0.5 and 0.75. The pulse periods were set to 10μs, 100μs, 1ms, 10ms and 100ms. For pulsed lasers the behaviour of the conductivity sensors was found to be the same as for the continuous mode. However, as would be expected, with decreasing mark-space ratio the difference between the illuminated and the reference device became less distinct. The pulse length did not influence the results in any of the experiments.

5.3.2. Gas Response to Illuminated SAW Sensor

In contrast to the conductivity sensors, which show little difference between the gas response of illuminated and unilluminated sensors, the SAW sensors showed a distinct difference in the gas response between illuminated and unilluminated films.

Figure 5.6 shows the response of a SAW sensor to exposure of 10ppm NO_2 for 300s without any laser illumination which serves as a reference for the following experiments. Due to experimental limitations it was not possible to have a reference device running simultaneously. The figure shows similar features as previous SAW sensing experiments: a distinct response but no recovery of the signal. For a consistent performance after each experiment the sensors were heated to 100°C for several hours and subsequently kept under stable temperature and flow conditions inside the test chamber overnight.

In Figure 5.7(a) the experiment of Figure 5.6 was repeated while illuminating the sensor with laser light in continuous mode. The frequency change upon gas exposure has clearly decreased. However, after approximately 800s the signal recovers quickly far below the original baseline.

The sensor response for the same experiment using a pulsed laser with a mark-space ratio of 0.5 and a period of 1ms is presented in Figure 5.7(b). This graph shows a larger change in frequency upon gas exposure with a recovery back to the original baseline. The above experiments were repeated for periods of 10μs and 100ms and very similar behaviour for response and recovery when exposed to NO_2.

5.3.3. Discussion of Illuminated Conductivity and SAW Gas Sensor Responses

The results for the conductivity and SAW response to NO_2 exposure suggested that laser illumination may have an effect on the gas adsorption and desorption behaviour of the sensor which is reflected in a significant change in SAW resonance frequency but only to a small extent in a change in conductivity.

In the previous section, which showed the gas sensor responses of unilluminated Pc sensors it was suggested that gas adsorption has two different components which could be ascribed to bulk diffusion and surface adsorption. It was also suggested that bulk diffusion mainly reflects as a response due to mass loading and only to a smaller extent in conductivity whereas surface adsorption has a dominating role in the electrical conductivity of the phthalocyanine film. This supports work previously reported on PbPc by Hsieh *et al* [11].

Laser illumination only produced a significant effect on the conductivity sensor for long exposure times, the recovery of the signal for a long exposure cycle improved. The slow response elements of the conductivity sensor are thought to be associated with bulk diffusion. The sensor response shown in Figure 5.7 may arise from an increased desorption of NO_2 molecules from the bulk of the Pc film. This should be reflected in a distinct response of the SAW sensor. Indeed, the SAW device which is believed to respond mainly to mass changes showed smaller response for a continuous wave illumination and a recovery to below the original baseline.

The data for SAW and conductivity sensors may be interpreted as the laser increasing the rate of desorption of the slow component of the adsorption mechanism (the bulk diffusion) but it has very little effect on surface adsorption. If true, in an ideal copper phthalocyanine gas sensor one of the two components should be eliminated to simplify its response behaviour. When either bulk diffusion or surface adsorption would be eliminated, the following sensor behaviour could be predicted from the results of the room temperature sensing experiments:

1. Elimination of bulk diffusion would result in a good response of the conductivity sensor to NO_2 exposure together with a very good recovery of the signal. The SAW sensor should show very little response to NO_2 since surface adsorption is thought to cause only a small change in mass loading compared to bulk diffusion.
2. Elimination of surface adsorption should reduce the overall response of the conductivity sensor to NO_2 exposure. It should recover more slowly than in the former case. Laser illumination would be expected to have a distinct effect on the sensing response of conductivity and SAW sensors. The SAW sensor should show a distinct response to NO_2 exposure.

Since it would certainly be impossible to fully eliminate one or the other mechanism this will be also referred to as changing the ratio of surface to bulk adsorption sites. From the two statements above it can be concluded that the

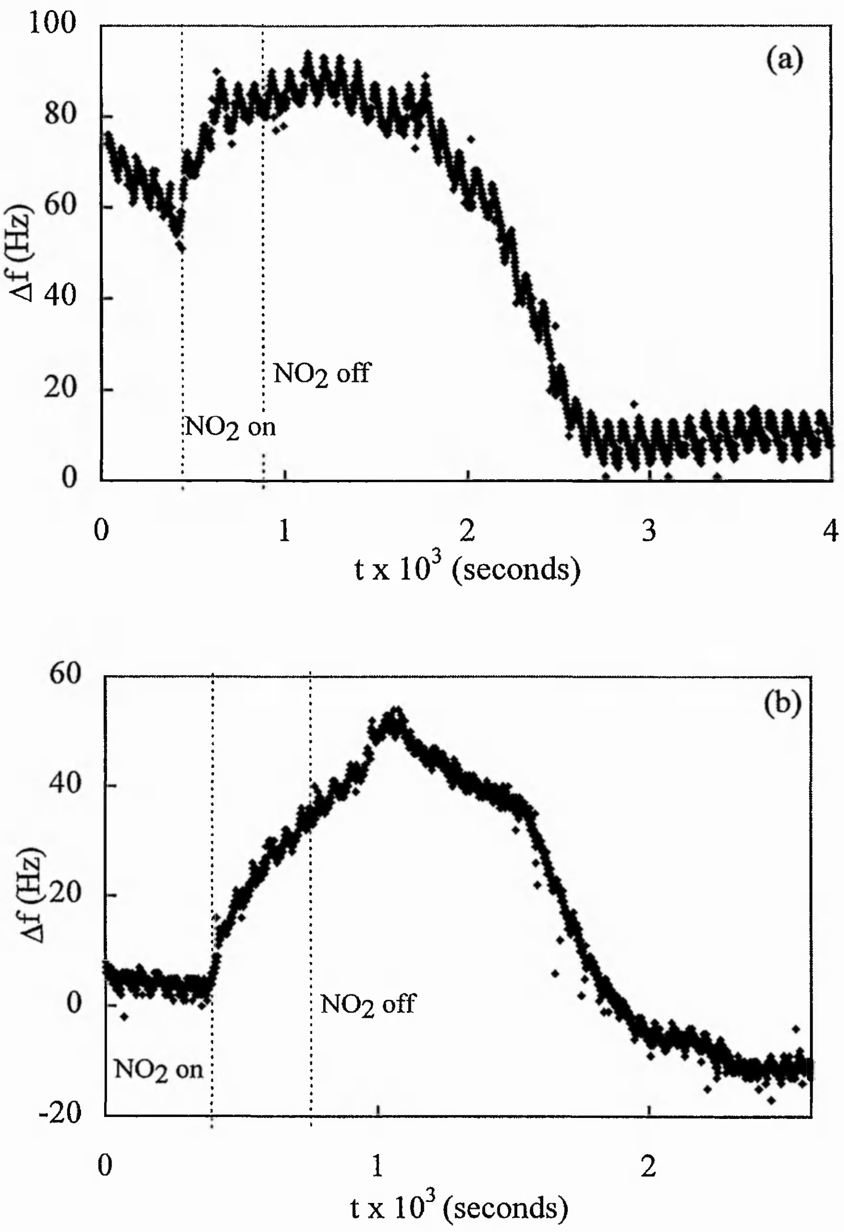

Figure 5.7: Response of the SAW sensor to 10ppm NO_2 for 300s (a) with continuous laser illumination and (b) with pulsed laser (mark-space ratio: 0.5, period: 1ms)

elimination of bulk diffusion in the CuPc layer would be preferable for conductivity sensors since it would accelerate the adsorption and desorption processes. In order to eliminate bulk diffusion one would have to fill the adsorption site in the bulk with a strong dopant, which has a significantly higher activation energy of desorption than oxygen for the same adsorption site.

In the next section results are presented for phthlocyanine layers which have been doped heavily with NO_2 to fill their bulk adsorption sites.

5.4. NO_2 Doping

In order to increase the ratio of surface to bulk adsorption sites the sensors were doped with NO_2. A batch of freshly evaporated sensors were stored in a dry atmosphere consisting of 100ppm NO_2 in nitrogen for approximately three weeks. Afterwards the sensors were held in a flow of dry air for two days [17].

5.4.1. Response of Doped Phthalocyanine Sensors to NO_2 Exposure

Figure 5.8 shows the response of a NO_2 doped conductivity sensor to exposure of different concentrations of nitrogen dioxide. The sensor shows a significant response to concentrations as low as 0.5ppm and the sensor fully recovered within 1700s. Furthermore, the response current of the sensor was one order of magnitude higher than that of the untreated phthalocyanine sensors. Heavy doping with NO_2 is thought to increase the number of charge carriers in the Pc material, which results in higher overall conductivity of the film and better response behaviour.

Initially, one would expect the sensitivity of the phthalocyanine sensor to suffer because of the heavy pre-exposure to nitrogen dioxide [18]. However, during the doping process NO_2 occupies the surface adsorption sites and also penetrates

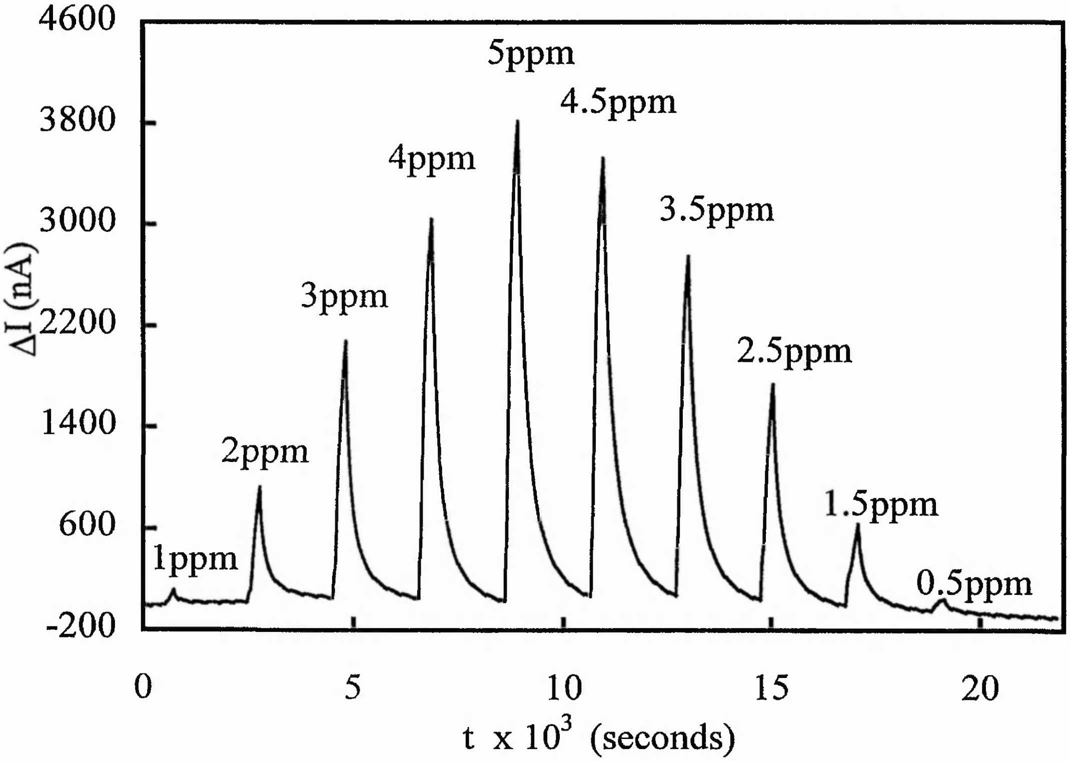

Figure 5.8: response of doped conductivity sensor to NO_2 exposures for 300s at room temperature, recovery time: 1700s

into the bulk of the phthalocyanine film [17]. If the doping process is sufficiently long most of the strongly binding sites in the bulk of the layer will be occupied. If the sensor is now kept under dry air conditions the NO_2 molecules on the surface adsorption sites will be replaced by oxygen whereas the majority of the bulk sites will remain occupied by NO_2 [19].

When the phthalocyanine film is repeatedly exposed to NO_2 again only the weakly binding surface adsorption sites are free to be occupied again. Although the amount of adsorbed molecules is quite small the response of the conductivity sensor will be good because surface adsorption site are the main contributors to conductivity changes.

The predictions of the previous section imply that the response of a SAW device should be comparatively small. In the experiments it was actually found that doped SAW sensors did not respond to NO_2 exposure at all. The amount of surface adsorbed molecules was probably too small to be detected as a mass loading response.

In comparison to untreated conductivity sensors [20], NO_2 doped Pc sensors show significant improvement in their gas sensing properties at room temperature. Improved sensitivity, recovery and stability of the sensor signal were demonstrated using this technique [21]. It was observed that the response of the doped conductivity and SAW sensor followed the predictions from the previous section for a high surface to bulk adsorption site ratio. Although the filling of the bulk adsorption site showed the expected result it would be interesting to investigate the effect of reducing surface adsorption. Since it is not possible to take away the surface of the film one option is to increase the ratio of bulk to surface adsorption sites to such an extend that the number of surface sites becomes negligible.

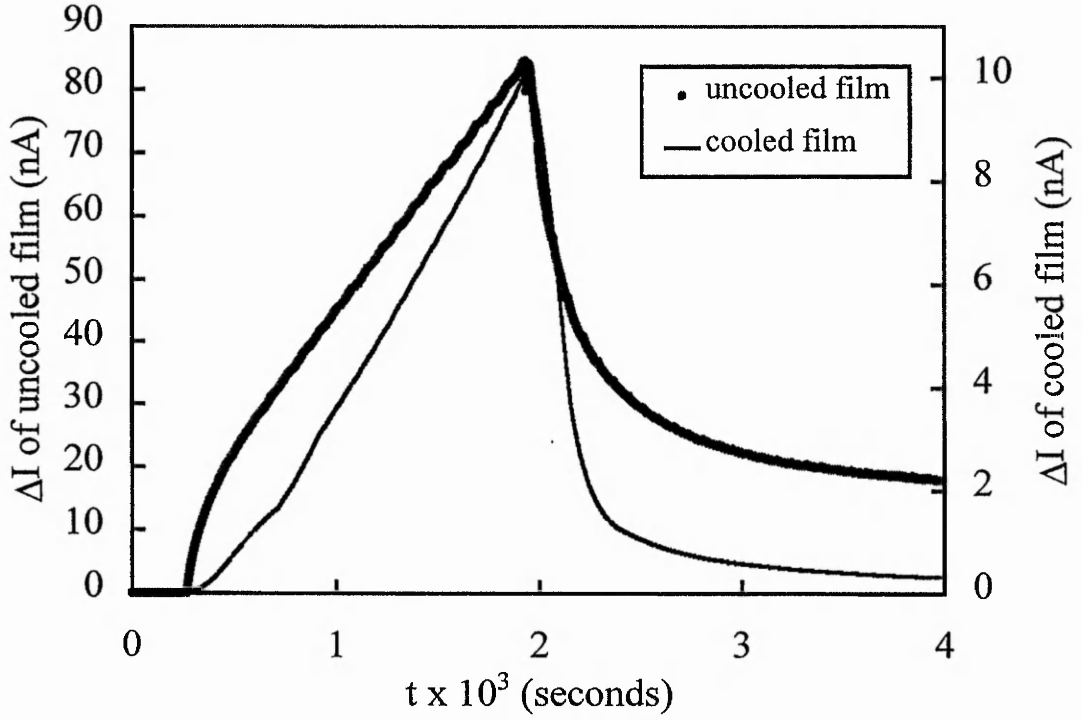

***Figure 5.9:* Comparison between uncooled and cooled conductivity sensor exposed to 2ppm NO_2 for 1700s**

To try to achieve this, abrupt cooling of the Pc film to liquid nitrogen temperature was considered. The idea was to increase stress within the crystal lattice of the phthalocyanine film and aid the microscopic cracking of the crystals. These fine cracks were intended to provide further bulk adsorption sites for NO_2 molecules. Experimental results for NO_2 exposure to phthalocyanine sensors which had been post-deposition cooled at liquid nitrogen temperature are presented in the next section.

5.5. Response of Post-Deposition Cooled Phthalocyanine Sensors to NO_2 exposure

After deposition of the Pc film, conductivity and SAW sensors were immersed in liquid nitrogen (77K) for approximately three minutes. It was thought that cooling to a very low temperature could result in microscopic cracks in the phthalocyanine layer [22]. These cracks would then aid access to additional bulk adsorption sites for the NO_2 gas. For a sufficiently large increase in the number of bulk adsorption sites the contribution of the surface adsorption sites to the overall response to conductivity and SAW sensors could be neglected. It was predicted that for a high ratio of bulk to surface adsorption sites there should be a long response and recovery time of the conductivity sensor, a good response of the SAW sensor and a more distinct effect of the laser.

5.5.1. Conductivity Sensor

Figure 5.9 shows the comparison between a cooled and an uncooled conductivity sensor during the same exposure cycle. The response of the cooled sensor is about one order of magnitude lower compared to that of the uncooled sensor. However, the cooled sensor has a recovery of the signal of 97% in the given time frame whereas the untreated device only recovered to about 77% relative to the maximum value.

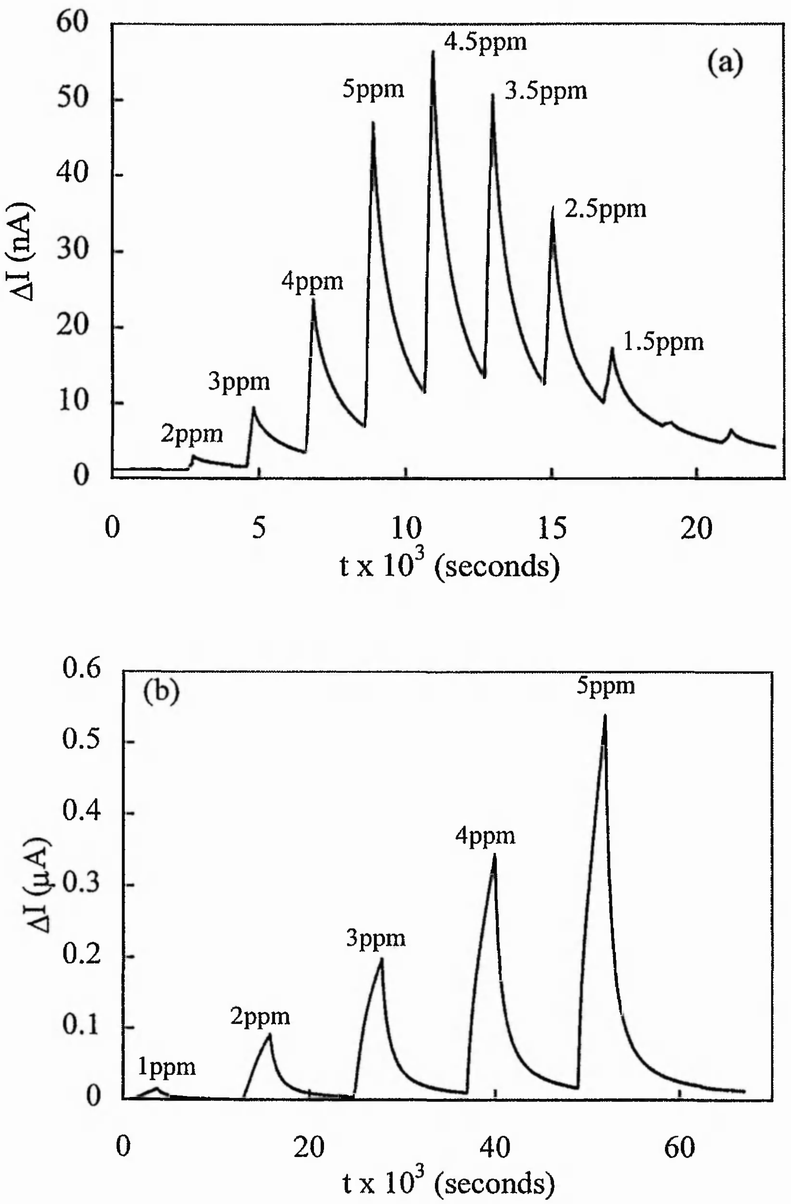

Figure 5.10: cooled sensor exposed to different concentrations of NO_2 with (a) 300s exposure and 1700s recovery time and (b) 3000s exposure and 9000s recovery time

Similar behaviour was observed by Hsieh et al [11] who reported improved recovery of amorphous PbPc which they ascribed to the increased number of bulk adsorption sites and better diffusion of the molecules into the bulk. The response behaviour of the cooled films may therefore be the result of a quasi-amorphous structure in the Pc overlayer.

Figure 5.10 shows the comparison between the responses of a cooled conductivity sensor to (a) short exposure and recovery time and (b) long exposure and recovery time. Figure 5.10(a) indicates that even for short exposures a recovery time of 1700s is not enough for a full recovery to the baseline. However, even for a long exposure time of 3000s (Figure 5.10(b)) the conductivity sensor shows very good recovery if the recovery time is sufficiently long.

5.5.2. Response of SAW Sensor with Cooled CuPc Layer to NO_2 Exposure

Figure 5.11(a) shows the response of a cooled SAW sensor to NO_2 exposure. Unlike the previous data for untreared Pc films, when the gas removed almost full recovery of the signal is obtained. In Figure 5.11(b) the cooled Pc layer of the SAW sensor was illuminated by the laser. It both cases the response of the sensors follow a similar pattern. However, the laser illuminated SAW sensor shows a frequency change, which is larger than that for the unilluminated SAW sensor by approximately a factor of 2.

5.5.3. Discussion of the Responses of Gas Sensors with Cooled CuPc Layers to NO_2 Exposure

It was shown in the previous section that the responses of the conductivity and SAW gas sensors with phthalocyanine film cooled at liquid nitrogen temperature after deposition follow a behaviour which could be ascribed to an adsorption process dominated by bulk diffusion.

The cooled conductivity sensors showed a response, which was about one order of magnitude smaller than that of the NO_2 doped sensors. However, the recovery of the signals was found to be almost complete given a sufficiently long recovery time. This may be attributed to a increased rate of diffusion as it has been reported for other phthalocyanine films with a low degree of order such as amorphous and spin coated films [11,12]. An increased rate of bulk diffusion may also be responsible for the improved recovery characteristic of the cooled SAW sensor. In contrast to the untreated SAW gas sensor which did not show any significant recovery the cooled sensor fully recovered from exposure to NO_2.

In Section 5.3 it was suggested that laser illumination has a significant effect mainly on the bulk adsorption sites. Other than for the untreated conductivity sensors where the laser had very little effect on the sensor response, the cooled conductivity devices showed an approximately three fold increase in response when illuminated with laser light (Figure 5.12). The cooled SAW devices also showed a significantly increased response upon NO_2 exposure when illuminated with the laser which agrees with the suggestions made in Section 5.3.

5.5.4. Discussion of the Responses Obtained from Cooled and Doped Sensors

In this section different ways to to improve the response behaviour of phthalocyanine gas sensors operated at room temperature have been discussed. It was suggested that two mechanisms contribute to the overall response behaviour of conductivity and SAW sensors: surface adsorption and bulk diffusion. Both of these mechanisms have significantly different properties

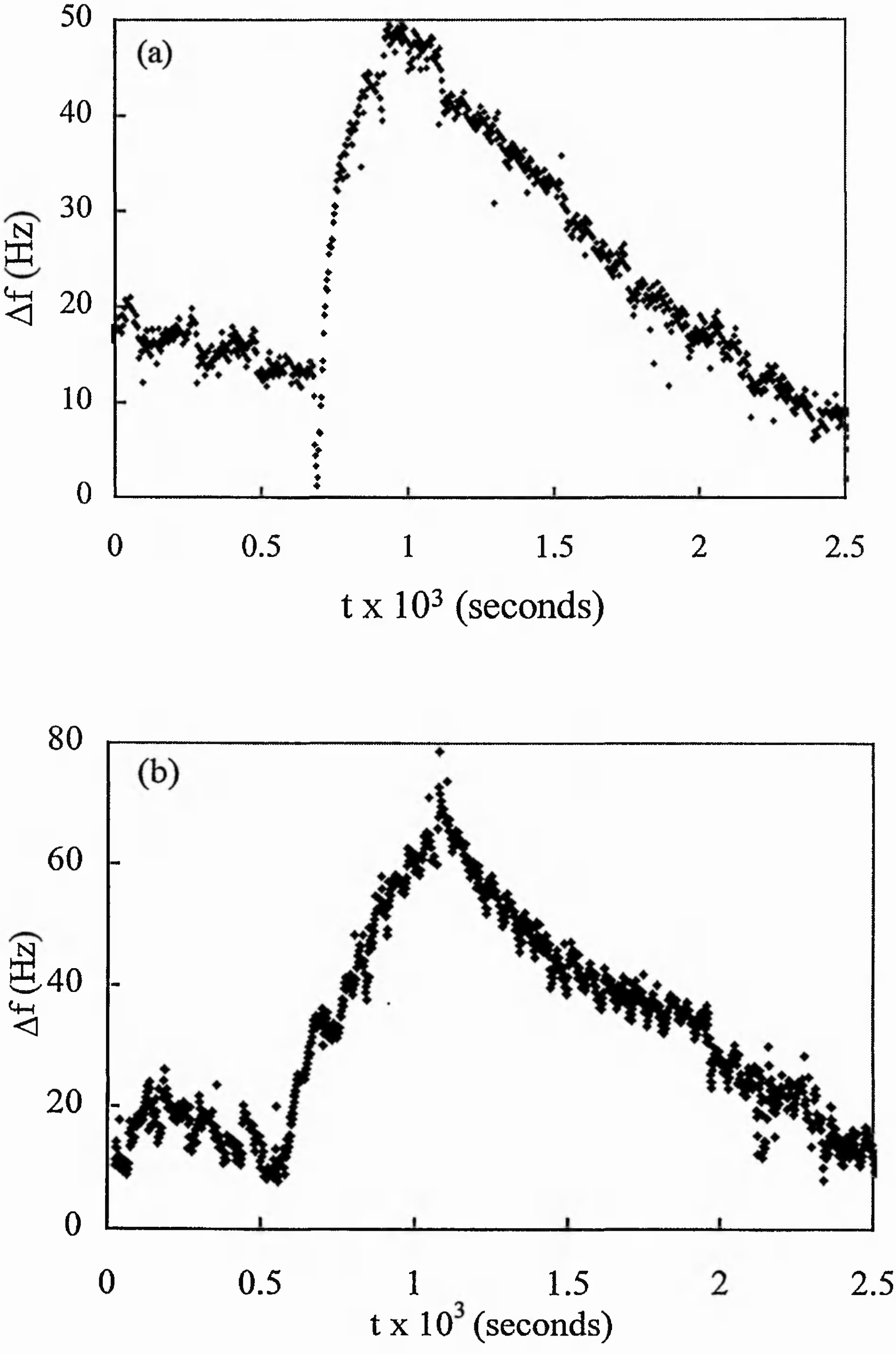

Figure 5.11: Comparison of the responses of cooled SAW devices to 10ppm NO_2 for 500s (a) without laser illumination and (b) with laser illumination

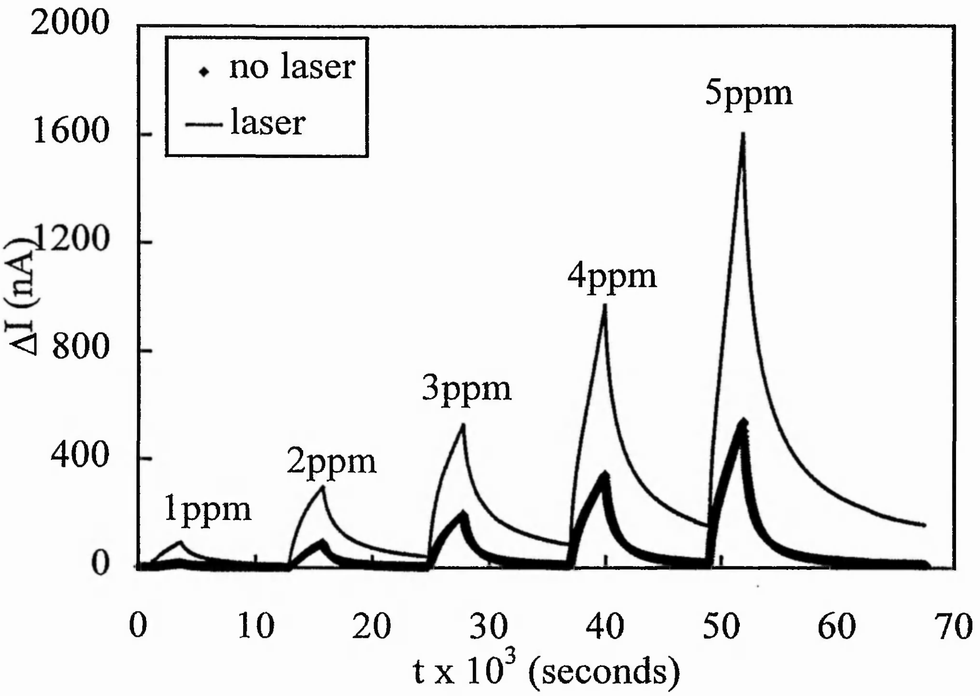

Figure 5.12: Comparison between response of cooled conductivity sensor for non-illuminated and illuminated phthalocyanine layer

and it was suggested that one or the other needs to be minimised in order to obtain clearer response patterns.

Doping with nitrogen dioxide was used to reduce the contribution of bulk diffusion. Doped conductivity sensors were found to have significantly improved properties for the detection of NO_2. It was suggested that post-deposition cooling of the phthalocyanine sensors may lead to an increase in the ratio of bulk to surface adsorption sites. Since the observations from the experiments with cooled PC sensor followed the predicted behaviour it was suggested that microscopic cracks in the PC film could lead to increased diffusivity [23]. Cooled conductivity and SAW sensors showed very good recovery after NO_2 exposure.

The advantage of both doped and cooled treatments to the sensors is their improved recovery, which makes their sensitivity virtually independent of the pre-exposure history of the phthalocyanine film. However, a steady state response is still obtained only after a very long period of time. In order to achieve a rapid determination of the concentration of the test gas it is necessary to investigate the kinetic responses of these sensors [24]. The next section describes the evaluation of the kinetic responses of doped and cooled phthalocyanine gas sensors in order to implement a fast and repeatable NO_2 sensing system, which operates at room temperature.

5.6. Kinetic Responses of CuPc Gas Sensors

This section outlines the kinetic responses of doped and cooled copper phthalocyanine conductivity sensor. Both sensor types show good recovery, which makes their sensitivity towards gas concentration virtually independent of the exposure history of the film. Initially, data were analysed in terms of the Langmuir adsorption model, which assumes a constant activation energy of adsorption [25]. If the activation energy of adsorption varies with surface coverage the Elovich model may be a more appropriate description of the sensor

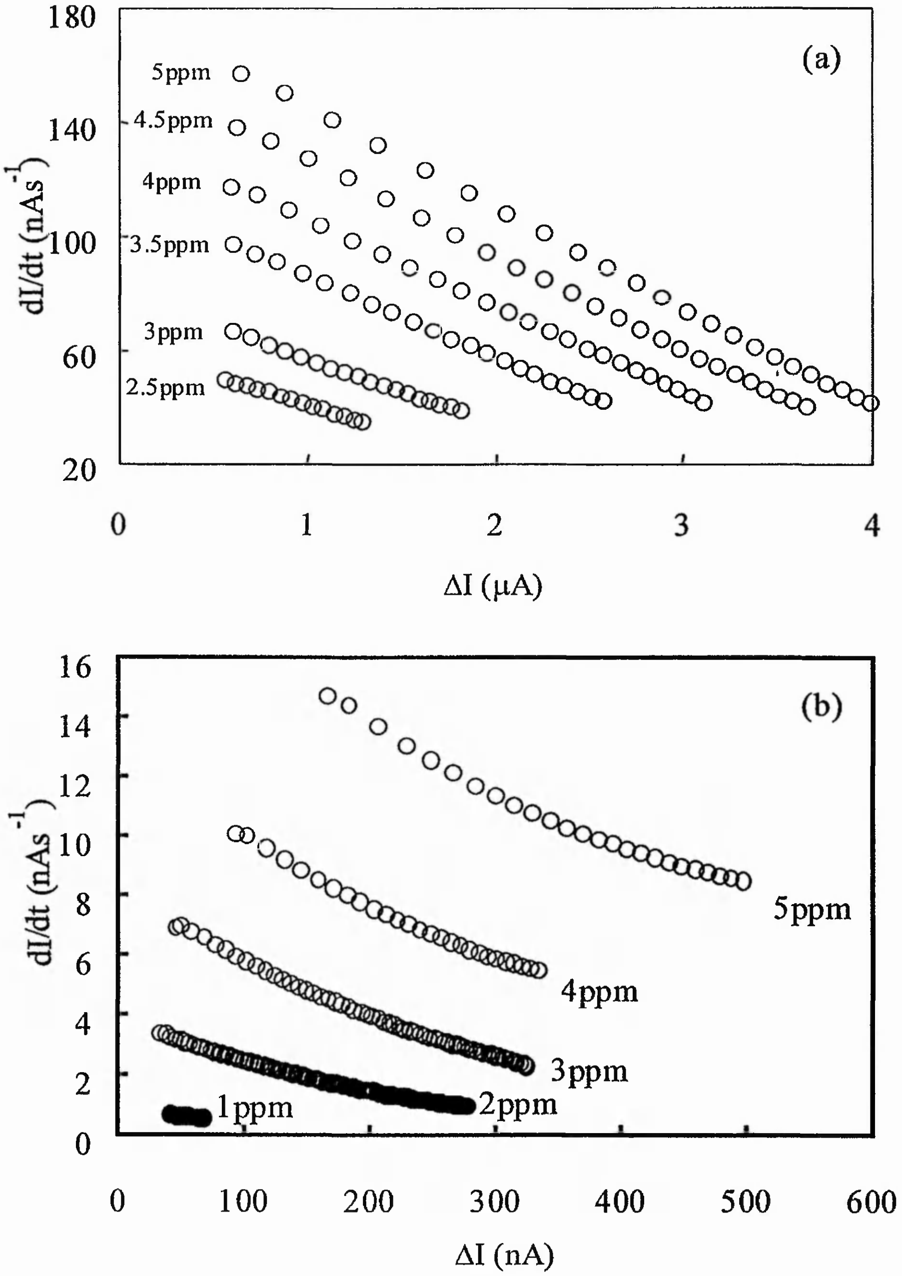

Figure 5.13: Langmuir plot of the initial response to different concentrations of NO_2 to (a) doped conductivity sensor and (b) cooled conductivity sensor

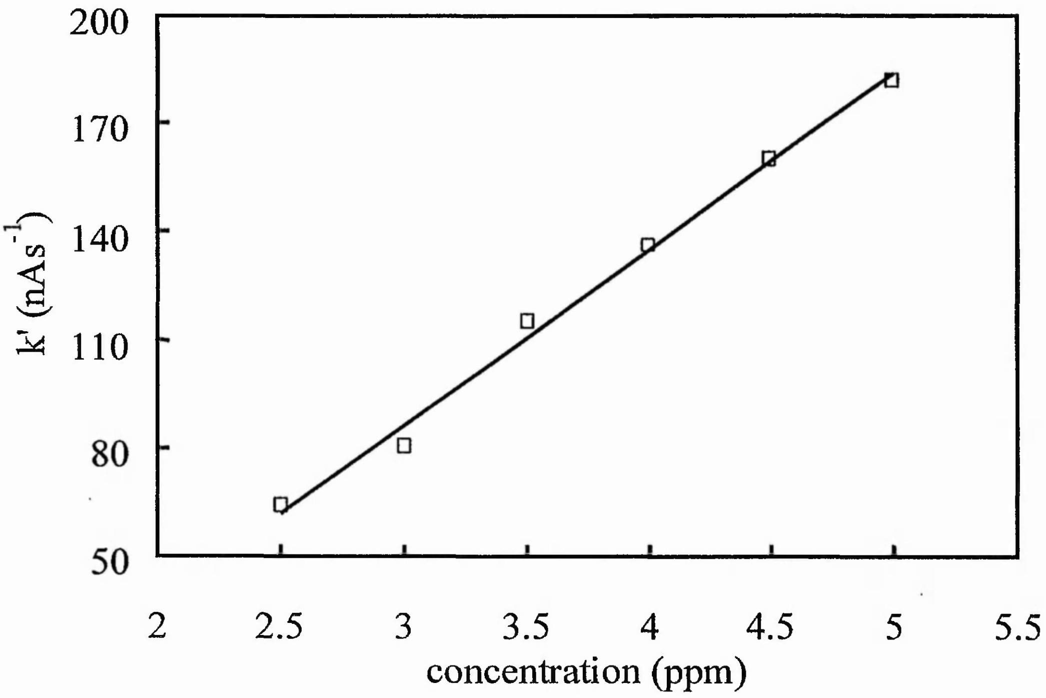

Figure 5.14: Correlation between the constant k' and the gas concentration for NO_2 exposure to a nitrogen dioxide doped conductivity sensor

response [26]. From the slopes of the Langmuir and Elovich plots, parameters (k' and a' respectively) can be extracted which are proportional to the concentration of the test gas [27].

Finally, a relationship between the maximum rate of adsorption and the gas concentration is introduced which allowed a fast and simple determination of the NO_2 concentration.

5.6.1. Kinetic Responses of Cooled and Doped Conductivity Sensors Assuming Constant Activation Energy of Adsorption (Langmuir Model)

The Langmuir adsorption model assumes that during the adsorption of gas on the surface of the solid there will be no change in activation energy of adsorption. If the Langmuir model is valid a plot of dI/dt against ΔI should be linear [27].

Figure 5.13 shows the Langmuir plots for (a) an NO_2 doped conductivity sensor and (b) a cooled conductivity sensor to NO_2 exposure with different concentrations. Clearly, the Langmuir plot of the doped sensor shows good linearity whereas the Langmuir plot of the cooled sensing device does not show a linear relationship between dI/dt and ΔI. This indicates that the activation energy of adsorption remains relatively constant for the doped device but shows significant variation for the cooled conductivity sensor. This behaviour may arise from the fact that NO_2 doping fills most of the strong adsorption sites of the phthalocyanine layer and only leaves some weakly binding sites available for gas adsorption. Assuming a proportional relationship between surface coverage and conductivity change the Langmuir equation can be written as:

$$\frac{dI}{dt} = k' - m' I \qquad (5.1)$$

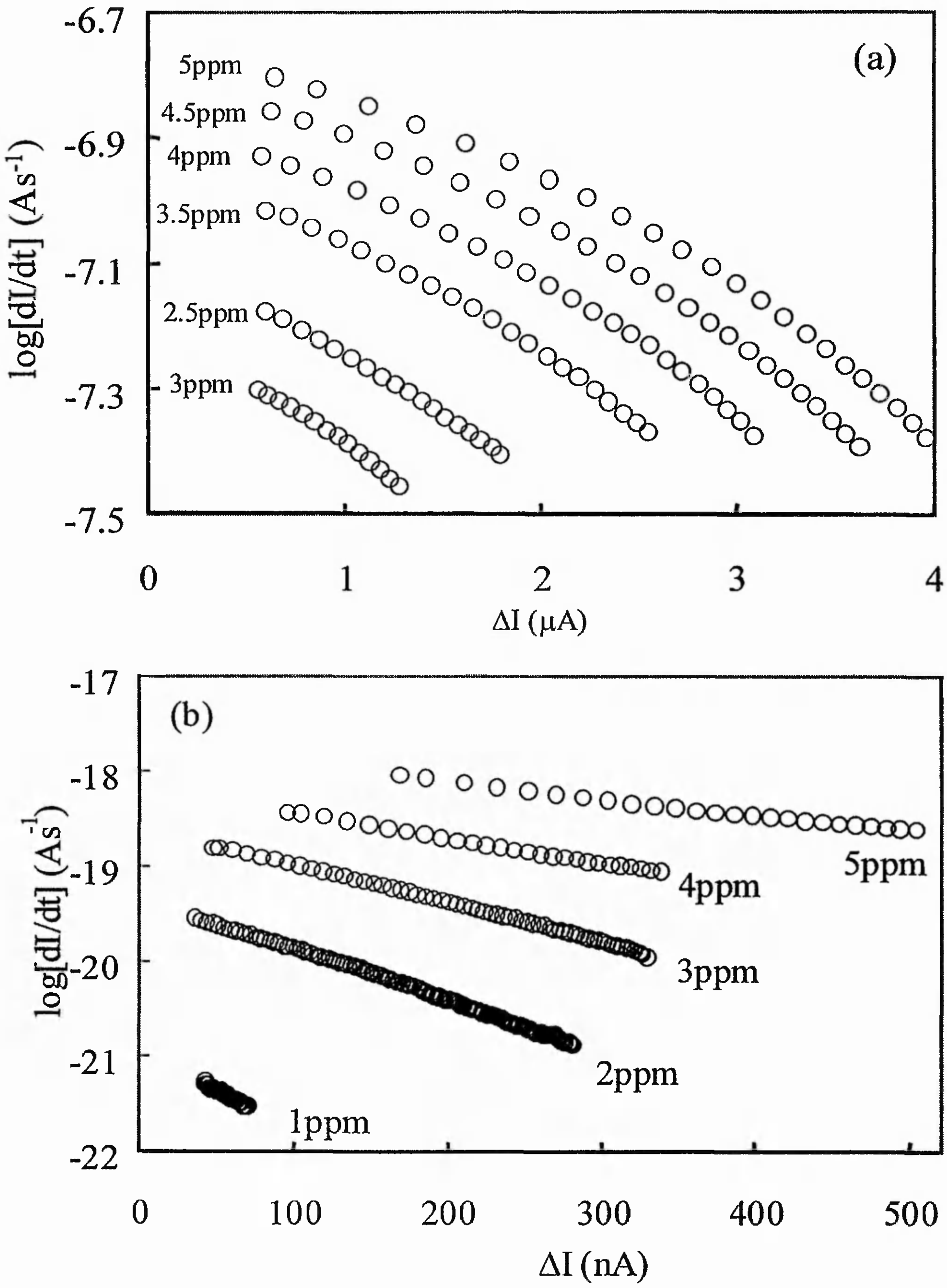

Figure 5.15: Elovich plots of the initial response to various concentrations of NO_2 for (a) doped and (b) cooled conductivity sensor

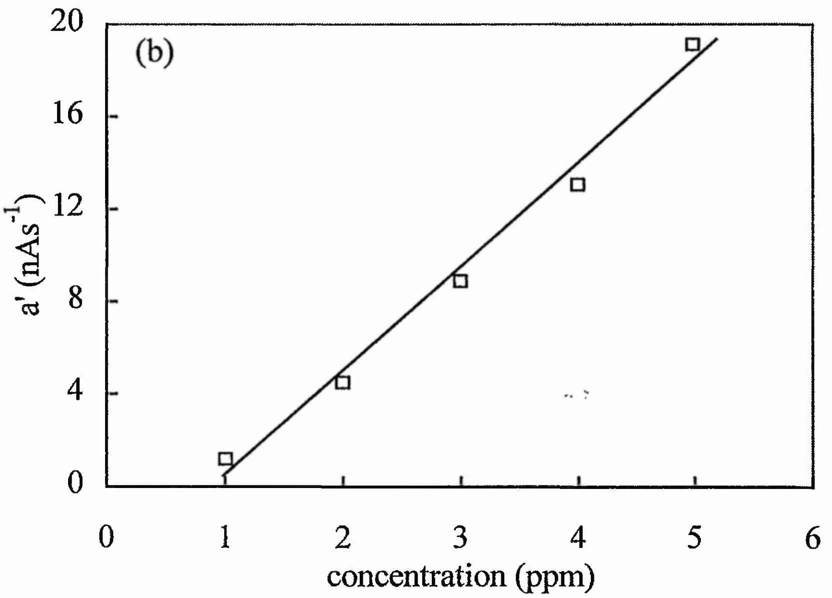

Figure 5.16: Correlation between the Elovich constant a' and the gas concentration for NO_2 exposure to a cooled conductivity sensor

with k' and m' being constants. Figure 5.14 shows that there is a good correlation between k' and the concentration of NO_2 for the doped conductivity sensor. This can be obtained within the first 200s of exposure and therefore allows a rapid quantification of the concentration of the test gas.

The data in Figure 5.13 suggest that the cooled CuPc conductivity sensor shows a variation in activation energy of adsorption. Bulk adsorption sites are believed to have much higher activation energies than surface sites [11]. Since all of these sites are available the activation energy can no longer be regarded as constant.

An adsorption with a variation in the activation energy, may be the case of the cooled sensor, is better described by the Elovich equation [28]. The application of this model to the cooled and doped conductivity sensor is discussed in the next section.

5.6.2. Kinetic Responses of Cooled and Doped Conductivity Sensors with Variation of Activation Energy of Adsorption (Elovich Model)

The Elovich adsorption model suggests that during the adsorption of gas on the surface of the solid there will be a change in activation energy of adsorption proportional to the surface coverage. If the Elovich model is valid a plot of $log[dI/dt]$ against ΔI should be linear [27].

Figure 5.15 shows the kinetic responses for cooled and doped conductivity sensors as Elovich plots. The Elovich adsorption model takes into account variations in activation energy with increasing surface coverage [29]. In the previous section it was found that the NO_2 doped conductivity sensor had a linear Langmuir plot and this implies that no significant variations in activation energy occured. This is also confirmed by the non-linearity of the Elovich plot for the doped sensor (Figure 5.15(a)).

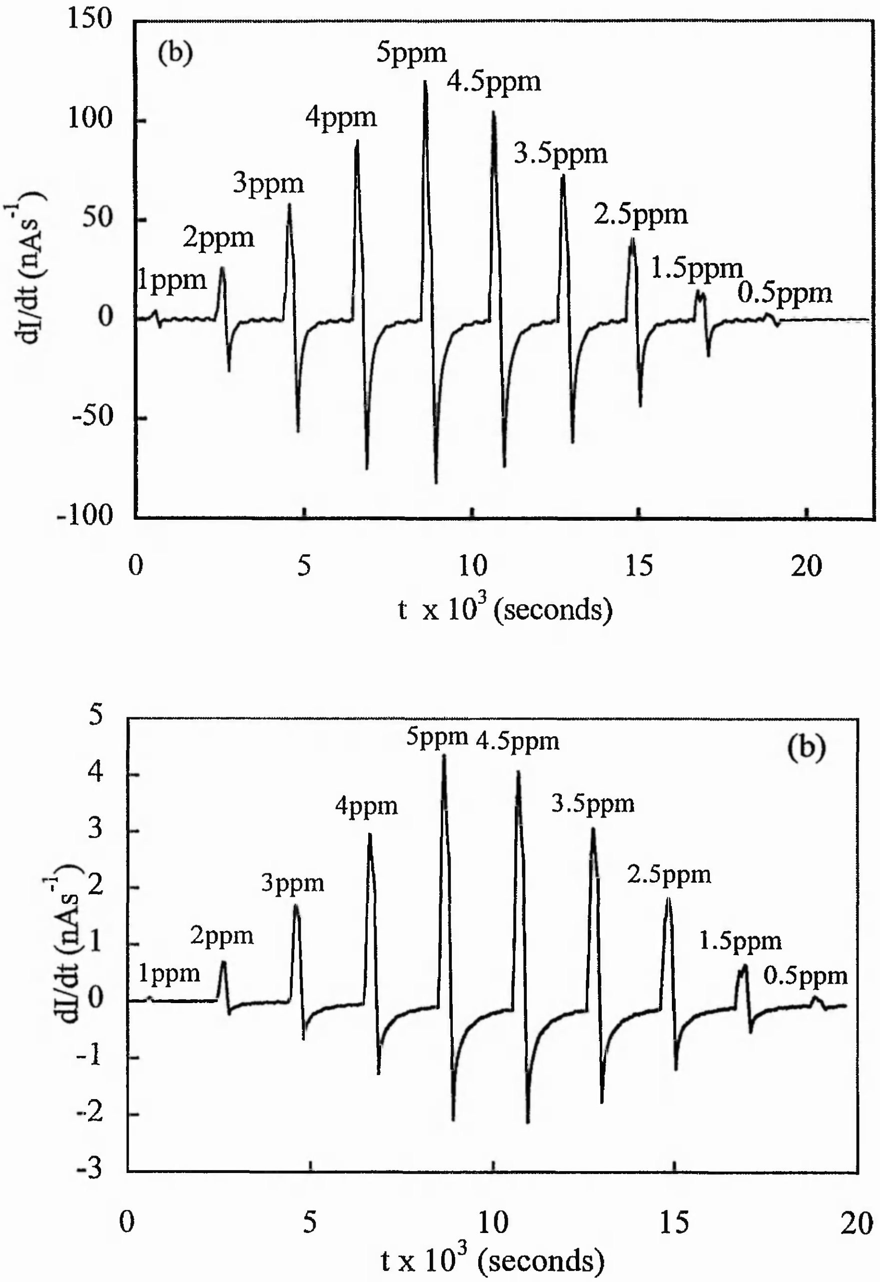

Figure 5.17:Plot of the derivative response to NO_2 exposure for (a) doped and (b) cooled conductivity sensor

The Langmuir plot of the cooled conductivity sensor however, suggested that the adsorption sites on this device do not have uniform activation energies. Hence, the strength with which NO_2 molecules are bound to the Pc layer varies significantly. The linearity of the plots in Figure 5.15(b) suggests that the kinetic response of the cooled sensor obeys the Elovich model. The linearity of the Elovich plot of the conductivity sensor is very distinct and this leads to the conclusion that there are a wide range of different adsorption sites available [30]. One possible explanation is that this is a result of structural changes in the CuPc film due to cooling.

In order to determine the concentration of the test gas with the cooled conductivity sensor, the Elovich parameter a' has to be extracted from the slope for each exposure cycle. Figure 5.16 shows the relationship between a' and the concentration of the test gas.

From the kinetic response patterns it can be seen that the responses of the cooled and the NO_2 doped sensor exemplify two extreme cases:

1. No variation in the activation energy of adsorption (doped sensor)
2. Wide variation in activation energy of adsorption (cooled sensor)

This behaviour shows that with post-deposition treatment of the sensors it was possible to enhance two distinct adsorption components, which could be ascribed to surface adsorption and bulk diffusion of the NO_2 molecules on CuPc. The different response kinetics of these processes may account for problems experienced with the use of CuPc gas sensors such as baseline drift, poor reversibility and dependence of the sensitivity on the exposure history of the film [20]. With doping and cooling of the phthalocyanine layer it was possible to reduce these problems. Additionally, it was possible to determine the test gas concentration after a short period of time by extracting the parameters *k'* and *a'* from the Langmuir and Elovich plots respectively.

In the last section of this chapter a method of determining the gas concentration is presented which works equally well for cooled and doped sensors and is relatively easy to obtain from the sensor responses.

5.6.3. Determination of the NO_2 Concentration by Using the Maximum Derivative Value

Before the exposure of a test gas to the sensor commences the surface coverage of the phthalocyanine with test gas molecules can be regarded as zero ($\theta_{t=0} = 0$). The initial rate of change in surface coverage must therefore have its maximum value at $t = 0$. This reduces the equations for the kinetic response to a similar form which only varies in a constant, hence:

$$\left(\frac{d\theta}{dt}\right)_{\theta=0} = k_a p \qquad (5.2)$$

for Langmuir adsorption and

$$\left(\frac{d\theta}{dt}\right)_{\theta=0} = ap \qquad (5.3)$$

for Elovich adsorption. These equations show that the maximum rate of adsorption is only dependent on the partial pressure (concentration) of the test gas.

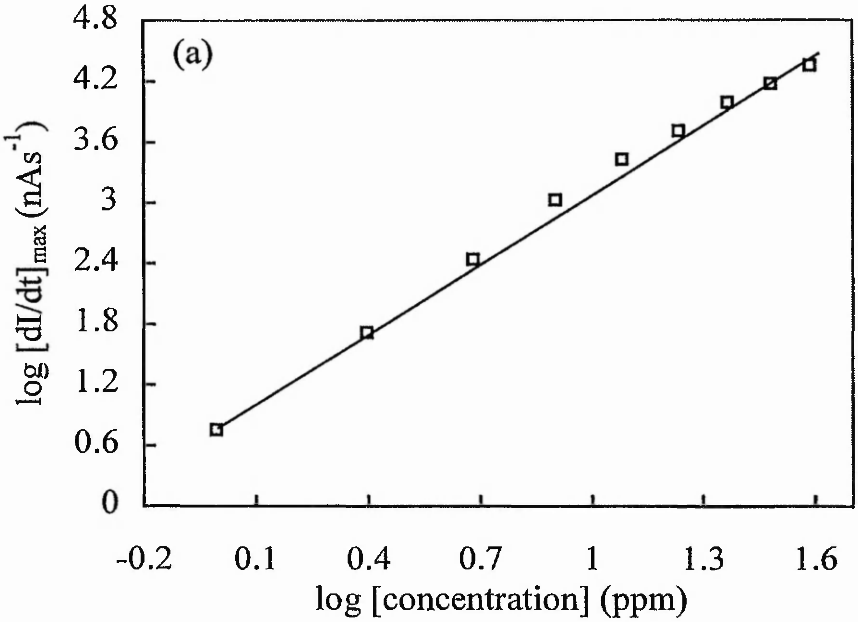

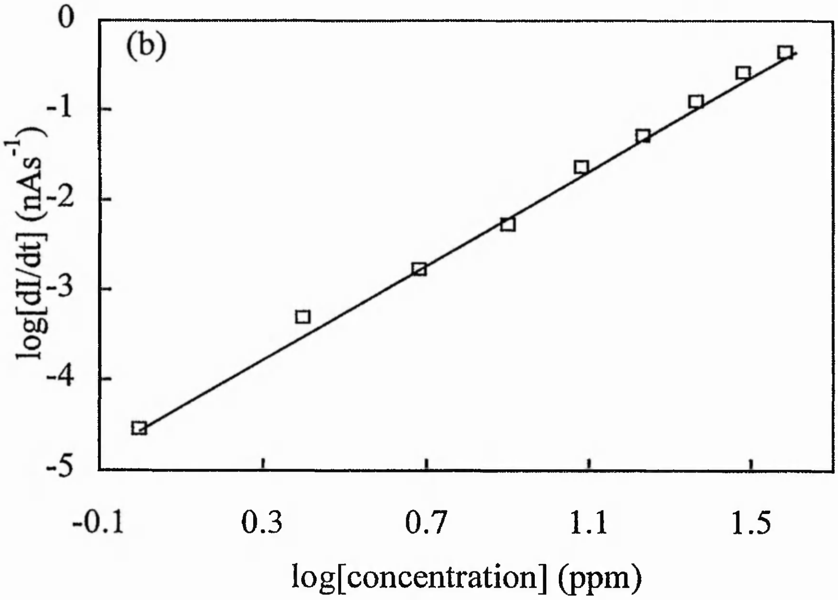

Figure 5.18: Double-log plot of the maximum derivative values for different gas exposures against their concentration for (a) doped and (b) cooled conductivity sensor

Figure 5.17 shows plots of the derivative responses to gas exposures with various concentrations obtained from (a) a doped and (b) a cooled conductivity sensor. In both cases the derivative value initially rises to a maximum. Subsequently, the derivative value decays during gas exposure. At the moment when the exposure is terminated the derivative value of the conductivity sensor response goes through its extreme minimum.

Figure 5.18 shows the correlation of the maximum derivative value for a gas exposure with the concentration of the test gas. The relationship of $(dI/dt)_{max}$ obeys a power law which is shown in the log-log plot.

This way of determining the concentration for the test gas works equally well for doped and cooled conductivity sensors and requires only an initial calibration. After a very short exposure time it provides a definite value for the maximum derivative and hence for the gas concentration. Furthermore, this value can be obtained from a simple analogue differentiator circuit without further processing.

This method of determining the maximum derivative value together with post-deposition treated conductivity sensors, which have a response independent of the exposure history of the phthalocyanine film could serve as the basis for the implementation of fast and reliable NO_2 detectors. The use of simple electronic circuits and low power consumption because of operation at room temperature could be prerequisites for the implementation of a portable phthalocyanine NO_2 sensor.

References

[1] I.Emilianov, V.Khatko, A.Tomochenko, Sens.Actu., **B47**, (1998), 158

[2] R.Zhou, F.Josse, W.Gölpel, Z.Z.Öztürk, Ö.Bekaroglu, Appl.Organomet.Chem., **10**, (1996), 557

[3] P.B.M.Archer, A.V.Chadwick, J.J.Miasik, M.Tamizi, J.D.Wright, Sens.Actu., **16**, (1989), 379

[4] Neil B McKeown, Phthalocyanine Materials Synthesis Structure and Function, Chemistry of Solid State Materials 6, (1998), 119

[5] G.Guillaud, J.Simon, J.P.Germain, Coord.Chem.Rev., **178**, (1998), 1433

[6] S.J.Martin, A.J.Ricco, Sens.Actu., **A21-A23**, (1990), 712

[7] A.J.Ricco, S.J.Martin, T.E.Zipperian, Sens.Actu., **8**, (1985), 319-333

[8] P.B.M.Archer, A.V.Chadwick, J.J.Miasik, M.Tamizi, J.D.Wright, Sens.Actu., **16**, (1989), 379

[9] H.-Y.Wang, J.B.Lando, Langmuir, **10**, (1994), 790

[10] Y.H.Ju, C.Hsieh, C.J.Liu, Thin Solid Films, **342**, (1999), 238

[11] C.Hsieh, C.J.Liu, Y.H.Ju, Thin Solid Films, **322**, (1998)

[12] W.Hu, S.Liu, D.Zhu, Thin Solid Films, **324**, (1998), 285

[13] X.Ding, S.Shen, H.Xu, Q.Zhou, Dyes and Pigments, **40**, (1999), 187

[14] J.G.Moser, Photodynamic Tumor Therapy, Gordon and Breach, (1998), 9

[15] X.Li, H.Xu, Q.Zhou, D.Jiang, L.Zang, A.Lu, Thin Solid Films, **324**, (1998), 277

[16] M.E.Musser, S.C.Dahlberg, Surf.Sci., **100**, (1980), 605

[17] Rudiono, S.Okazaki, M.Takeuchi, Thin Solid Films, **334**, (1998), 187

[18] J.D.Wright, A.V.Chdadwick, B.Meadows, J.J.Miasik, Mol.Cryst.Liq.Cryst., **93**, (1983), 315

[19] A.DeHaan, M.Debliquy, A.Decroly, Chem.Sens., **I**, (1998), 183

[20] S.Dogo, J.-P.Germain, C.Maleysson, A.Pauly, Thin Solid Films, **219**, (1992), 257

[21] M.I.Newton, T.K.H.Starke, G.McHale, M.R.Willis, Thin Solid Films, **360**, (2000), 10

[22] J.M.Langaron, N.M.Dixon, W.Reed, J.M.Pastor, B.J.Kip, Polymer, **40**, 1999, 2569

[23] X.Li, S.Shen, Q.Zhou, D.Jiang, A.Lu, Thin Solid Films, **324**, (1998), 274

[24] A.K.Ray, M.J.Cook, S.C.Thorpe, S.Mukhopadhyay, Phys.Stat.Sol., **140**, (1993), K85

[25] H.E.Avery, Basic Reaction Kinetics and Mechanisms, MacMillan, (1974), 123

[26] C.Aharoni, F.C.Tompkins, Adv.Catal., **21**, (1970), 1

[27] G.Zhou, R.Gould, Thin Solid Films, **317**, (1998), 436

[28] J.Langton, P.Day, J.Chem.Soc.,Faraday Trans., **2**, (1982), 1675

[29] A.W.Adamson, Physical Chemistry of Surfaces, J.Wiley and Sons Inc., USA, (1990), 700

[30] G.G.Fedoruk, D.I.Sagadiak, A.V.Misevich, A.E.Pochtenny, Sens.Actu., **B48**, (1998), 351

Chapter 6: Conclusion and Further Work

This project studied the NO_2 gas sensing properties of conductivity and acoustic wave sensors with copper phthalocyanine sensitising layers operated at room temperature. The following chapter reviews the work that was undertaken and presents a summary of the important results. Finally, this chapter suggests work that can be carried out in this field.

6.1. Conclusion

The aim of this project was to investigate the use of CuPc as a gas sensor for operating at room temperature with properties comparable to gas sensors operated at elevated temperatures. NO_2 was chosen as test gas for its environmental significance and its well known interaction with CuPc.

Preliminary experiments were carried out in order to establish the gas delivery system, produce SAW and conductivity sensor devices, understand their properties and overcome problems arising from the equipment and the nature of the experiment. It was found that SAW sensors have sufficient sensitivity to detect mass loading of the Pc film due to gas adsorption. A set of gas sensing experiments at elevated temperatures repeated gas sensing work by other researchers and provided the basis for room temperature experiments. The experiments at elevated temperature clearly indicated the importance of understanding response kinetics in order to achieve fast measurements of the test gas concentration.

Initially, room temperature gas sensing experiments were carried out using a simple vacuum sublimed copper phthalocyanine film on conductivity and SAW sensors in order to detect conductivity and mass loading changes of the film. The room temperature sensing properties of normal vacuum sublimed CuPc films were found to be insufficient in terms of sensitivity, recovery and response time for detection of NO_2 in the ppm range and required further develpoment. From the significant difference in the response of conductivity and SAW devices it was suggested that gas adsorption on CuPc could follow two different mechanisms: surface adsorption and bulk diffusion. The different characteristics of the response components result in a very complex response behaviour of the sensors, showing a sensitivity to gas concentrations which is dependent on the exposure history of the phthalocyanine film.

In order to improve the gas sensing properties of the conductivity and surface acoustic wave sensors the phthalocyanine layer was illuminated by a 30mW laser diode. It was anticipated that photo excitation of the copper phthalocyanine material upon laser exposure would alter its response characteristics. The experimental results indicated that the laser had a significant effect on the response component of the sensors which was ascribed to bulk diffusion but only little effect on the response component ascribed to surface adsorption.

Preliminary work suggested that conductivity devices were dominated by surface adsorption and SAW response by bulk diffusion. A reduction of one component was believed to lead to a much more controllable response of the sensors upon gas exposure. It was suggested that a Pc film, which would only allow for surface adsorption of gas molecules, should show very good gas sensing properties such as fast response and full recovery.

In order to minimise the response component ascribed to bulk diffusion and promote surface adsorption component, Pc films were doped with NO_2 in order to fill the bulk adsorption sites. Experiments showed that the doped conductivity sensors responded remarkably well to nitrogen dioxide exposure. Films showed rapid response and almost full recovery as well as a sensitivity comparable to Pc sensors at elevated temperatures.

A further set of experiments was carried out to investigate the behaviour of the sensor when the response component ascribed to surface adsorption is minimised. This could be achieved by increasing the ratio of bulk to surface adsorption sites so that the number of surface adsorption sites becomes negligible. To increase this ratio the sensors with Pc films were cooled at liquid nitrogen temperature prior to room temperature gas sensing experiments which was believed to generate microscopic cracks providing improved access to bulk adsorption sites. Both SAW and conductivity sensors showed nearly full recovery of the signal after NO_2 exposure. Laser illumination of the cooled devices, which was believed to affect mainly bulk diffusion, significantly increased the response of SAW and conductivity sensors to NO_2 exposure.

In addition to good sensor properties it is important for practical applications to determine the test gas concentration in as short time as possible. Therefore, it was necessary to investigate the response kinetics of the phthalocyanine gas sensors. The doped and the cooled sensor were chosen for the study because they represent domination of surface adsorption and bulk diffusion respectively.

Initially, the Langmuir model of adsorption was applied to the response of the conductivity sensors. This model represents the case where the adsorption is dominated by a single activation energy. This was found to be approximately true for the doped sensor where most of the strongly binding adsorption sites are believed to be filled and only weakly binding sites remain with a very small variation in activation energy. From the slopes of the Langmuir plots for the doped sensors a parameter k' was extracted which is proportional to the concentration of the test gas. This parameter can be obtained within the first minutes of gas exposure.

The response of the cooled sensor to gas exposure was believed to be dominated by bulk diffusion which should have a large variation in activation energies of adsorption. The Elovich adsorption model takes these variations into account. An analysis of the conductivity sensor responses to gas exposure with the Elovich model indicates that the cooled sensor shows very good correlation whereas the doped sensor does not. From the Elovich plots of the cooled conductivity sensor, a parameter a' was extracted which was proportional to the concentration of the test gas. This parameter also could be obtained within the first minutes of gas exposure.

Finally, a method was proposed which allows a quantification of gas concentrations equally well for doped and cooled phthalocyanine conductivity sensors. In the initial phase of the gas exposure the rate of adsorption will be at maximum. In both cases (doped and cooled) this maximum value of adsorption rate follows a power law relationship with the test gas concentration. It can therefore be used for determination of the concentration of the test gas. The maximum derivative value can be obtained right at the beginning of an exposure cycle.

In conclusion, a systematic study of the effect of post-deposition treatedment of CuPc thin film devices has been carried out for room temperature detection of NO_2 in the ppm range.

6.2. Future Work

This work investigated the surface treatment for copper phthalocyanine based NO_2 sensors in order to improve sensing characteristics. Drift problems and variations in sensitivity are greatly reduced, and nearly full recovery of the signal was achieved. The post-deposition treatment of the films resulted from an adsorption model which involves a fast and a slow response component. These surface treatments could also be applied to improve the sensing properties of other phthalocyanine materials such as lead phthalocyanine which is known to have higher sensitivity to NO_2 gas then CuPc.

In this work one technique was used to dope the phthlocyanine layer with nitrogen dioxide to fill strong adsorption sites. Other doping agents that bind more strongly to phthalocyanines may cause even quicker response and recovery. They could have the effect of improving the long term stability of the sensor if they had slower desorption from the filled sites. The choice of doping agent (e.g. oxidising or reducing) could also influence the selectivity of the phthalocyanine sensor.

Selectivity is a key problem for chemical sensors. Phthalocyanines are known to be cross-sensitive to a range of different gases of oxidising and reducing nature. Sensor arrays with pattern recognition software are often used to determine the gas composition in a system. In order to achieve this the sensors in an array should have widely different response characteristics. If the response characteristics of the individual sensors are well understood the learning period of the neural network will be much quicker and the determination of the gas composition will be more precise. Phthalocyanine sensors with a response behaviour which can be described by a simple adsorption model such as the Langmuir model would be well suitable for implementation in a sensor array. A variety of responses could be achieved by using different metallo-phthalocyanines with varying surface treatments. To analyse the data the maximum rate of current change could be used since it is fast and independent of exposure times.

Environmental monitoring becomes increasingly important with higher pollution due to industrial and domestic emissions. Phthalocyanine sensors respond well to main pollutants of the atmosphere such as nitrogen dioxide and ozone. However, humidity with its reducing character will interfere with the sensor performance, especially when the sensor is operated at room temperature. Therefore, it would be important to investigate the influence of humidity to the gas sensing properties of room temperature phthalocyanine sensors.

Phthalocyanines materials show some promise for implementation in cheap and effective gas sensing systems. Further investigations have to be carried out to pass the transition from a material which merely responds to gas exposure to a sensitive, selective and reliable sensing device. This work will require a multidisciplinary approach and remains a great challenge for many researches all over the world.

APPENDIX

may not be singular in joint space. Also, find the singularity-free regions in Cartesian space corresponding to only the nonsingular regions in joint space.

(iii) *Step 3:* Make a desired path or trajectory within the nonsingular regions in Cartesian space.

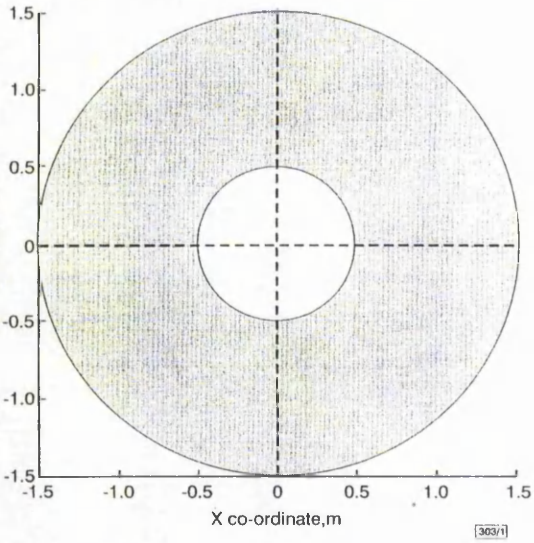

Fig. 1 *Singularity-free regions in Cartesian space*

Boundary lines do not belong to nonsingular regions
◎ semi-singular region
○ nonsingular region

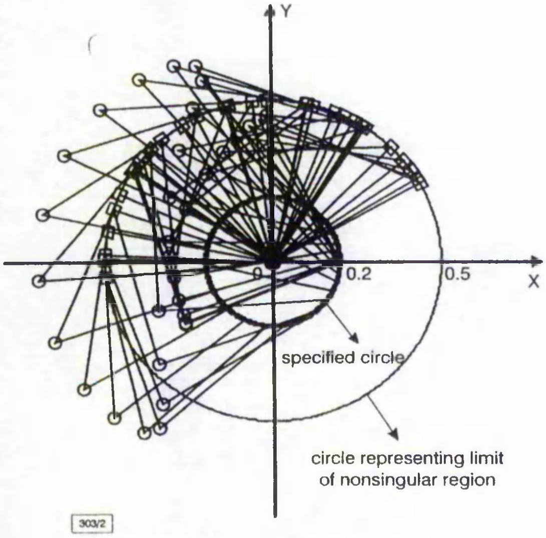

Fig. 2 *Snapshot of robot motion for circle tracking task*

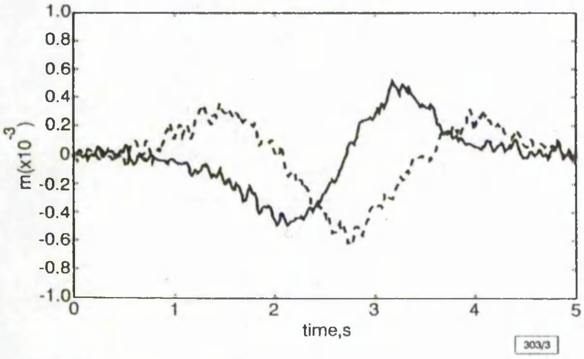

Fig. 3 *Position tracking error (e)*

——— X-co-ordinate
- - - - Y-co-ordinate

Simulation: The simulated manipulator is a three-link planar robot arm with one passive joint moving on a horizontal plane [3]. It is assumed that the third joint (q_3) is passive. The numerical real and nominal robot parameters used are the same as those given in [3]. The disturbance is a bounded random noise.

The singular regions in joint space found for the simulated manipulator are as follows: $\Omega_1 = \{q : q_2 = 0(\text{rad}) \; \forall \; q_1,q_3\}$, $\Omega_2 = \{q : q_2 = \pi(\text{rad}) \; \forall \; q_1,q_3\}$, $\Omega_3 = \{q : q_2 = 2\pi(\text{rad}) \; \forall \; q_1,q_3\}$. Fig. 1 shows the singularity-free region in Cartesian space for the simulated underactuated robot. The robot task used is that the end-effector circulates once along the specified circle.

In the control simulation, the singularity-free desired path $x^2_{ed}(t) + y^2_{ed}(t) = 0.2^2$ is used. Simulation results for the circular motion of the end-effector are shown in Figs. 2 and 3.

Conclusions: A stable, robust adaptive Cartesian control with fault tolerance for underactuated manipulators has been proposed to overcome actuator and/or brake failures and uncertainties. The proposed control method does not need *a priori* knowledge of the accurate dynamic parameters and the exact uncertainty bounds. To guarantee the availability of the proposed controller, singularity-free Cartesian path planning has been achieved. The proposed control scheme is useful and robust for uncertain underactuated robot systems with many applications, such as fault-tolerant robots, robots working in hazardous environments (space, underwater, nuclear plants), etc.

© IEE 1998
29 June 1998
Electronics Letters Online No: 19981191

Jin-Ho Shin and Ju-Jang Lee (*Department of Electrical Engineering, Korea Advanced Institute of Science and Technology (KAIST), 373-1, Kusong-dong, Yusong-gu, Taejon, 305-701, Korea*)

E-mail: jhshin@iliad.kaist.ac.kr, jjlee@ee.kaist.ac.kr

References

1 ORIOLO, G., and NAKAMURA, Y.: 'Control of mechanical systems with second-order nonholonomic constraints: underactuated manipulators'. Proc. IEEE 30th Conf. on Decision and Control, December 1991, pp. 2398–2403

2 ARAI, H., TANIE, K., and TACHI, S.: 'Dynamic control of a manipulator with passive joints in operational space', *IEEE Trans. Robot. Autom.*, 1993, **RA-9**, (1), pp. 85–93

3 SHIN, J.-H., and LEE, J.-J.: 'Robust adaptive control of underactuated robot manipulators in Cartesian space'. Proc. 1997 IEEE/RSJ Int. Conf. Intelligent Robots and Systems, Grenoble, France, 7–11 September 1997, pp. 491–497

Surface acoustic wave device design for gas sensing applications

M.I. Newton, T.K.H. Starke, G. McHale, M.R. Willis and A. Krier

A dual delay line surface acoustic wave device designed for gas sensing applications is described. The viability of this design is demonstrated using data showing the response to NO_2 with a sensitising layer of lead phthalocyanine.

Introduction: The use of surface acoustic wave (SAW) oscillators incorporating sensitising layers for gas detection has been extensively reported and reviewed [1, 2]. A dual delay line configuration using two identical SAW oscillators, one coated with a gas sensitive layer and one uncoated, is often employed to provide compensation for environmental changes such as temperature and pressure [3, 4]. Using a simple interdigital transducer on an appropriate piezoelectric substrate, surface acoustic (Rayleigh) waves are launched equally in both directions perpendicular to the fingers. This is normally considered to be undesirable in an oscillator circuit as the SAW energy launched in the opposite direction to the detection transducer provides an additional 6dB of attenuation to be overcome by the amplifier. In this work, an SAW design was investigated which used a separate interdigital transducer for the oscillator frequency detection utilising this 'unwanted' SAW component. This configuration removed the usual requirement for a power splitter to be provided in the oscillator circuit and hence reduced the gain requirements of the amplifiers. A range of sensitising layers have previously been reported in the literature for SAW gas sensing applications. To demonstrate the viability of this SAW design for gas sensing, we present data using a lead phthalocyanine (PbPc) sensitising layer. This material is well-known to respond to a range of gases [4, 6, 7] including nitrogen dioxide which we have used for our example gas.

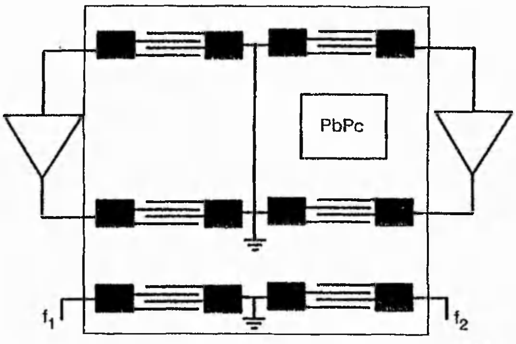

Fig. 1 *Schematic diagram of SAW device design*

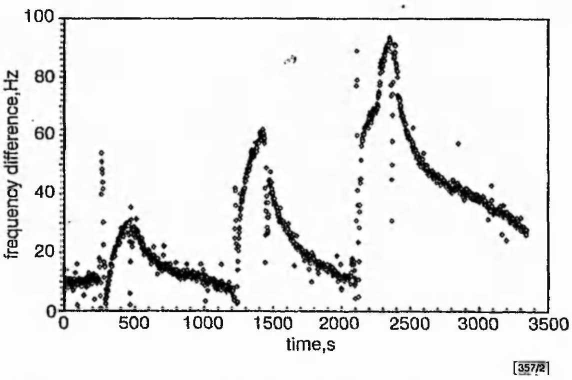

Fig. 2 *Transient response of device to 5, 10 and 15ppm of NO_2*

Experimental: In Fig. 1 we show a schematic diagram of the SAW sample design. For the oscillator circuit, an interdigital transducer (IDT) separation of 7.5mm was used and for the detection transducer, there was a separation of 1.5mm. Devices were fabricated on 128° rotated Y-cut lithium niobate substrates propagating along the X-axis. Each interdigital transducer consisted of 10 finger pairs of finger width and spacing 24.9μm and an aperture of 2081μm; these gave a resonant frequency of 35.5MHz. Between the IDTs on one of the SAW paths, a film of PbPc of thickness 160nm was deposited at a deposition rate of 0.1nm/s directly onto the lithium niobate surface; the PbPc was purified by train sublimation prior to deposition. The SAW device was mounted in a test chamber which was held at a constant temperature of 82°C. The gas delivery system comprised a source of 100ppm NO_2 in N_2 and a source of pure N_2 which were mixed to give the required concentration while delivering a constant flow rate of 250ml/min to the test chamber. The oscillator frequencies, f_1 and f_2, were measured by two interfaced frequency meters and values were subtracted to give the frequency difference.

Results: In Fig. 2, we show the transient response of the device to NO_2. At 250s, 5ppm of NO_2 was introduced into the test chamber followed by an N_2 only purge at 460s. This was followed at 1200s by the introduction of 10ppm of NO_2 and followed by an N_2 only purge at 1440s. Finally, at 2100s, 15ppm of NO_2 was introduced into the test chamber followed by a N_2 only purge at 2360s. This sensitivity and speed of response is comparable with previously reported data for conventional SAW devices with a PbPc overlayer [4]. The working frequency of 35.5MHz in these test devices is relatively low for surface acoustic wave devices. Since the sensitivity to surface mass loading of SAWs is known to increase with frequency [2], moving to higher frequencies should allow these devices to be sensitive to NO_2 in the sub-parts per million range.

Conclusion: A dual delay line surface acoustic wave device design has been investigated for gas sensing applications. The device utilises a separate IDT for frequency detection in addition to the usual oscillator circuit. Using a lead phthalocyanine sensitising layer, these devices have been shown to be sensitive to NO_2 in the parts per million range.

Acknowledgments: The authors wish to thank D. Campbell and B. Hartmann for their technical assistance.

©IEE 1998

2 July 1998
Electronics Letters Online No: 19981163

M.I. Newton, T.K.H. Starke and G. McHale (*Department of Chemistry and Physics, The Nottingham Trent University, Clifton Lane, Nottingham NG11 8NS, United Kingdom*)

M.R. Willis (*Department of Chemistry, The University of Nottingham, University Park, Nottingham, NG7 2RD, United Kingdom*)

A. Krier (*Advanced Materials and Photonics Group, School of Physics and Chemistry, Lancaster University, Lancaster, LA1 4YB, United Kingdom*)

References

1 BENES, E., GROSCHL, M., BURGER, W., and SCHMID, M.: 'Sensors based on piezoelectric resonators', *Sens. Actuators A*, 1995, **48**, pp. 1–21

2 GRATE, J.W., MARTIN, S.J., and WHITE, R.M.: 'Acoustic wave microsensors', *Anal. Chem.*, 1993, **65**, pp. A940–A948

3 REBIERE, D., DUCHAMP, G., PISTRE, J., HOUMMADY, M., HAUDEN, D., and PLANADE, R.: 'Surface acoustic wave NO_2 sensor: influence of humidity', *Sens. Actuators B*, 1993, **13–14**, pp. 642–645

4 RICCO, A.J., MARTIN, S.J., and ZIPPERIAN, T.E.: 'Surface acoustic wave gas sensors based on film conductivity changes', *Sens. Actuators*, 1985, **8**, pp. 319–333

5 BECKER, H., VON SCHICKFUS, M., and HUNKLINGER, S.: 'A new sensor principle based on the reflection of surface acoustic waves', *Sens. Actuators*, 1996, **54**, pp. 618–621

6 NIEUWENHUIZEN, M.S., NEDERLOF, A.J., and BARENDSZ, A.W.: 'Metallophthalocyanines as chemical interfaces on surface acoustic wave gas sensors for nitrogen dioxide', *Anal. Chem.*, 1988, **60**, pp. 230–235

7 RAPP, M., BINZ, D., KABBE, I., VON SCHICKFUS, M., HUNKLINGER, S., FUCHS, H., SCHREPP, W., and FLEISCHMANN, B.: 'New high-frequency high-sensitivity SAW devices for NO_2 gas detection in the sub-ppm range', *Sens. Actuators B*, 1991, **4**, pp. 103–108

Velocity of surface acoustic waves in metallised PE $LiNbO_3$

D. Čiplys and R. Rimeika

The velocity of surface acoustic waves in proton-exchanged 128°-rotated *Y* cut *X* propagation lithium niobate with a Cu or Al thin film deposited on the sample surface has been measured using acousto-optic techniques in a wide frequency range. The electrical and mechanical perturbations of the propagation surface introduced by the metal film affects the acoustic velocity, thus providing a mean for its accurate control.

Introduction: Propagation of surface acoustic waves (SAWs) in proton-exchanged (PE) lithium niobate ($LiNbO_3$) has attracted considerable interest in recent years because of promising applications in integrated acousto-optic devices [1]. The SAW velocity has been studied on a free surface of PE $LiNbO_3$ for various crystal cuts and acoustic propagation directions [2 – 5]. The general feature observed is the SAW dispersion arising due to the formation of an $H_xLi_{1-x}NbO_3$ layer at the surface of an $LiNbO_3$ substrate [6]. For practical purposes, the surface of an SAW device is often covered by a thin metal film (e.g. plate electrodes, gratings etc.). However, there was no data available on the SAW velocity in metallised proton-exchanged lithium niobate. In this Letter, we report the experimental measurements of the SAW velocity performed in PB 128° rotated *Y*-cut $LiNbO_3$ with a thin Cu or Al film deposited on the crystal surface.

Experimental techniques: The samples were single crystal plates of dimensions 20 × 8 × 1.5mm³. The SAW propagation direction was

ELSEVIER
TSF 13047
Thin Solid Films 000 (2000) 1–3
thin solid films
www.elsevier.com/locate/tsf

Letter

The effect of NO_2 doping on the gas sensing properties of copper phthalocyanine thin film devices

M.I. Newton[a,*], T.K.H. Starke[a], G.M. Hale[a], M.R. Willis[b]

[a]Department of Chemistry and Physics, The Nottingham Trent University, Clifton Lane, Nottingham, NG11 8NS UK.
[b]Department of Chemistry, The University of Nottingham, University Park, Nottingham, NG7 2RD UK.

Received 25 August 1999; accepted 1 October 1999

Abstract

In this work we report the effect on the NO_2 gas sensing properties of initially doping CuPc thin films with oxygen (in air) and NO_2 for room temperature operation. The pre-treatment with NO_2 is shown to improve the gas sensing properties by providing both an increase in the magnitude of the conductivity change for a given NO_2 concentration and a significant improvement in the recovery time. Data presented suggest that a simple time derivative of the change in current may provide a measure of concentration for real time gas sensing applications.
© 1999 Elsevier Science S.A. All rights reserved.

Keywords: Phthalocyanine; Nitrogen dioxide; Thin film; Gas sensor

1. Introduction

Phthalocyanines are an extensively investigated class of organic dye material, which are weakly semiconducting. Their thermally stable nature makes them suitable for thin film deposition by thermal sublimation; much of the work on these materials is reviewed by Leznoff and Lever [1]. These materials have also shown promise for photoconductive and photovoltaic response of which the current state of research has also been extensively reviewed by Whitlock et al. [2], Law [3] and Martin et al. [4]. It has been widely reported that oxygen acts as a dopant in phthalocyanines and is also responsible for the formation of a space charge region near rectifying electrodes. As a consequence, many workers have used exposure to air for days before depositing the top metal contact in sandwich structures, in order to oxygen dope the devices; after this time the oxygen doping is thought to be complete. Musser and Dahlberg [5] investigated the transient effect of oxygen adsorbed on to NiPc using the photovoltaic response and reported both a reversible and irreversible effect.

Different metal substituted phthalocyanines have been shown to respond to the presence of strongly reacting gases such as NO_2, NH_3 and Cl_2 [6–8]. Archer et al. [9] extensively investigated the influence of heat treatment and gas-exposure history on NO_2 detection with MPc films. One of their conclusions was that the previous exposure of MPc films to different gases played a crucial role in the gas sensing response. Experiments using earthed guard rings by Archer et al. [9] and VanEwyk et al. [10] have suggested that it is a surface conductivity responsible for the response to NO_2 rather than a bulk effect. The modelling of the adsorption/desorption of NO_2 on MPc thin films has more recently attracted interest [11,12]. Zhou and Gould have suggested that information about NO_2 concentration may be derived from the initial conductivity changes of a MPc film, rather than from data obtained under saturation conditions. They have suggested that the initial response of CuPc films to NO_2 follow the Elovich equation: $d\theta/d\theta = a\exp(-b\theta)$, where $d\theta/dt$ represents the rate of change of surface coverage θ and a and b are constants. By assuming that the change in electrical conductivity is proportional to the change in surface coverage [13], the change in current under constant bias then gives $d\Delta I/dt = a'\exp(b'\Delta I)$, where the value of a' may be correlated to the NO_2 concentration. In this work we compare the effect on the NO_2 gas sensing properties of initially doping CuPc films with oxygen (in air) and NO_2. It will be demonstrated that the pre-treatment with NO_2 improves the gas sensing properties by providing both an increase in the magnitude of the conductivity change for a given NO_2 concentration and an improvement in the recovery time.

---

[*] Corresponding author. Tel.: 44-115-9486656; fax: + 44-115-9486636.
E-mail address: michael.newton@ntu.ac.uk (M.I. Newton)

0040-6090/99/$ - see front matter © 2000 Elsevier Science S.A. All rights reserved.
PII: S0040-6090(99)00870-6

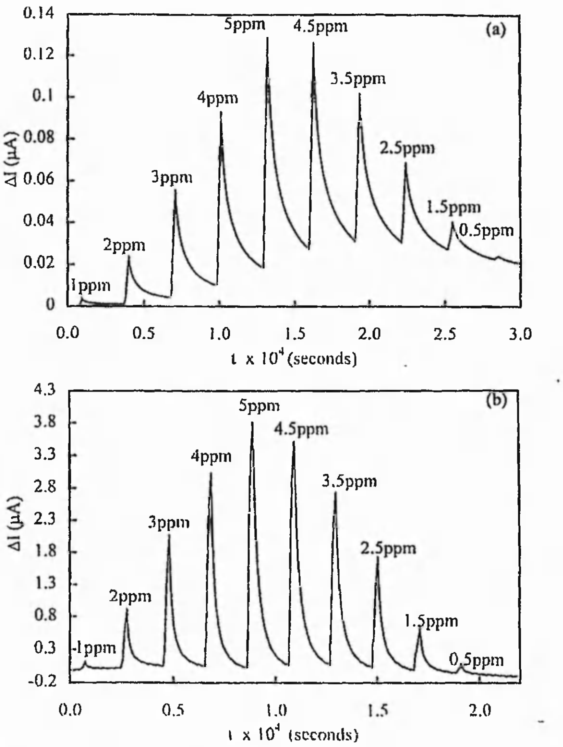

Fig. 1. (a) Response of a CuPc device to a sequence of 300 s exposures to NO_2 in the range 0.5–5 ppm with 2700 s between each exposure. (b) Response of a NO_2 doped CuPc device to a sequence of 300 s exposures to NO_2 in the range 0.5–5 ppm. with 1700 s between each exposure.

2. Experimental

The devices used in these experiments consisted of interdigital transducers (IDTs) with a CuPc overlayer. The IDTs were made of gold on glass using photolithography and used 20 finger pairs of length 2 mm and equal finger widths and spaces of 25 μm. The CuPc was deposited by thermal evaporation at a rate of 0.1 nm/s, on to a room temperature substrate producing films in the alpha phase of approximate thickness 160–200 nm. The CuPc was obtained from Fluke and purified by entrain sublimation prior to deposition. Immediately after deposition, the devices to be doped with NO_2 were placed in a 100 ppm NO_2 in N_2 atmosphere for four weeks: the other devices were stored in dry air. Conductivity changes in the CuPc films were measured by applying a constant bias of 1 V to each device and monitoring the current using Keithley model 485 picoammeters: the IDT geometry used produced an initial device resistance of typically 15 MΩ. The devices were mounted in a temperature controlled enclosure in an atmosphere of zero grade air (Air Products 2500 generator) provided at a constant flow rate of 1 l/min. The NO_2 was supplied by Air Products in the form of 100 ppm. NO_2 in N_2. The substrate temperature, gas flow controllers and electrical data collection were all controlled using a microcomputer: all data presented here is for room temperature measurements.

3. Results and discussion

Fig. 1 shows the change in current (ΔI) of an undoped sample for a sequence of 300 s exposures to NO_2 in the range 0.5–5 ppm. Fig. 2 shows the same sequence for a NO_2 doped device. The doped device shows an order of magnitude increase in the current change for the same NO_2 exposure. The time between exposures was 1700 for the doped and 2700 s for the undoped to allow for the much slower recovery time. Zhou and Gould [11] have reported that CuPc devices, under their test conditions, follow a simple Elovich model for surface coverage. In Fig. 2a we show the Elovich plot for the doped device. By extracting the value a' from these plots, we show the NO_2 concentration as a function of a' in Fig. 2b. Our data would suggest that, although we observe a similar relationship between NO_2 concentration and a' as that observed by Zhou and Gould, the linear region for the Elovich plot is limited. For real time gas sensing, a more appropriate analysis may be a simple time derivative of ΔI. In Fig. 3a we show the data from Fig. 1b plotted as the time derivative ($d\Delta I/dt$). From this data, the height of the differential peak would suggest to be a measure of NO_2 concentration. This is

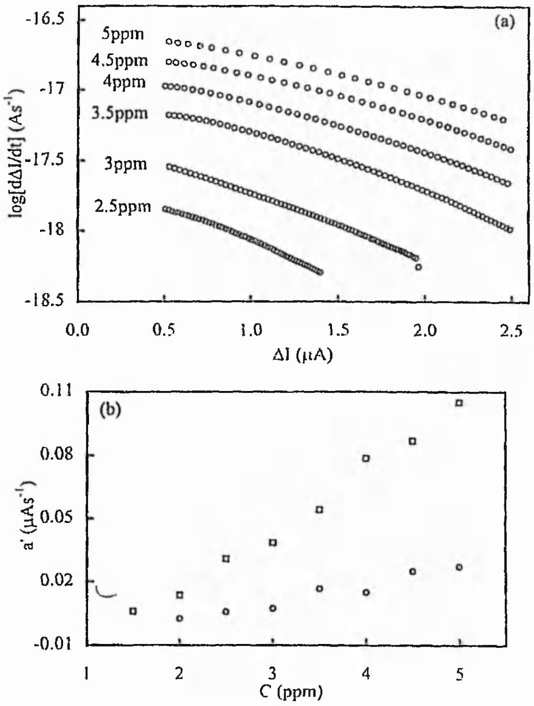

Fig. 2. (a) Elovich plot for the NO_2 doped CuPc device. (b) The NO_2 concentration plotted as a function of a' for the undoped (circles multiplied by a factor of 20) and NO_2 doped (squares) devices.

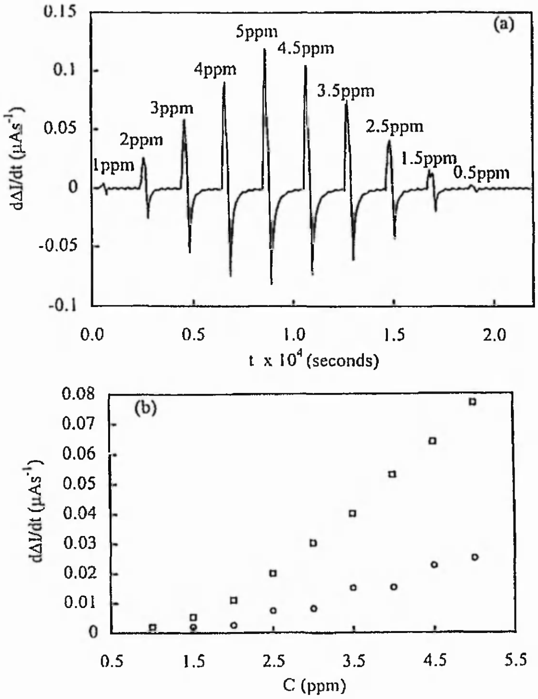

Fig. 3. (a) The data from Fig. 1b showing dΔI/dt as a function of time. (b) The peak in the dΔI/dt plotted as a function of NO_2 concentration for the undoped device (circles multiplied by a factor of 20) and for the NO_2 doped device (squares).

demonstrated in Fig. 3b, which shows the peak in the differential (dΔI/dt) as a function of concentration for both doped and undoped devices.

4. Conclusion

The effect on the NO_2 gas sensing properties of an initial doping of CuPc films with oxygen (in air) and NO_2, has been investigate for room temperature operation. The pre-treatment with NO_2 has been shown to improves the gas sensing properties by providing both an increase in the magnitude of the conductivity change for a given NO_2 concentration and a significant improvement in the recovery time. Data has been analysed using the Elovich equation, which provides a relationship between NO_2 concentration and a' however a simple time derivative of the change in current may also provide a measure of concentration for real time gas sensing applications.

References

[1] C.C. Lenznoff, A.B.P. Lever, Phthalocyanines, Properties and Applications, VCH publishers, 1989, pp. 1–3.
[2] J.B. Whitlock, P. Panayotatos, G.D. Sharma, M.D. Cox, R.R. Sauers, G.R. Bird, Opt. Eng. (1993) 32.
[3] K.-Y. Law, Chem. Rev. 93 (1993) 449.
[4] M. Martin, J.J. Andre, J. Simon, Nouv. J. Chim. 5 (1981) 485.
[5] M.E. Musser, S.C. Dahlberg, Surf. Sci. 100 (1980) 605.
[6] T.A. Jones, B. Bott, Sensors and Actuators 9 (1986) 27.
[7] S.J. Qin, B. Bott, Sensors and Actuators B 3 (1991) 255.
[8] K. Moriya, H. Enomoto, Y. Nakamura, Sensors and Actuators B 14 (1993) 412.
[9] P.B.M. Archer, A.V. Chadwick, J.J. Miasik, M. Tamizi, J.D. Wright, Sensors and Actuators 16 (1989) 379.
[10] R.L. VanEwyk, A.V. Chadwick, J.D. Wright, J.C.S. Faraday, Thin Solid Films 76 (1980) 2194.
[11] Q. Zhou, R.D. Gould, Thin Solid Films 317 (1998) 436.
[12] Y.H. Ju, C. Hsieh, C.J. Liu, Thin Solid Films 342 (1999) 238.
[13] J.W. Gardner, M.Z. Iskandarani, B. Bott, Sensors and Actuators B 9 (1992) 133.

The Nottingham Trent University

Libraries &
Learning
Resources

The Boots Library: 0115 848 6343
Clifton Campus Library: 0115 848 6612
Brackenhurst Library: 01636 817049